DTIC FILE COPY

AD-A189 678

ELECTROMAGNETIC SCATTERING BY AN EXPONENTIALLY DISTRIBUTED ROUGH SURFACE WITH THE INTRODUCTION OF A ROUGH SURFACE GENERATION TECHNIQUE

THESIS

Thomas K. Roseman, B.S.E.E.
Captain, USAF

AFIT/GE/ENG/87D-55

DTIC
ELECTE
MAR 0 7 1988
S H

DEPARTMENT OF THE AIR FORCE
AIR UNIVERSITY
AIR FORCE INSTITUTE OF TECHNOLOGY

Wright-Patterson Air Force Base, Ohio

DISTRIBUTION STATEMENT A
Approved for public release;
Distribution Unlimited

88 3 01 060

AFIT/GE/ENG/87D-55

ELECTROMAGNETIC SCATTERING BY AN EXPONENTIALLY DISTRIBUTED ROUGH SURFACE WITH THE INTRODUCTION OF A ROUGH SURFACE GENERATION TECHNIQUE

THESIS

Thomas K. Roseman, B.S.E.E.
Captain, USAF

AFIT/GE/ENG/87D-55

DTIC
ELECTE
MAR 0 7 1988
S D
H

Approved for public release; distribution unlimited

AFIT/GE/ENG/87D-55

ELECTROMAGNETIC SCATTERING BY AN EXPONENTIALLY DISTRIBUTED ROUGH SURFACE WITH THE INTRODUCTION OF A ROUGH SURFACE GENERATION TECHNIQUE

THESIS

Presented to the Faculty of the School of Engineering

of the Air Force Institute of Technology

Air University

In Partial Fulfillment of the

Requirements for the Degree of

Master of Science in Electrical Engineering

Thomas K. Roseman, B.S.E.E.

Captain, USAF

November 1987

Approved for public release; distribution unlimited

Preface

This study is intended to add to the available technology for the modeling of electromagnetic scattering from random rough surfaces. Two primary contributions are made in this thesis. First, a true joint exponential probability density function is introduced as a new model for rough surface representation and it's electromagnetic scattering properties are studied. Second, a digital technique is developed to generate rough surfaces using only marginal density functions. The electromagnetic scattering properties of these surfaces are then found using standard scattering prediction techniques.

As usual with this type of effort, no one person can take full credit. A great deal of the credit must go my advisor, Dr. Vital Pyati, who derived the true exponential pdf used in this thesis and whose assistance at several key points in the development of this thesis was critical. A very special thanks goes to Lt Col Wm. Baker without whom this thesis might never have gotten past the point of being just an assembly of mathematical problems with no solutions. Additionally I would like to thank Dr. Robert J. Papa of RADC, one of the recognized authorities in the field of rough surface scattering, for lending his valued assistance. I also thank Mr. Jim Common of AFWAL/AAWP-3 for his assistance with the Radar Cross Section prediction code, Dr. Peter S. Maybeck, and all the rest of the AFIT faculty. Finally, I would like to thank John, Pam and the rest of the outstanding staff of the AFIT Library for their excellent support.

DTIC COPY INSPECTED 1

on For
By
Dist
Dist
A-1

On a personal level I want to thank my classmates, the greatest bunch of people I have ever had the opportunity to be associated with. A special note of appreciation goes to Lt Clarence Reif with whom I had the pleasure of working especially close with throughout this thesis. All of them made this last year and a half very special to me. Mostly, however, I want to thank my family for all of their support. To my wife Tami, your the greatest, thanks for all of your patience and help. Finally, to my son Chuckie, thank you for being here to remind what it is all about.

Tom Roseman

Table of Contents

List of Figures

List of Tables

List of Symbols

Symbol/Acronym

RCS - radar cross section

jpdf - joint probability density function

pdf - probability density function

$p_2^G()$ - joint Gaussian pdf

$p_2^{ET}()$ - joint Exponential-type pdf

$p_2^E()$ - joint Exponential pdf

$p^G()$ - marginal Gaussian pdf

$p^{ET}()$ - marginal Exponential-type pdf

$p^E()$ - marginal Exponential pdf

ζ_1 - surface height random variable at point (x_1, y_1)

ζ_2 - surface height random variable at point (x_2, y_2)

ρ - correlation coefficient (also $\rho(r)$)

r - distance between two points on the surface (argument of $\rho()$)

h^2 - variance of the surface heights

sgn() - signum function

J_n - bessel function of order n

I_n - modified bessel function of first kind, order n

K_n - modified bessel function of second kind, order n

ℓ - correlation length

EMS - electromagnetic scattering

j - square root of (-1)

E - electric field intensity

$\underline{E}$ - complex electric field intensity (E*exp(-jωt))

$\underline{\overline{E}}$ - complex electric field intensity vector

H, $\underline{H}$, $\underline{\overline{H}}$ - magnetic field quantities

μ - complex permeability

ε - complex permittivity

ρ - charge density within the context of the Stratton-Chu equations

ψ - free space Green's function

$\hat{n}$ - outward unit normal vector from a point on a surface

$*$ - complex conjugate operator

ω - radian frequency of the electromagnetic field

$k_o, \overline{k}$ - free space wave number and free space wave vector

$\hat{k}$ - unit wave vector equal to $\overline{k} / k_o$

$\overline{r}$ - vector from point (x_1, y_1) to point (x_2, y_2)

$R_{\parallel}$, $R_{\perp}$ - parallel and perpendicular Fresnel reflection coefficients

Z,Y - intrinsic impedance and admittance of the reflecting surface

$\hat{\eta}$ - unit vector indirection of observation point from a point on the surface

$\langle\ \rangle$ - expected value operator

CF - characteristic function

$\Upsilon_1()$, $\Upsilon_2()$ - marginal and joint characteristic functions

$\delta()$ - delta function

s - defined as ($s=2h/\ell$), atan(s) is the mean surface slope

$\overline{Z}(t_i)$ - correlated vector of surface heights

$\overline{W}(t_i)$ - uncorrelated vector of surface heights

$\overline{R}$ - matrix of correlation coefficients, correlation matrix

$\sqrt{\ }$ - Cholesky square root matrix operator

$\Gamma()$ - gamma function

Abstract

The purpose of this investigation is to extend the capability of statistical modeling for the problem of electromagnetic scattering by random rough surfaces. A majority of prior studies considered the well known Gaussian joint probability density function (pdf), partly because of its mathematical convenience. About 25 years ago, a second pdf called exponential type was introduced and has since been used by several workers in the field. In this thesis it is shown that this exponential-type pdf fails to meet an essential statistical requirement. To remedy this situation, an exponential pdf that satisfies all the statistical requirements is derived. The scattering properties of surfaces modeled by this new exponential pdf are then formulated.

In the second part of this thesis a user-oriented computer program is developed to create random surfaces whose statistical description is at the will of the user requiring only the input of a monovariate pdf. By using this program, the average radar cross section properties of surfaces modeled by the Gaussian and exponential pdf's are investigated further. Finally, applications of the work completed in this thesis to problems needing further investigation are outlined.

ELECTROMAGNETIC SCATTERING BY AN EXPONENTIALLY DISTRIBUTED ROUGH SURFACE WITH THE INTRODUCTION OF A ROUGH SURFACE GENERATION TECHNIQUE

I. Introduction

1. Background

The theory of scattering of electromagnetic waves from rough surfaces has many applications. Among these are effects of roughness upon the reflectance of optical devices [21], the effects of rough terrain and multipath propagation on radar system performance [14] and the remote sensing of surface roughness parameters [25], [8]. The ability to predict and control the rough surface scattering phenomena is dependent upon ones ability to accurately model the rough surfaces themselves.

Extensive research has gone into rough surface scattering theory where the rough surface is modeled by a joint probability density function (jpdf). In these models the surface heights are random variables. However, the research has been limited to the use of only two types of joint densities as rough surface models. In addition, one of these two jpdf's has characteristics which make its use as a surface model inappropriate. Therefore, development of scattering properties of surfaces with different jpdf representation as well as a better overall understanding of rough surface scattering is desirable.

As noted by Pyati, for a joint probability density function to properly represent a surface, it must not only satisfy the statistical properties required of a second order jpdf but it also must satisfy any additional conditions imposed by the physics of the problem (4:3). Clearly, two such physical conditions should be that:

(1) As the distance between any two points (r) on the surface goes to infinity, the heights, ζ_1 and ζ_2, at the two points should be statistically independent.

(2) As the distance between any two points on the surface goes to zero, the probability that the two points are equal in height should go to one.

The two jpdf's that are commonly used in the current literature to represent random rough surfaces are the joint Gaussian pdf (Eq (1))

$$p_2^G(\zeta_1,\zeta_2;r) = \frac{1}{2\pi h^2\left[1-\rho^2(r)\right]^{1/2}} \exp\left\{-\frac{\zeta_1^2 - 2\zeta_1\zeta_2\,\rho(r) + \zeta_2^2}{2\,h^2\left[1-\rho^2(r)\right]}\right\} \tag{1}$$

$\zeta_{1,2} \equiv$ surface heights at points (x_1,y_1) and (x_2,y_2)

$\rho(r) \equiv$ the correlation function

$h^2 \equiv$ variance of $\zeta_{1,2}$

and the joint exponential-type pdf (Eq (2)).

$$p_2^{ET}(\zeta_1,\zeta_2;r) = \frac{3}{2\pi h\left[\,1 - \rho^2(r)\right]^{1/2}} \times \exp\left\{-\left[\frac{\zeta_1^2 - 2\zeta_1\zeta_2\rho(r) + \zeta_2^2}{\frac{1}{3}h^2\left[1 - \rho^2(r)\right]}\right]^{1/2}\right\} \tag{2}$$

The joint Gaussian pdf satisfies conditions (1) and (2) and is a valid jpdf for representing rough surfaces. The exponential-type jpdf fails to satisfy condition 1, some consequences of which will be shown in this thesis, and may therefore not be valid for rough surface representation.

Pyati has derived the following true exponential joint probability density function that satisfies both of the physical conditions given above [17:8]:

$$P_2^E(\zeta_1,\zeta_2;r) = \frac{1}{\left[4h^2(1-\rho^2)\right]} \exp\left\{-\left[\frac{|\zeta_1| + |\zeta_2|}{h\ (1-\rho^2)}\right]\right\}$$

$$\times\left\{I_o\left[\frac{2\rho(\ |\zeta_1|\ |\zeta_2|)^{1/2}}{h\ (1-\rho^2)}\right] + (8/\pi^2)\ \mathrm{sgn}(\zeta_1)\ \mathrm{sgn}(\zeta_2)\right.$$

$$\left.\times\sum_{n=o}^{\infty}\frac{1}{(2n+1)}\ I_{2n+1}\left[\frac{2\rho(\ |\zeta_1|\ |\zeta_2|)^{1/2}}{h\ (1-\rho^2)}\right]\right\} \qquad (3)$$

where

I_n ≡ n^{th} order modified bessel function of the first kind

sgn(x) ≡ the sign of x or zero if x = zero.

The scattering properties of surfaces modeled by the above exponential jpdf will be studied here.

In addition to the lack of density functions to use as models, there has heretofore never been presented a method by which the the predicted scattering from the existing models could be checked against the scattering from real surfaces that meet the statistics. This thesis will address this problem.

2. Statement of the Problem

The problem is divided into two primary parts. Part A will involve the prediction of the average RCS per unit area of a surface represented by Pyati's exponential jpdf using somewhat traditional rough surface scattering theory. Part B involves the development of an entirely new approach to the prediction of rough surface scattering for surfaces represented by probability density functions.

3. Assumptions and Limitations

The following assumptions will be made in this thesis:

(1) The radii of curvature of the surface irregularities are large with respect to a wavelength. This restriction permits one to use the physical optics method to solve the electromagnetic integral equations introduced in the next chapter.

(2) Multiple scattering and shadowing will be ignored.The effects of shadowing are being accounted for in another thesis by Reif [19] concurrent with this one.

(3) The surfaces will be assumed to be perfect conductors.

(4) The correlation length ℓ is assumed to be much less than the either dimension of the surface. For instance, if the surface is chosen to be a rectangle with transverse dimensions of Lx and Ly, $\ell \ll$ Lx, Ly. This condition makes certain that the scattering is a result of the ensemble surface roughness rather than from a statistically small portion of the surface that may not be representative of the surface as a whole.

(5) The Gaussian correlation coefficient model, $\rho(r) = \exp[-r^2/\ell^2]$, will be used be used to maintain consistency with previous calculations based upon Eqs (1) and (2), [20:721] thus allowing direct comparisons of the results.

4. Approach

For Part A of the analysis a general solution for the average RCS per unit area of rough surfaces represented by joint probability density functions is formulated from the Stratton-Chu integral equation for electromagnetic scattering. The general solution arrived at is that which was previously obtained by Beckmann [5]. The general solution is then applied to Pyati's exponential jpdf and the results are compared to those for Gaussian and exponential-type surfaces.

In Part B, a technique is developed that allows the creation of correlated rough surfaces from the one dimensional marginal pdf of the surface heights. This technique is then used to create rough surfaces that obey Gaussian and exponential statistics. The physical optics radar cross sections of these surfaces is then calculated using a standard RCS prediction software package. These results are then compared to the predictions in Part A.

5. Support

The only support required for Part A is an IBM™ personal computer system and associated software, all of which are the personal property of the author. The RCS prediction package required for Part B is owned by AFWAL/AAWP-3 and is hosted on their VAX 11/785. A personal copy of this code along with access to the VAX was provided by AFWAL/AAWP-3.

II. Theory

In this section two equations for the average RCS per unit area of random rough surfaces will be derived. The derivation of each equation involves assumptions and approximation that will be pointed out as they occur.

1. Stratton-Chu and Helmholtz Equations

A starting point for discussions of electromagnetic scattering theory is the set of equations known as the Stratton-Chu integral equations (Eqs (4) and (5)) [23:466].

$$\bar{E}(P') = \frac{1}{4\pi} \oint_V \left[j\omega\mu \bar{J}\psi - \bar{J}^* \times \nabla\psi + \frac{1}{\varepsilon}\rho\nabla\psi \right] dv$$

$$- \frac{1}{4\pi} \oint_S \left\{ j\omega\mu \left(\hat{n} \times \bar{H} \right)\psi + \left(\hat{n} \times \bar{E} \right) \times \nabla\psi + \left(\hat{n} \cdot \bar{E} \right)\nabla\psi \right\} ds \quad (4)$$

$$\bar{H}(P') = \frac{1}{4\pi} \oint_V \left[j\omega\varepsilon \bar{J}^*\psi - \bar{J} \times \nabla\psi + \frac{1}{\mu}\rho^* \nabla\psi \right] dv$$

$$+ \frac{1}{4\pi} \oint_S \left\{ j\omega\varepsilon \left(\hat{n} \times \bar{E} \right)\psi - \left(\hat{n} \times \bar{H} \right) \times \nabla\psi - \left(\hat{n} \cdot \bar{H} \right)\nabla\psi \right\} ds \quad (5)$$

The above equations were derived by applying the vector analog of Green's theorem to Maxwell's field equations [23:464,465]. The left side of the equations represent the complex electric and magnetic field vectors at a point P' located within the closed volume of the first

integral of either equation. The closed surface of the second integral is that surface which encloses the volume of the first integral. Within the context of these equations, ρ is the charge density within the closed volume and $\bar{J}$ represents any current sources within the volume. The operator (*) indicates that the complex conjugate of the quantity is to be used. The $\bar{E}$'s and $\bar{H}$'s within the second integral of Eqs (4) and (5) represent the total electric and magnetic fields at the interior surface of the volume. The symbol ψ is the free-space Green's function. This scenario is depicted in Fig. 1.

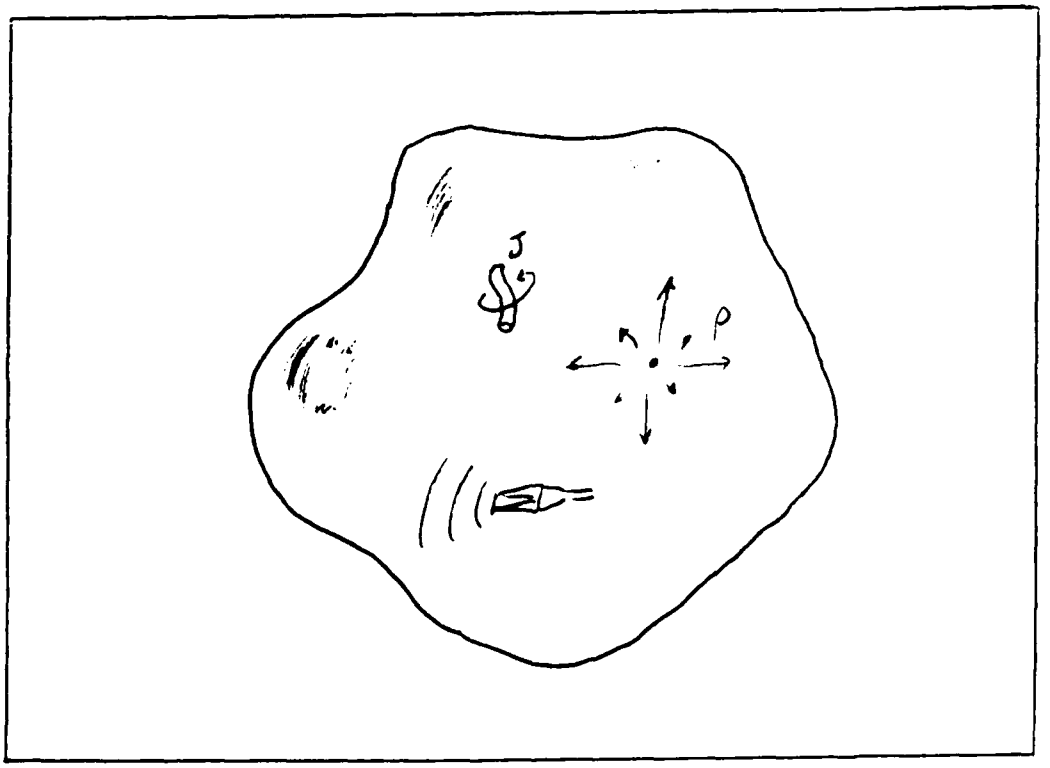

Fig. 1. Geometry Associated with the Stratton-Chu Equations

The geometry of the rough surface scattering problem to be worked in this thesis is that of an open surface, Fig. (2).

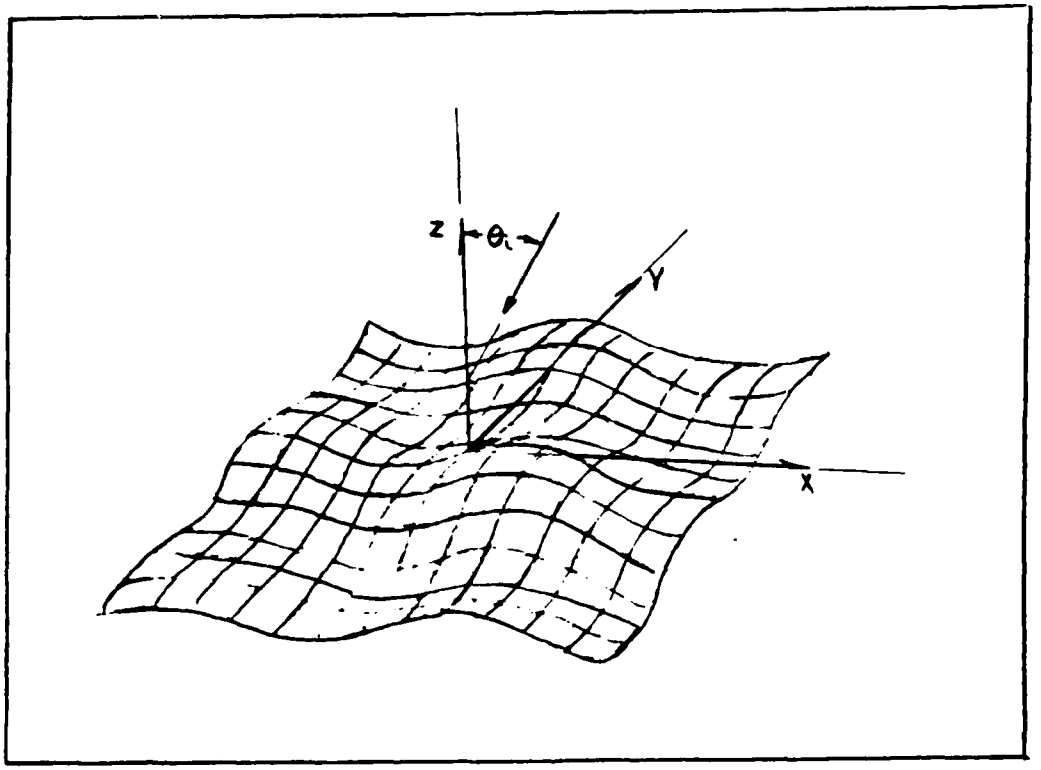

Fig. 2. Rough Surface Geometry

The Stratton-Chu equations can be simplified somewhat since the environment surrounding the target can be assumed to be source free. This may seem to be a contradiction since there must obviously be some source of the original electromagnetic fields that are to be scattered by the target. This contradiction is resolved by realizing that when the RCS of a target is being considered, only those fields scattered from the

target in the direction of the receiver are of any concern. Certainly there may be additional fields at the observation point P'. But, if they are not traveling along a vector in a direction from the target, or are not a result of the scattering of the transmitted wave from the target, they may be set to zero. With this simplification then, the Stratton-Chu equations can be written without the first integral of each equation.

$$\underline{\bar{E}}(P') = -\frac{1}{4\pi}\oint_s \left\{ j\omega\mu\left(\hat{n}\times\underline{\bar{H}}\right)\psi + \left(\hat{n}\times\underline{\bar{E}}\right)\times\nabla\psi + \left(\hat{n}\cdot\underline{\bar{E}}\right)\nabla\psi \right\} ds \quad (6)$$

$$\underline{\bar{H}}(P') = +\frac{1}{4\pi}\oint_s \left\{ j\omega\varepsilon\left(\hat{n}\times\underline{\bar{E}}\right)\psi - \left(\hat{n}\times\underline{\bar{H}}\right)\times\nabla\psi - \left(\hat{n}\cdot\underline{\bar{H}}\right)\nabla\psi \right\} ds \quad (7)$$

Although the scattering geometry of the rough surfaces under study do not coincide with the geometry for which the Stratton-Chu equations were derived these equations can still be used if one simply considers the rough surface to be a portion of a closed surface (Fig. (3)). Electromagnetic fields will be present at the rough surface but will be set to zero over the remainder of the imaginary closed surface. Setting the fields outside of the rough surface equal to zero causes the tangential fields over the entire closed surface to be discontinuous. Stratton shows [23:468-470] that the discontinuity can be accounted for by the addition of a line integral around the contour of the open surface. With this addition the Stratton-Chu equations are given by Eqs (8) and (9).

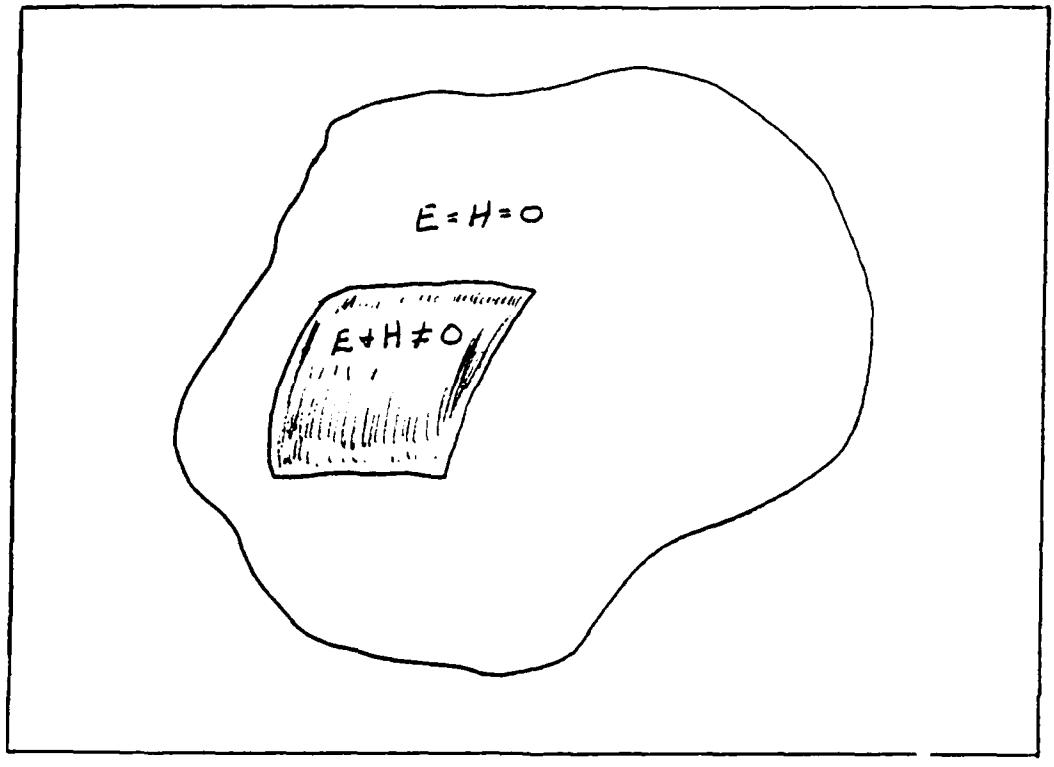

Fig. 3. Modified Stratton-Chu Scattering Geometry

$$\underline{\bar{E}}(P') = -\frac{1}{4\pi}\oint_s \left\{ j\omega\mu\left(\hat{n}\times\underline{\bar{H}}\right)\psi + \left(\hat{n}\times\underline{\bar{E}}\right)\times\nabla\psi + \left(\hat{n}\cdot\underline{\bar{E}}\right)\nabla\psi \right\} ds$$

$$-\frac{1}{j\omega\varepsilon}\;\frac{1}{4\pi}\oint_c \nabla\psi\left(\underline{\bar{H}}\cdot d\bar{l}\right) \qquad (8)$$

$$\underline{\bar{H}}(P') = +\frac{1}{4\pi}\oint_s \left\{ j\omega\varepsilon\left(\hat{n}\times\underline{\bar{E}}\right)\psi - \left(\hat{n}\times\underline{\bar{H}}\right)\times\nabla\psi - \left(\hat{n}\cdot\underline{\bar{H}}\right)\nabla\psi \right\} ds$$

$$-\frac{1}{j\omega\mu}\;\frac{1}{4\pi}\oint_c \nabla\psi\left(\underline{\bar{E}}\cdot d\bar{l}\right) \qquad (9)$$

These equations can be transformed into yet another form [23:469]:

$$4\pi\,\underline{\bar{E}}(P') = -\int_s \left[\,\underline{\bar{E}}\,\frac{\partial\,\psi}{\partial\,\hat{n}} - \psi\,\frac{\partial\,\underline{\bar{E}}}{\partial\,\hat{n}}\,\right] ds \; - \frac{1}{i\omega\varepsilon}\oint_c \nabla\psi\left[\,\underline{\bar{H}}\cdot d\bar{l}\,\right]$$

$$+\oint_c \psi\,\left[\underline{\bar{E}}\times d\bar{l}\right] \tag{10}$$

$$4\pi\,\underline{\bar{H}}(P') = -\int_s \left[\,\underline{\bar{H}}\,\frac{\partial\,\psi}{\partial\,\hat{n}} - \psi\,\frac{\partial\,\underline{\bar{H}}}{\partial\,\hat{n}}\,\right] ds - \frac{1}{i\omega\mu}\oint_c \nabla\psi\left[\,\underline{\bar{E}}\cdot d\bar{l}\,\right]$$

$$+\oint_c \psi\,\left[\underline{\bar{H}}\times d\bar{l}\right] \tag{11}$$

The first and last integrals of each equation come from Eqs (8) and (9) by applying Green's theorem relating surface integrals to line integrals. The second integral is of course the added term for the edge scattering effects. The first integrals of Eqs (10) and (11)

$$4\pi\,\underline{\bar{E}}(P') = -\int \left[\,\underline{\bar{E}}\,\frac{\partial\,\psi}{\partial\,\hat{n}} - \psi\,\frac{\partial\,\underline{\bar{E}}}{\partial\,\hat{n}}\,\right] ds \tag{12}$$

$$4\pi\,\underline{\bar{H}}(P') = -\int \left[\,\underline{\bar{H}}\,\frac{\partial\,\psi}{\partial\,\hat{n}} - \psi\,\frac{\partial\,\underline{\bar{H}}}{\partial\,\hat{n}}\,\right] ds \tag{13}$$

are known as the Helmholtz Integral equations. The Helmholtz equations are exact for source free closed surfaces.

2. Approximations

Exact solutions to the equations of the previous section have not been found except in very limited cases. In general, any solution to these electromagnetic scattering equations is facilitated by the imposition of one or more approximations. This subsection discusses several approximations that will be made in this thesis.

2.1 Far Field Approximation and Plane Waves

If one only considers observation points (P's) that are very far from the scattering surface several simplifications can be made. The first simplification is that the incident fields at the surface may be considered plane waves. This will be useful when the physical optics approximation is made and the angle of incidence at each point along the surface needs to be known. If the incident fields are not considered to be planar, determining this angle of incidence becomes a significant problem.

The incident planar electric field can be written

$$\bar{E} = \frac{1}{4\pi R} \exp\left[\mp j(\omega t - \bar{k}\cdot\bar{r})\right]\left(E_x\hat{x} + E_y\hat{y} + E_z\hat{z}\right) \qquad (14)$$

Because the field quantity is only the real part of Eq (14), the sign of the remaining complex exponential term is inconsequential. Since the time dependence of the fields is henceforth going to be suppressed, the

negative sign will be used. This will make the remaining term in the exponential positive. The complex electric and magnetic fields can now be written:

$$\bar{\underline{E}} = \frac{\bar{\underline{E}}_o}{4\pi R} \exp(j\bar{k}\cdot\bar{r}) \quad ; \qquad \bar{\underline{H}} = \frac{\bar{\underline{H}}_o}{4\pi R} \exp(j\bar{k}\cdot\bar{r}) \tag{15}$$

Another important result of the far field approximation is that terms containing higher orders of 1/R may be neglected. Letting $\hat{\eta}$ be a unit vector directed from a point on the scattering surface to the observation point P'

$$\hat{\eta} \equiv \frac{\bar{R}}{R} \tag{16}$$

the following approximations that will prove useful may also be obtained [2:19].

$$\psi = \frac{\exp(jkR_o - jk\hat{\eta}\cdot\bar{r})}{R_o} \tag{17}$$

$$\text{Lim}_{R\to\infty} \nabla\psi = \text{Lim}_{R\to\infty} \left(\frac{1}{R} - jk\right)\psi\,\hat{\eta} = \left(-jk\right)\psi\,\hat{\eta} \tag{18}$$

$$(\hat{n} \times \underline{\overline{H}}) \cdot \nabla\nabla\psi = \frac{d^2\psi}{dR^2} \left[(\hat{n} \times \underline{\overline{H}}) \cdot \hat{\eta} \right] \hat{\eta} =$$

$$\psi \left[\frac{2}{R^2} - \frac{2jk}{R} - k^2 \right] \left[(\hat{n} \times \underline{\overline{H}}) \cdot \hat{\eta} \right] \hat{\eta} = - k^2 \psi \left[(\hat{n} \times \underline{\overline{H}}) \cdot \hat{\eta} \right] \hat{\eta} \qquad (19)$$

$$(\hat{n} \times \underline{\overline{E}}) \cdot \nabla\nabla\psi = \frac{d^2\psi}{dR^2} \left[(\hat{n} \times \underline{\overline{E}}) \cdot \hat{\eta} \right] \hat{\eta} =$$

$$\psi \left[\frac{2}{R^2} - \frac{2jk}{R} - k^2 \right] \left[(\hat{n} \times \underline{\overline{E}}) \cdot \hat{\eta} \right] \hat{\eta} = - k^2 \psi \left[(\hat{n} \times \underline{\overline{E}}) \cdot \hat{\eta} \right] \hat{\eta} \qquad (20)$$

2.2 The Physical Optics Approximation

The Stratton-Chu and Helmholtz equations are of a family called integral equations. That is, the term on the left of each equation is equal to the integral of some function of itself. This is easier seen by expanding the expressions for the fields along the interior surfaces as

$$\underline{\overline{E}}_{\text{total}}(x,y,z) \Big|_{\text{sur}} = \underline{\overline{E}}_{\text{scattered}}(x,y,z) \Big|_{\text{sur}} + \underline{\overline{E}}_{\text{incident}}(x,y,z) \Big|_{\text{sur}} \qquad (21)$$

$$\underline{\overline{H}}_{\text{total}}(x,y,z) \Big|_{\text{sur}} = \underline{\overline{H}}_{\text{scattered}}(x,y,z) \Big|_{\text{sur}} + \underline{\overline{H}}_{\text{incident}}(x,y,z) \Big|_{\text{sur}} \qquad (22)$$

while noting that the left side of each equation is

$$\bar{E}_{scattered}(x,y,z)\Big|_{P'} \quad \text{or} \quad \bar{H}_{scattered}(x,y,z)\Big|_{P'}$$

In general, integral equations of this type are not easily solved. In fact, closed form solutions of the scattering integrals have been found for only a few simple geometries such as spheres and infinite cylinders (The solutions for these shapes is facilitated by the fact that their geometries are specified by a single coordinate of an orthogonal coordinate systems). Therefore, several approximate solution methods to the scattering problem have been formulated. One such approximation is called physical optics. The physical optics concept is to approximate the fields at the surface by some function of the incident fields only. Thus, the integral scattering equations become definite integrals.

The most common physical optics approximation is the tangent plane approximation where the fields at each point on the surface are set equal to that field which would be present at the point if the surface were an infinite plane tangent to that point. "Then the incident field at every point on the surface may be broken up into components, $\bar{E}^i$ in

the plane of incidence, and $\underline{\bar{E}}^i_\perp$. normal to the plane of incidence. The scattered field given by each of these incident field components is then given by" [20:55]

$$\underline{\bar{E}}^s_\perp = R_\perp \; \underline{\bar{E}}^{\,i}_\perp \tag{23}$$

$$\hat{k}^{spec} \times \underline{\bar{E}}^s_{\shortparallel} = R_{\shortparallel} \left(\hat{k}^i_o \times \underline{\bar{E}}^i_{\shortparallel} \right) \tag{24}$$

where $\hat{k}^{spec}$ is a unit vector in the specular direction of scattering and [5:21]

$$R_\perp = \frac{\cos\theta_i - \sqrt{Y^2 - \sin^2\theta_i}}{\cos\theta_i + \sqrt{Y^2 - \sin^2\theta_i}} \tag{25}$$

$$R_{\shortparallel} = \frac{Y^2\cos\theta_i - \sqrt{Y^2 - \sin^2\theta_i}}{Y^2\cos\theta_i + \sqrt{Y^2 - \sin^2\theta_i}} \tag{26}$$

In the above equations Y is the intrinsic admittance of the reflecting medium, θ_i is the incident angle with respect to the surface normal, and the propagating medium is taken to be free space.

The tangent plane approximation is valid only when the radius of curvature at points along the surface are much greater than the wavelength of the incident fields thus limiting the effects of the phase shift caused by non-flat surfaces. This will not be discussed in detail

since there are many fine references that cover physical optics [20:55-59], [10:119-130] and [14:454-458]. The important consequence of this fact is that only rough surfaces with no sharp peaks or valleys will be covered in the pursuing calculations. The Gaussian correlation coefficient used in this thesis forces surfaces to meet this criteria as long as the wavelength is kept small compared to a correlation length.

2.3 The Infinite Conductivity Approximation

For any surface for which z is not constant (see Fig. 2) the normal to the surface is a function of x and y. This will make the plane of incidence and angle of incidence a function of x and y. This in turn complicates the determination of the local reflection coefficients. A common practice which reduces this complication is to assume that the scatterer is a perfect conductor so that the admittances in Eqs (25) and (26) go to infinity and thus $R_{\perp} = -1$ and $R_{\parallel} = +1$. The scattered electric and magnetic fields are then given by the relationships

$$\underline{\overline{E}}_{\perp}^{scat} = - \underline{\overline{E}}_{\perp}^{i} \tag{27}$$

$$\hat{k}^{spec} \times \underline{\overline{E}}_{\parallel}^{scat} = \hat{k}_{o}^{i} \times \underline{\overline{E}}_{\parallel}^{i} \tag{28}$$

This results in the total fields at the surface being given by

$$\hat{n} \times \underline{\overline{E}}_{surf} = \hat{n} \times (\underline{\overline{E}}_{i} + \underline{\overline{E}}_{scat}) = 0 \qquad (29)$$

$$\hat{n} \times \underline{\overline{H}}_{surf} = 2\hat{n} \times \underline{\overline{H}}_{i} \qquad (30)$$

This simplifies the problem in that the angle of incidence dependence of the surface fields is removed. The dependence on the normal to the surface at a given point remains.

3. Solution Ignoring Surface Slopes

In this section an equation that gives the average RCS per unit area for a random rough surface will be developed by starting with Eqs (8) and (9). Applying Stokes theorem to the line integrals one finds that [2:18]:

$$\oint_C \nabla\psi \left(\underline{\overline{H}} \cdot d\overline{l} \right) = \int_s \left\{ -\left[(\hat{n} \times \underline{\overline{H}}) \cdot \nabla \right] - j\omega\varepsilon (\hat{n} \cdot \underline{\overline{E}}) \right\} \nabla\psi \, ds \qquad (31)$$

$$\oint_C \nabla\phi \left(\underline{\overline{E}} \cdot d\overline{l} \right) = \int_s \left\{ -\left[(\hat{n} \times \underline{\overline{E}}) \cdot \nabla \right] - j\omega\mu (\hat{n} \cdot \underline{\overline{H}}) \right\} \nabla\phi \, ds \qquad (32)$$

By substituting Eqs (17), (19) and (20) into Eqs (31) and (32), substituting these results into Eqs (8) and (9) one can write [2:21]

$$\underline{\overline{E}}\,(P') = \frac{j\omega\mu\ e^{jkR}}{4\pi\ R} \int_s \left\{ (\hat{n}\times\underline{\overline{H}}) - \hat{\eta}\cdot(\hat{n}\times\underline{\overline{H}})\hat{\eta} - Y\ (\hat{n}\times\underline{\overline{E}})\times\hat{\eta} \right\} e^{-jk\hat{\eta}\cdot\overline{r}}\ ds \quad (33)$$

while Eq (9) effectively becomes

$$\underline{\overline{H}}\,(P') = \frac{j\omega\varepsilon\ e^{jkR}}{4\pi\ R} \int_s \left\{ (\hat{n}\times\underline{\overline{E}}) - \hat{\eta}\cdot(\hat{n}\times\underline{\overline{E}})\hat{\eta} - Z\ (\hat{n}\times\underline{\overline{H}})\times\hat{\eta} \right\} e^{-jk\hat{\eta}\cdot\overline{r}}\ ds \quad (34)$$

where Z and Y are the intrinsic impedance and admittance of the propagating medium. Using the infinite conductivity identity that the tangential component of the surface electric field is zero and that $\hat{n}\times\underline{\overline{H}} = 2\hat{n}\times\underline{\overline{H}}^{i}$, these equations become

$$\underline{\overline{E}}\,(P') = \frac{j\omega\mu\ e^{jkR}}{2\pi\ R} \int_s \left\{ (\hat{n}\times\underline{\overline{H}}^{i}) - \hat{\eta}\cdot(\hat{n}\times\underline{\overline{H}}^{i})\hat{\eta} \right\} e^{-jk\hat{\eta}\cdot\overline{r}}\ ds \quad (35)$$

$$\underline{\overline{H}}\,(P') = \frac{jke^{jkR}}{2\pi\ R} \int_s \left\{ (\hat{n}\times\underline{\overline{H}}^{i})\times\hat{\eta} \right\} e^{-jk\hat{\eta}\cdot\overline{r}}\ ds \quad (36)$$

Since either the electric fields or the magnetic fields at the observation point may be used to determine the RCS of the scattering surface, Eq (36), being the simpler of the two, will be used.

Recalling that $\hat{\eta}$ is the unit vector originating at a point on the surface and in the direction of the observation point P', the far field condition gives that this vector will be constant over the surface of integration. Therefore this cross product will be taken outside of the integrand using the relationship that $\bar{A} \times \bar{B} = - \bar{B} \times \bar{A}$. Also, using the rectangular coordinate system with the height of the surface above the z=0 plane be given by the random variable $\zeta(x,y)$, the following identities can be written:

$$\hat{n} = \frac{-\frac{\partial \zeta}{\partial x}\hat{x} - \frac{\partial \zeta}{\partial y}\hat{y} + \hat{z}}{\sqrt{\left(\frac{\partial \zeta}{\partial x}\right)^2 + \left(\frac{\partial \zeta}{\partial y}\right)^2 + 1}} \tag{37}$$

$$ds = dx\, dy \sqrt{\left(\frac{\partial \zeta}{\partial x}\right)^2 + \left(\frac{\partial \zeta}{\partial y}\right)^2 + 1} \tag{38}$$

Substitution of Eqs (37) and (38) into Eq (36) results in [2:33]

$$\bar{H} = -\frac{jke^{jkR}}{2\pi R}\hat{\eta} \times \int_s \left\{\left(-\frac{\partial \zeta}{\partial x}\hat{x} \times \bar{H}^i - \frac{\partial \zeta}{\partial y}\hat{y} \times \bar{H}^i + \hat{z} \times \bar{H}^i\right)\right\} e^{-jk\hat{\eta}\cdot\bar{r}}\, dx\, dy \tag{39}$$

At this point the approximation that the slope terms are very small will be applied reducing Eq (39) to

$$\underline{\bar{H}}\ (P') = -\frac{jke^{jkR}}{2\pi R}\,\hat{\eta} \times \int_s \left\{ \hat{z} \times \underline{\bar{H}}^i \right\} e^{-jk\hat{\eta}\cdot\bar{r}}\ dx\ dy \qquad (40)$$

From Eq (15) the incident magnetic field can be written

$$\underline{\bar{H}}^{\,i} = \underline{\bar{H}}_0^{\,i}\ e^{j\bar{k}^i\cdot\bar{r}} \qquad (41)$$

where the polarization and time dependence of the field are contained in $\underline{\bar{H}}_0^{\,i}$ and $\bar{r}$ is given by $\bar{r} = x\,\hat{x} + y\,\hat{y} + \zeta(x,y)\,\hat{z}$. The magnetic field can then be written [2:41]

$$\underline{\bar{H}}\ (P') = -\frac{jke^{jkR}}{2\pi R}\,\hat{\eta} \times \left\{ \hat{z} \times \underline{\bar{H}}_o^i \right\} \int_s e^{j(\bar{k}^i - k\hat{\eta})\cdot\bar{r}}\ dx\ dy \qquad (42)$$

Restricting the derivation to the case of backscatter where $\bar{k}^i$ is equal to $-k\hat{\eta}$ and thus $\hat{k}^i$ equals $-\hat{\eta}$, Eq (42) becomes

$$\underline{\bar{H}}\ (P') = -\frac{jke^{jkR}}{2\pi R}\,\hat{k}^i \cdot \left\{ \hat{z} \times \underline{\bar{H}}_o^i \right\} \int_s e^{2j\bar{k}^i\cdot\bar{r}}\ dx\ dy \qquad (43)$$

By breaking $\bar{k}^i$ up into its $\hat{x}$, $\hat{y}$, and $\hat{z}$ components and performing the dot product one arrives at

$$\underline{\bar{H}}(P') = \frac{jke^{jkR}}{2\pi R}\hat{k}^i \times \left\{ \hat{z} \times \underline{\bar{H}}_o^i \right\}$$

$$\times \int_s \exp\left[2j\left(k_x^i x + k_y^i y + k_z^i \zeta(x,y) \right) \right] dx\, dy \qquad (44)$$

The cross product can be easily performed for the case of backscatter by using the triple cross product identity [22:17]

$$\bar{A} \times (\bar{B} \times \bar{C}) = (\bar{A}\cdot\bar{C})\bar{B} - (\bar{A}\cdot\bar{B})\bar{C} \qquad (45)$$

resulting in

$$\hat{k}^i \times \left\{ \hat{z} \times \underline{\bar{H}}_o^i \right\} = \left(\hat{k}^i \cdot \underline{\bar{H}}_o^i \right) \hat{z} - \left(\hat{k}^i \cdot \hat{z} \right) \underline{\bar{H}}_o^i \qquad (46)$$

Since $\underline{\bar{H}}_o^i$ is orthogonal to $\hat{k}^i$ the first dot product is zero. The second dot product is simply the projection of the incident wave vector upon the z axis. Therefore, Eq (46) reduces to

$$\hat{k}^i \times \left\{ \hat{z} \times \underline{\bar{H}}_o^i \right\} = -k_z^i \underline{\bar{H}}_o^i = \cos(\theta_i)\, \underline{\bar{H}}_o^i \qquad (47)$$

and Eq (44) becomes

$$\underline{\bar{H}}(P') = \frac{jke^{jkR}}{2\pi R} \cos(\theta_i) \underline{\bar{H}}_o^i \int \exp\left[2j\left(k_x^i x + k_y^i y + k_z^i \zeta(x,y) \right) \right] dx\, dy \qquad (48)$$

Equation (48) is easily checked for validity by setting the random surface height variable equal to zero. With this substitution, the surface slopes are exactly zero and so Eq (48) should give the physical optics solution for a flat plate. Direct integration of Eq (48) with $\zeta(x,y)=0$ and the application of the RCS formula given by

$$\langle RCS \rangle = \frac{4\pi R^2 \langle |\bar{\underline{H}}(P')| \rangle^2}{|\bar{\underline{H}}_o^i|^2} \tag{49}$$

results in the RCS being

$$\frac{k^2}{\pi} \cos^2(\theta)\, L_x^2\, L_y^2\, \mathrm{sinc}^2(k_y L_y)\, \mathrm{sinc}^2(k_x L_x) \tag{50}$$

Equation (50) is the physical optics solution for the RCS of an infinitely conducting flat plate with sides L_x and L_y [10:121].

The next step then is to take the average of Eq (48) with respect to the random variable $\zeta(x,y)$.

$$\langle \bar{\underline{H}}(P') \rangle = \frac{jke^{jkR}}{2\pi R} \cos(\theta_i) \bar{\underline{H}}_o^i \int_s \exp\left[2j\left(k_x^i x + k_y^i y\right)\right] \langle \exp(2jk_z^i \zeta) \rangle \, dx \, dy \tag{51}$$

The solution above gives the expected value of $\bar{\underline{H}}(P')$. This value is relatively meaningless for very rough surfaces because the magnetic field is a complex quantity. The large variations in phase caused by the rough surface will cause the phase of this term to vary wildly. Therefore

$\langle \underline{\bar{H}}(P') \rangle$ gives little information about $\langle |\underline{\bar{H}}(P')| \rangle$ which is the contributor in incoherent measurement systems. To clarify this a simple example will be given.

The expected value of a complex number is written as

$$\langle \underline{\bar{H}}(P') \rangle = \langle \text{Re } \underline{\bar{H}}(P') \rangle + j \langle \text{Im } \underline{\bar{H}}(P') \rangle$$

Table I shows what misleading things can happen in the extreme case of 180° phase variation

TABLE I

Comparison of the Average of a Complex Quantity with the Average of its Magnitude

Re $\underline{\bar{H}}(P')$	Im $\underline{\bar{H}}(P')$	$\langle \text{Re } \underline{\bar{H}}(P') \rangle$	$\langle \text{Im } \underline{\bar{H}}(P') \rangle$	$\langle \lvert \underline{\bar{H}}(P') \rvert \rangle$
1	-1	0	0	$\sqrt{2}$
-1	1			

With this in mind, its obvious that in order to find the average RCS of the surface, Eq (49) one must solve for $\langle |\underline{\bar{H}}(P')| \rangle^2$.

The expected magnitude of the magnetic field at P', $\langle|\underline{\bar{H}}(P')|\rangle^2$, can be written $\langle\underline{H}(P')\underline{H}(P')^*\rangle$. Multiplying Eq (51) by it's complex conjugate results in

$$\underline{H}(P')\underline{H}(P')^* = \frac{k^2\cos^2(\theta)}{4\pi^2R^2}\,|\underline{\bar{H}}_o^{\,i}|^2 \times \int_s \exp\left[2j\left(k_x^i x + k_y^i y\right)\right] \exp(2jk_z^i\zeta)\,dx\,dy \times \int_s \exp\left[-2j\left(k_x^i x' + k_y^i y'\right)\right] \exp(-2jk_z^i\zeta')\,dx'\,dy' \tag{52}$$

By combining the two integrals and taking the average with respect to the random surface heights, the expected value of the magnitude of the scattered magnetic field can be written

$$\langle\underline{H}(P')\underline{H}(P')^*\rangle = \frac{k^2\cos^2(\theta)}{4\pi^2R^2}\,|\underline{\bar{H}}_o^{\,i}|^2 \times \int_s\int_s \exp\left[2j\left(k_x^i(x-x') + k_y^i(y-y')\right)\right] \langle\exp(2jk_z^i(\zeta-\zeta'))\rangle\,dx\,dy\,dx'dy' \tag{53}$$

At this time a substitution will be made for the sake of shorthand and also to match more closely the notation of the common literature on this subject [5], [20]and [16]. The following parameters are defined and simplified for the case of backscatter

$$v_x = 2k_x^i = k\left[\sin(\theta_i)-\sin(\theta_s)\cos(\phi_s)\right] = 2k\sin(\theta) \tag{54}$$

$$v_y = 2k_y^i = k\left[-\sin(\theta_i)\sin(\phi_s)\right] = 0 \tag{55}$$

$$v_z = 2k_z^i = k\left[-\cos(\theta_i)+\cos(\theta_s)\right] = -2k\cos(\theta) \tag{56}$$

With this notation Eq (53) becomes

$$\langle|\underline{\bar{H}}(P')|\rangle^2 = \frac{k^2\cos^2(\theta)}{4\pi^2R^2}\,|\underline{\bar{H}}_o^{\,i}|^2 \cdot \int_{-Lx/2}^{Lx/2}\int_{-Ly/2}^{Ly/2}\int\int\exp\left[j\left(v_x(x-x')+v_y(y-y')\right)\right]\langle\exp(jv_z(\zeta-\zeta'))\rangle\,dx\,dy\,dx'dy' \tag{57}$$

Here v_y has been left in for the time being although it is equal to zero for the case of backscatter. The inclusion of the limits of integration indicate that each surface integral is to be integrated over a rectangle that is Lx by Ly. It will be seen later that the shape and size of the surface is inconsequential so long as it is many correlation lengths in the x and y directions.

The averaged term within the integrand, $\langle \exp(jv_z(\zeta-\zeta')) \rangle$, is by definition the joint characteristic function of the pdf evaluated for v_z and $-v_z$ [7:428] and will be denoted by $\Upsilon(v_z,-v_z;r)$. It is the two dimensional fourier transform of the joint pdf and is a function of the correlation coefficient which is itself a function of the distance between the two points (x,y) and (x',y') given by r.

Barrick [2:45-48] shows the steps necessary to make a total transformation of Eq (57) into a polar coordinate integral that can be integrated over the characteristic function. First, define the distance between points as

$$r_x = (x-x') \quad , \quad r_y = (y-y') \quad \text{and} \quad r = \text{sqrt}(r_x^2 + r_y^2) \qquad (58)$$

Then

$$\langle |\underline{\bar{H}}(P')| \rangle^2 = \frac{k^2 \cos^2(\theta)}{4\pi^2 R^2} |\underline{\bar{H}}_o^i|^2 \int_{-Lx/2}^{Lx/2} \int_{-Ly/2}^{Ly/2} \left[\int_{-Lx/2-x'}^{Lx/2-x'} \int_{-Ly/2-y'}^{Ly/2-y'} \exp\left[j\left(v_x r_x + v_y r_y\right)\right] \Upsilon(v_z,-v_z;r)\, dr_x dr_y \right] dx'dy' \qquad (59)$$

The polar coordinate r has already been defined as $\text{sqrt}(r_x^2 + r_y^2)$ so all that remains is to define ϕ and the limits of integration. Since

neither of the data points (x,y) or (x',y') are as yet fixed, the easiest way to define ϕ is as Barrick did [7:79]:

$$x-x' = r\cos(\phi) \quad \text{and} \quad y-y' = r\sin(\phi) \tag{60}$$

This definition is especially facilitating since the left hand terms appear in the integrand. Transforming the limits of integration is not so trivial a task but is facilitated by the fact that for very rough surfaces, the joint characteristic function goes to zero monotonically within only a few surface correlation lengths. Reserving the definitions of "very rough" and "a few correlation lengths" until the analysis section where these terms are examined more closely, suffice it to say that this allows the finite surface to be expanded into an infinite surface without affecting the value of the integral.

Then

$$\langle|\underline{\overline{H}}(P')|\rangle^2 = \frac{k^2\cos^2(\theta)}{4\pi^2R^2}\,|\underline{\overline{H}}_o^{\,i}|^2 \int_{-Lx/2}^{Lx/2}\int_{-Ly/2}^{Ly/2} dx'\,dy' \int_0^{2\pi}\int_0^{\infty} \exp\left[j\left(v_x r\cos(\phi)+v_y r\sin(\phi)\right)\right] \Upsilon(v_z,-v_z;r)\,dr\,d\phi \tag{61}$$

The first integration is trivial resulting in

$$\langle|\underline{\bar{H}}(P')|\rangle^2 = \frac{k^2\cos^2(\theta)}{4\pi^2R^2}\,Lx\,Ly\,|\underline{\bar{H}}_o^{\,i}|^2$$

$$\int_0^{2\pi}\int_0^{\infty} \exp\left[j\left(v_x r\cos(\phi)+v_y r\sin(\phi)\right)\right]\chi(v_z,-v_z;r)\,dr\,d\phi \qquad (62)$$

Before proceeding the difference between coherent and diffuse scattering must be understood. Coherent scattering is that portion of the scattered field that follows the same pattern as would the scattered field if the surface were not rough. For the rectangular surfaces under consideration here, the coherent pattern is that given by Eq (50). As the surface gets progressively rougher, diffuse scattering will become more dominant. The diffuse scattering is the random scattering pattern that tends to fill in the nulls of the coherent pattern and reduce the power in the coherent lobes. A very rough surface is one which has only diffusely scattered power.

If a surface is not very rough and has a coherent component remaining in the scattered field, the expansion of the surface to infinite dimensions will cause the RCS to also go to infinity. This problem can be avoided if one subtracts out the coherent part of the power within the integration. The coherent power can be eliminated by subtracting $\langle \underline{\bar{H}} \rangle \langle \underline{\bar{H}}^* \rangle$ from the $\langle \underline{\bar{H}}\ \underline{\bar{H}}^* \rangle$. This is equivalent to subtracting the square of the one dimensional characteristic function

from the joint (two dimensional) characteristic function. With this modification and integrating over ϕ as shown by Beckmann [5:181-184]

$$\langle|\underline{\bar{H}}(P')|\rangle^2=\frac{k^2\cos^2(\theta)}{2\pi R^2}L_xL_y|\underline{\bar{H}}_o^i|^2\int_0^\infty rJ_0(r\sqrt{v_x+v_y})\left[\chi_2-\chi_1^2\right]dr \qquad (62)$$

where $\chi_2=\chi(v_z,-v_z;r)$ and $\chi_1=\chi_1(v_z)$ is the characteristic function of the one dimensional marginal distribution which goes to zero as the surface gets rougher and v_z increases. This is easily converted to a radar cross section per unit area by dividing by the area of the surface and employing Eq(49).

$$\langle RCS\rangle = 2k^2\cos^2(\theta)\int_0^\infty rJ_0(r\sqrt{v_x+v_y})\left[\chi_2-\chi_1^2\right]dr \qquad (64)$$

Recall that the above Eqs (63) and (64) give only the diffusely scattered is power and are only valid for surfaces where the surface slopes can be ignored.

4. Beckmann's Solution

Beckmann starts with the Helmholtz integral equation for the electric field given by Eq (12) and repeated here [5:19]:

$$\underline{\overline{E}}(P') = \frac{1}{4\pi} \int \left[\underline{\overline{E}} \frac{\partial \psi}{\partial \hat{n}} - \psi \frac{\partial \underline{\overline{E}}}{\partial \hat{n}} \right] ds \tag{65}$$

Obviously, Beckmann has ignored the line integrals introduced by the fact that the scatterer is not a closed surface . But, as stated by Barrick states, these terms are small and proportional to $\sin(\theta)$ [2:14]. Therefore, Beckmann's solution should not suffer from this deficiency at near normal incidence. As the angle of incidence increases, the shadowing function, $S(\theta)$, begins to dominate the solution, again making the line integral terms inconsequential (see Reif [19]).

Continuing with the Beckmann's derivation, the normal derivative of any quantity is given by the relationship [22:62]

$$\frac{\partial \psi}{\partial n} = \nabla \psi \cdot \hat{n} \tag{66}$$

Using the $\nabla \psi$ given by Eq (20) and the scalar quantities for the electric fields Beckmann gives the following physical optics

relationships for the fields at the surface [5:20]

$$|\bar{\underline{E}}| = (1+R)E \tag{67}$$

$$\left|\frac{\partial \bar{\underline{E}}}{\partial \hat{n}}\right| = (1-R)E(j\bar{k}^i \cdot \hat{n}) \tag{68}$$

where the R's are the Fresnel reflection coefficients. Substitution of these quantities into the Helmholtz equation results in

$$E(P) = \frac{E^i}{4\pi} \int\int \left[(1+R)(-j\bar{k}^s\psi) - \psi(1-R)(j\bar{k}^i)\right] \cdot \hat{n}\, ds \tag{69}$$

which in turn can be reduced to

$$E(P) = \frac{E^i}{4\pi R} \frac{j\, e^{jkR}}{} \int\int \left[(2R)(\bar{k}^i \cdot \hat{n}) \exp(2j\bar{k}^i \cdot \bar{r})\right] ds \tag{70}$$

in the case of backscatter where $\bar{k}^s = -\bar{k}^i$.

Beckmann does not state such, but Eqs (67) and (68) hold only for $\bar{\underline{E}}_\perp$ where $R \cong -1$. For $\bar{\underline{E}}_\parallel$ where $R \cong +1$, the field at the surface is not double the incident field as indicated by Eq (67) nor is the normal derivative of the field equal to zero as indicated by Eq (68). The equations only hold for the portion of $\bar{\underline{E}}_\parallel$ that is normal to the surface. For that portion of the field that is parallel to the surface, the equations hold with R set to -1. Fortunately, when the scalar terms are added as they are in Eq (69), the result is still Eq (70).

Continuing with Beckmann's derivation, Eq (68) is substituted into Eq (70) for the surface normal vector and Eq (38) is substituted in for the differential surface. Also, the magnitude of the Fresnel reflection coefficient is replaced with unity for the case of perfect conductivity yielding

$$E(P) = \frac{E^i \; j \; e^{jkR}}{2\pi R} \iint (\bar{k}^i) \cdot (-\zeta_x' \hat{x} - \zeta_y' \hat{y} + \hat{z}) \exp(2j\bar{k}^i \cdot \bar{r}) \, dxdy \qquad (71)$$

Instead of simply dropping the slope terms in Eq (71) Beckmann removes them by employing integration by parts legitimately. Expanding the integral portion of Eq (80) it can be written as

$$I = \iint (-k_x \zeta_x' - k_y \zeta_y' + k_z) \exp[(2j)(k_x x + k_y y + k_z \zeta)] \, dxdy \qquad (72)$$

For the case of backscatter where $k_y = 0$, Eq (72) can be written as the sum of two integrals

$$I = \iint (-k_x \zeta_x') \exp[(2j)(k_x x + k_z \zeta)] \, dxdy + \iint (k_z) \exp[(2j)(k_x x + k_z \zeta)] \, dxdy \qquad (73)$$

Upon integrating the first integral by parts one gets

$$I = \int \left[\left(\frac{-k_x}{2jk_z} \right) \exp\left[(2j)(k_x x + k_z \zeta) \right] \right]_{-Lx/2}^{Lx/2} dy + \iint \left(\frac{k_x^2}{k_z} \right) \exp\left[(2j)(k_x x + k_z \zeta) \right] dxdy + \iint (k_z) \exp\left[(2j)(k_x x + k_z \zeta) \right] dxdy \quad (74)$$

Beckmann shows that the first integral represents an edge term and is negligible [5:31]. Summing the second and third integrals one gets

$$I = \iint \left(\frac{k_x^2}{k_z} + k_z \right) \exp\left[(2j)(k_x x + k_z \zeta) \right] dxdy \quad (75)$$

Since $k_x = k\sin(\theta)$ and $k_z = k\cos(\theta)$, the terms can be summed to yield

$$\left(\frac{k_x^2}{k_z} + k_z \right) = \left(\frac{k_x^2}{k_z} + \frac{k_z^2}{k_z} \right) = \frac{k}{\cos(\theta)} = k \sec(\theta) \quad (76)$$

Thus

$$E(P) = \frac{jkE^i e^{jkR}}{2\pi R} \sec(\theta) \iint \exp\left[(2j)(k_x x + k_z \zeta) \right] dxdy \quad (77)$$

Equations (77) and Eq (48) are practically identical in form except the $\cos(\theta)$ term in Eq (48) is replaced by a $\sec(\theta)$ term and the magnetic field

is replaced by the electric field in Eq (77). Therefore, the same procedures can be used to transform Eq (77) as were used to transform Eq (48) into Eq (64) and the final result for the average RCS per unit area is

$$\langle RCS \rangle = 2k^2 \sec^2(\theta) \int_0^{\infty} rJ_0(r\sqrt{v_x}) \left[\tau_2 - \tau_1^2 \right] dr \qquad (78)$$

This result is the same as that of Beckmann [5:79] with the exception that Beckmann's result is in terms of average reflectance. Beckmann's solution is also true for the more general case of three dimensional bistatic scattering [5:720]. Transforming Beckmann's three dimensional bistatic scattering with finite conductivity solution into RCS units one gets

$$\langle RCS \rangle = |\beta_{hv}|^2 \, 2k^2 \int_0^{\infty} rJ_0(r\sqrt{v_x + v_y}) \left[\tau_2 - \tau_1^2 \right] dr \qquad (79)$$

where $|\beta_{hv}|^2$ is a polarization scattering matrix whose elements are given in reference [5]. For the case of backscatter and infinite conductivity, $|\beta_{hv}|^2$ reduces to $\sec^2(\theta)$.

5. Summary

In this section two equations were derived to give the average diffuse RCS per unit area from a random rough surface. The first solution , Eq (64), was found by making the assumption that the surface slopes were essentially zero. The second solution, Eq (78), was facilitated by the fact that the contour integrals around the outer edge of the surface were set to zero. In comparing the Eqs (64) and (78) it is clear that the only difference between them is that Eq (64) has a cosine term where Eq (78) has a secant term. Thus at incident angles very close to zero, these two solutions will give the same results. As will be seen in the next section, the diffuse backscatter from surfaces with small surface slopes is concentrated within small angles of incidence and thus Eqs (64) and (78) will give essentially the same results. As the slopes of the surfaces increase, the diffuse power is backscatter is present over a larger range of incident angles where Eqs (64) and (78) do not give the same results. Since Eq (78) is valid for these rougher surfaces as well as for the surfaces with small surface slopes, it will be the solution used throughout the remainder of this thesis.

III. ANALYSIS

This chapter is devoted to numerical computations and interpretation of the results. The sections in this chapter consist of

Part A:

1) A comparison of the three pdf's presented in Chapter I with respect to their ability to represent rough surfaces.

2) The calculation of the average RCS per unit area from a surface represented by the exponential pdf (Eq (3)) along with a comparison of these results to those for the Gaussian pdf and for the exponential-like pdf.

Part B:

3) The computer generation of surfaces meeting various statistics.

4) The computed average RCS for the computer generated surfaces.

Part A

1. Three PDF's

In this section the three pdf's presented in Chapter I will be analyzed with respect to their ability to represent rough surfaces. As stated in Chapter I, two of the probability density functions, the Gaussian and the exponential-type, have been used in the past by

workers studying the electromagnetic scattering from rough surfaces. Of these two pdf's, it will be shown that only the Gaussian pdf can reasonably be expected to represent a realizable rough surface.

This author, along with others [4] defines a realizable rough surface as one for which decorrelation of the surface height random variables implies statistical independence. Some may argue that simply because the variables do not become independent does not infer that either variable influences the other in a manner which precludes the use of the pdf from representing logical surfaces. Rather than contest this argument the exact influence of one variable over the other will be examined using conditional probabilities. Since the bivariate Gaussian pdf is a well documented density which decorrelates into two statistically independent monovariate Gaussian pdf's, it will be looked at first and used as the basis of comparison.

1.1 The Joint Gaussian pdf

There are several ways of determining the statistical independence of random variables in a multivariate pdf. A sufficient condition given by Davenport is that when the correlation coefficient is equal to zero, the joint distribution can be written as a product of the marginal distributions [7:167]. Integrating the joint Gaussian pdf with respect to ζ_1 it is found that the marginal distribution on ζ_2 is

$$p^G(\zeta_2) = \frac{1}{\sqrt{2\pi}\, h} \exp\left[- \frac{\zeta_2^2}{2h^2} \right] \tag{80}$$

Since the joint distribution is symmetric, ζ_1 can be substituted for ζ_2 in the above equation to get the marginal distribution on ζ_1. Setting ρ equal to zero in Eq (1)

$$p^G(\zeta_1,\zeta_2;0) = p^G(\zeta_1)\ p^G(\zeta_2) \tag{81}$$

thus establishing the fact that decorrelation implies statistical independence given the joint Gaussian pdf.

Figure 4 illustrates the effect of the correlation coefficient upon the joint Gaussian pdf. With ρ set to zero , Fig. 4a, one simply gets the symmetric Gaussian curve which states that the probability of $\zeta_1 = z_1$ and $\zeta_2 = z_2$ is dependent only upon the magnitude of $(z_1^2 + z_2^2)$. When the points are closer together there is a dependence between ζ_1 and ζ_2 such that the chance of z_1 being equal to z_2 is increased while the probability that z_1 will differ significantly from z_2 is decreased. This trend is shown in Figs. 4b and 4c where ρ is equal to .5 and .95 respectively. With ρ=.95 it is seen that the probability that $z_1 = z_2$ is very high as it should be since the points are very close to each other. When ρ=1 the joint density function becomes

$$\delta(\zeta_1-\zeta_2)\ p^G(\zeta_1) \tag{82}$$

indicating that the two random variables represent the same point [4].

Another way to state statistical independence in the context of surface height random variables is to say that the probability of a point (x,y) being at height z_0 is totally independent of the height of a

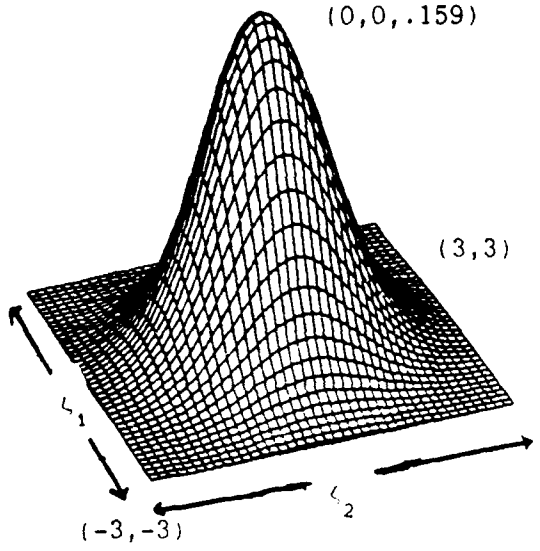

Fig. 4a. Joint Gaussian pdf with ρ=0

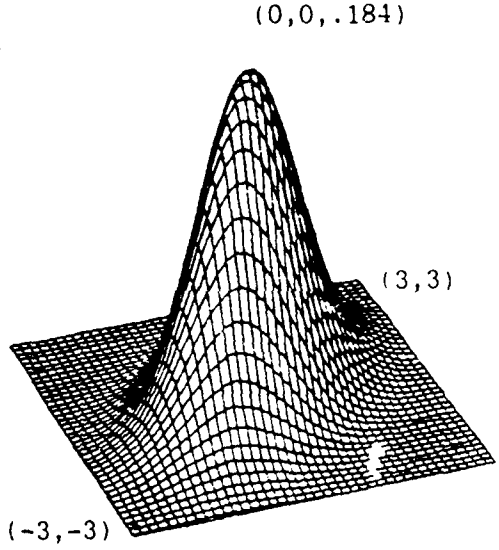

Fig. 4b. Joint Gaussian pdf with ρ=.5

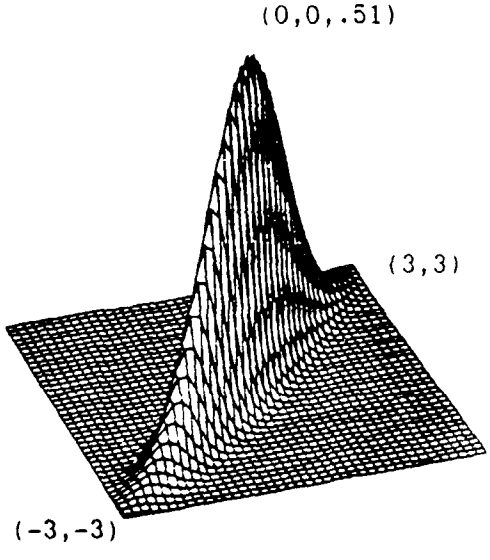

Fig. 4c. Joint Gaussian pdf with ρ=.95

point at (x',y') as long as the two points are separated by a great distance. Using the definition of conditional probability [7:160]

$$p(\zeta_1|\zeta_2;\rho) = \frac{p(\zeta_1,\zeta_2;\rho)}{p(\zeta_2)} \tag{83}$$

where $p(\zeta_1|\zeta_2)$ gives the probability of ζ_1 based on a given ζ_2 and ρ, a necessary condition for statistical independence can then be written as

$$p(\zeta_1|\zeta_2;\rho) = p(\zeta_1) \tag{84}$$

Substituting the joint and marginal Gaussian pdf's into Eq (83) gives the conditional Gaussian density function

$$p^G(\zeta_1|\zeta_2;\rho) = \frac{1}{\sqrt{2\pi(1-\rho^2)}} \exp\left[\frac{-(\zeta_1-\rho\zeta_2)^2}{2(1-\rho)}\right] \tag{85}$$

which is graphed out in Fig. 5 for the same values of ρ as was the joint pdf.

With ρ=0 the relationship of Eq (85) is illustrated that the probability of ζ_1 is not a function of ζ_2. With ρ=.5 the center of the curve tends towards the $\zeta_1 = \zeta_2$ line (it is actually at the $\zeta_1 = .5\zeta_2$ line) while the variance of the curve decreases. With ρ=.95 knowledge

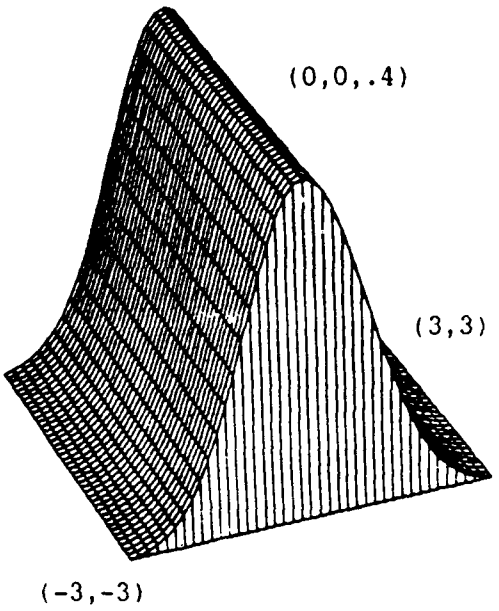

Fig. 5a. Conditional Gaussian pdf, ρ=0

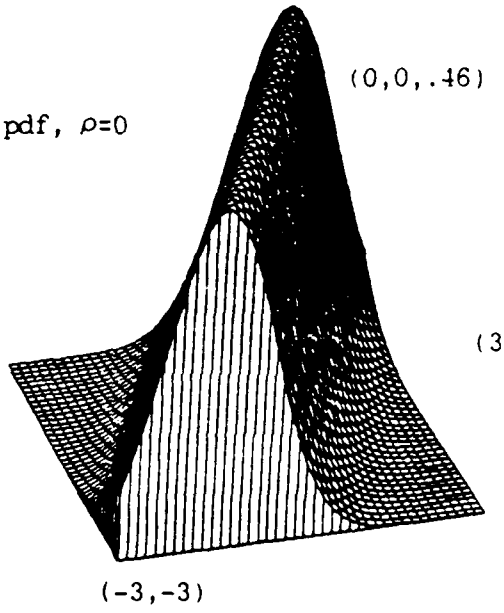

Fig. 5b. Conditional Gaussian pdf, ρ=.5

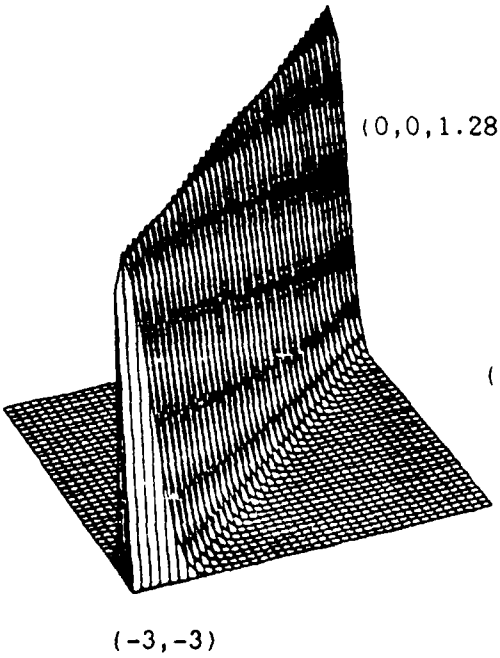

Fig. 5c. Conditional Gaussian pdf, ρ=.95

of ζ_2 almost completely determines ζ_1 as the trend towards

$$p^G(\zeta_1|\zeta_2;\rho) = \delta(\zeta_1-\zeta_2) \tag{86}$$

becomes apparent.

1.2 Exponential-Type pdf

Having established some of the desired features in a joint pdf it is time to examine the exponential-type pdf Eq (2) which has been used by many as an alternate to the joint Gaussian pdf for rough surface representation. Figure 6 graphs the exponential-type pdf for ρ=0, .5 and .95. There are many similarities between these graphs and the corresponding graphs for the joint Gaussian pdf. It is these similarities that may have lead others to use this pdf as a rough surface model. What is not readily apparent from these graphs is that the joint exponential-type density function is not equal to the product of its marginals at ρ=0 and and thus the decorrelated random variables are not statistically independent.

The fact that the exponential-type jpdf is not equal to the product of its marginals at ρ=0 is easily verified by checking at the point $\zeta_1 = \zeta_2$=0. The marginal pdf as derived by Papa and Lennon [15:59] is

$$p^{ET}(\zeta_1) = \frac{3}{\pi h^2} |\zeta_1| K_1\left(\sqrt{3}\,|\zeta_1|\right) \tag{87}$$

where K_1 is a first order modified Bessel function. Setting h=1 and using the value of $xK_1(x)$=1 for x=0 from [1:379] one gets

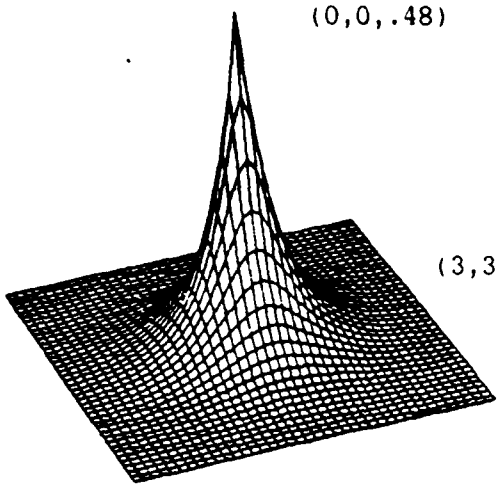

Fig. 6a. Joint Expo-type pdf, ρ=0

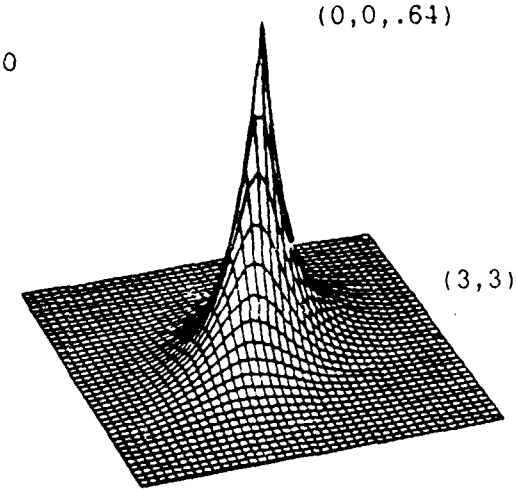

Fig. 6b. Joint Expo-type pdf, ρ=.5

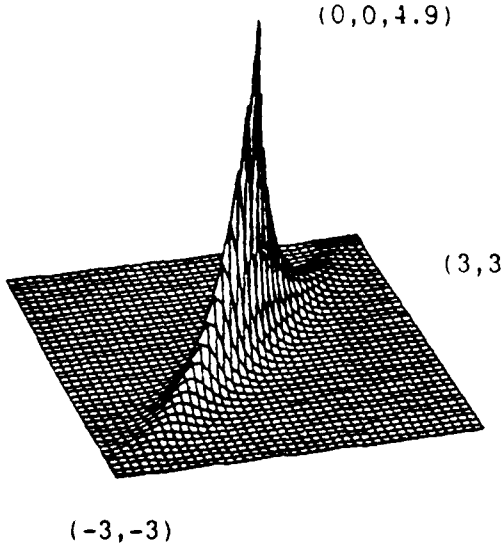

Fig. 6c. Joint Expo-type pdf, ρ=.95

$$p^{ET}(\zeta_1=0) = \frac{\sqrt{3}}{\pi} \quad \text{thus} \quad \left[p^{ET}(\zeta_1)\right]^2 = \frac{3}{\pi^2} \tag{88}$$

which does not equal $3/(2\pi)$, the value of the jpdf evaluated at zero.

The more critical question of the relationship between ζ_1 and ζ_2 is answered in Fig. 7 which graphs the conditional pdf's for the exponential-type jpdf at the different values of ρ. The fact that all of the graphs show a spreading of the conditional density function on ζ_1 as $|\zeta_2|$ gets large is a curiosity but does not prohibit the jpdf from representing rough surfaces. The fact that the conditional density function at $\rho=0$ shows that the density on ζ_1 is a strong function of ζ_2 does prohibit its use.

The exponential-type conditional pdf at $\rho=0$ is odd indeed for a pdf that is to represent rough surfaces. The increase in the variance of ζ_1 as $|\zeta_2|$ increases indicates that if the height $\zeta(x,y)$ is very high, the probability that the height at a point (x',y') which is very far from point (x,y) is modified so that very large positive and negative heights become more probable at the point (x',y'). Meanwhile, heights around the mean become less probable. The same behavior is observed if the height at point (x,y) is very large and negative. Although this author can offer no mathematical proof as to why this is impossible for physical surfaces, it seems that this is the only logical conclusion.

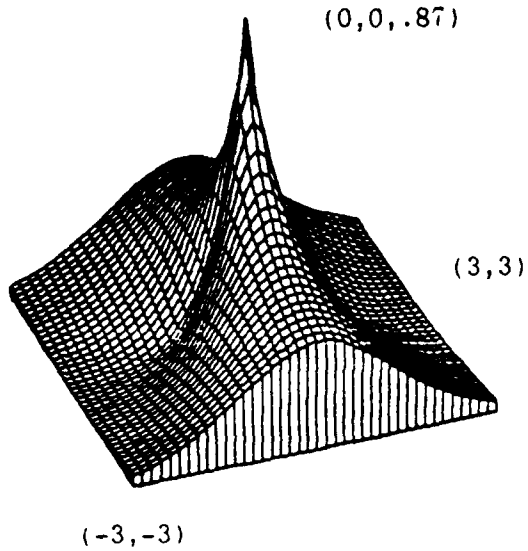

Fig. 7a. Conditional Expo-type pdf, ρ=0

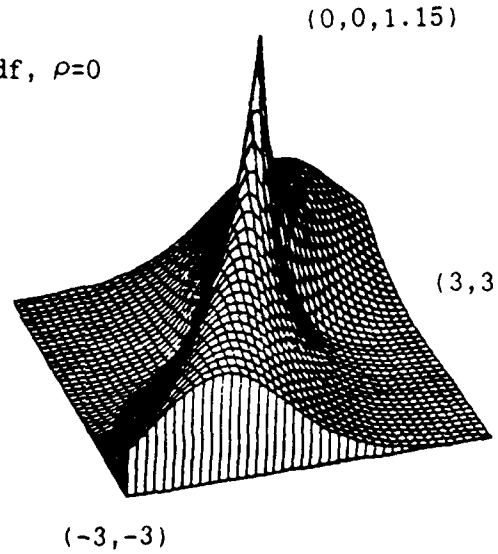

Fig. 7b. Conditional Expo-type pdf, ρ=.5

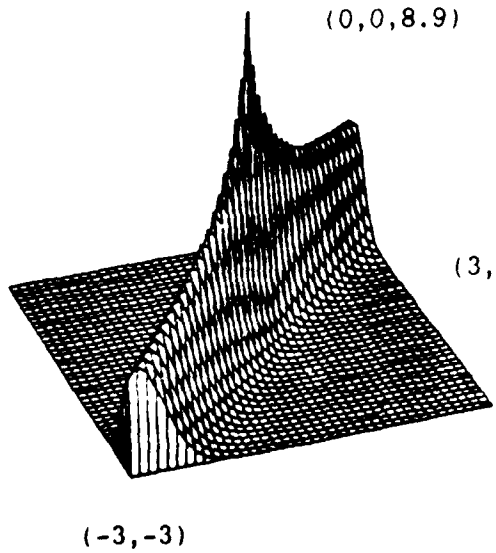

Fig. 7c. Conditional Expo-type pdf, ρ=.95

1.3 True Exponential pdf

The final jpdf to be evaluated is the exponential pdf introduced by Pyati , Eq (3), and it is pictured in Fig. 8. A noticeable distinction of this pdf is that it does not have the circular symmetry at ρ=0. This is simply because at ρ=0 the exponential JPDF reduces to the product of its marginals

$$f^E(\zeta_1,\zeta_2;0) = \frac{1}{4h^2}\exp\left[-\frac{|\zeta_1| + |\zeta_2|}{h}\right] \tag{89}$$

which has constant probability along the $|\zeta_1|+|\zeta_2|$ = C lines, where C is any constant instead of the $\zeta_1^2+\zeta_2^2$= C lines as did the previous two pdf's. The same trend as seen in the other pdf's as ρ approaches one is apparent in Figs. 8b and 8c. Figure 8c is perhaps not as clean as it should be based on the fact that as ρ approaches 1, a large number of the higher ordered modified bessel functions are needed to calculate accurate data points for the exponential pdf. Since each of these modified bessel functions is represented by a truncated infinite series in the computer program that calculated the surface graphs, increased error is present as more terms are needed. The trend, however, is obvious and the fact that this series tends to

$$\begin{aligned} f^E(\zeta_1,\zeta_2;1) &= \delta(\zeta_1-\zeta_2)\ f^E(\zeta_2) \\ &= \delta(\zeta_1-\zeta_2)\ \frac{1}{2h}\exp\left[-\frac{|\zeta_1|}{2h}\right] \end{aligned} \tag{90}$$

as $\rho \to 1$ is verified when the characteristic function of Eq (3) is shown to be equal to 1 at ρ = 1 (see Fig. 12).

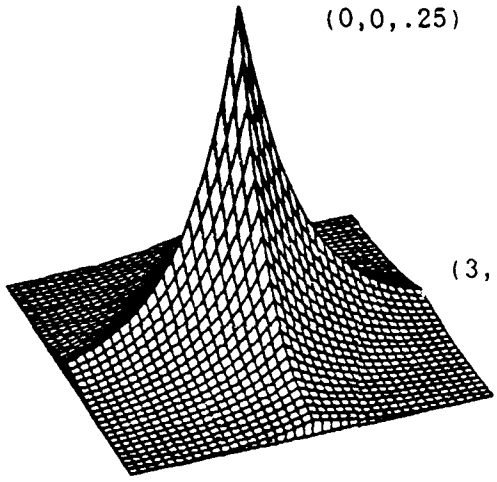

Fig. 8a. Joint Exponential pdf, ρ=0

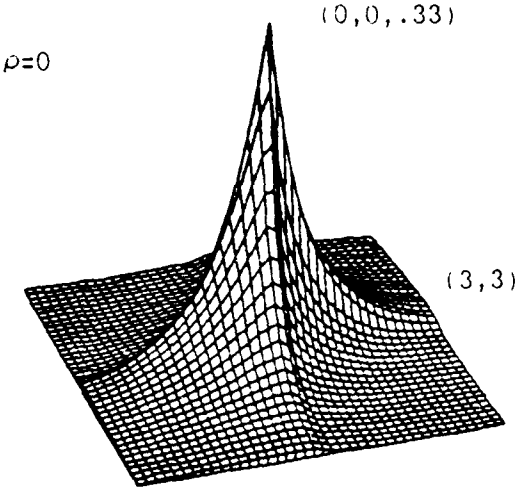

Fig. 8b. Joint Exponential pdf, ρ=.5

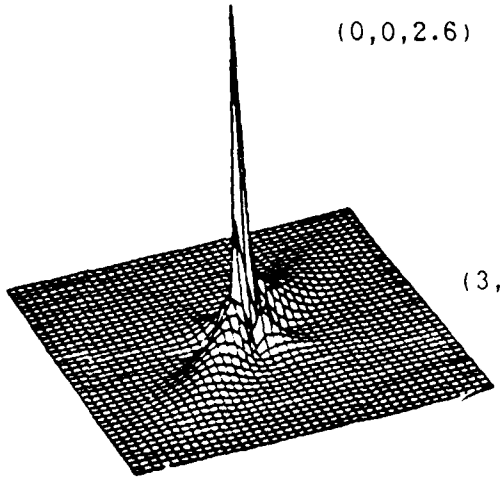

Fig. 8c. Joint Exponential pdf, ρ=.95

The graphs of the conditional probability of ζ_1 given ζ_2 and ρ (Fig. 9) show the necessary condition that when $\rho=0$ the probability of ζ_1 is independent of ζ_2. The above stated relationships as ρ increases are evident in Figs. 9b and 9c within the limits of the numerical inaccuracy stated in the previous paragraph.

In summary, it has been shown that the true exponential JPDF satisfies the condition of decorrelating into statistically independent pdf's while the exponential-type pdf has been shown to be inappropriate for representing rough surfaces.

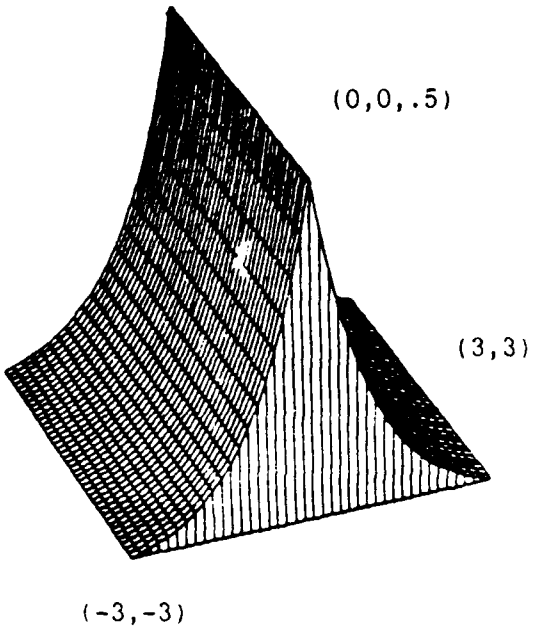

Fig. 9a. Conditional Exponential pdf, ρ=0

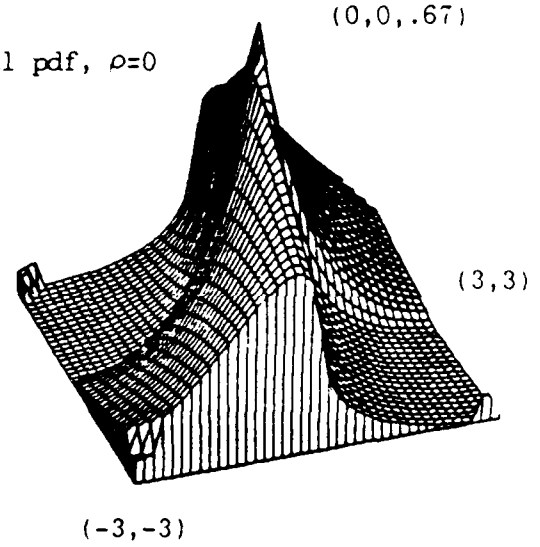

Fig. 9b. Conditional Exponential pdf, ρ=.5

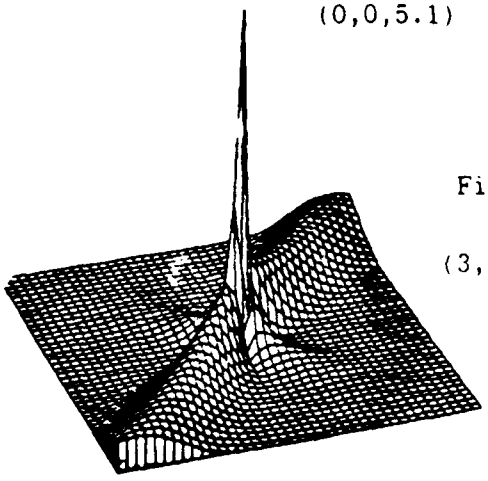

Fig. 9c. Conditional Exponential pdf, ρ=.95

12. RCS's Using Specified Density Functions

In this section the steps required to calculate the average diffuse RCS's per unit area are presented for all three jpdf's. Henceforth the fact that only the diffusely scattered power is being considered will be assumed unless otherwise stated.

2.1 The Characteristic Functions

To calculate the average RCS per unit area of a rough surface given a specific pdf, one must first calculate the characteristic functions of the joint pdf and the one dimensional marginal pdf's. The joint characteristic function of a bivariate pdf is given by [7:428]

$$\Upsilon_2(v_1,v_2) = \langle \exp(jv_1\zeta_1 + jv_2\zeta_2) \rangle \tag{91}$$

Making the backscatter substitution that $v_2 = -v_1 = -v_z$ this becomes

$$\Upsilon_2(v_z,-v_z) = \langle \exp(jv_z\zeta_1 - jv_z\zeta_2) \rangle \tag{92}$$

which, for convenience, will henceforth be referred to simply as the joint characteristic function without reference to the particular arguments. The one dimensional characteristic functions are given by

$$\Upsilon_1(v_z) = \langle \exp(jv_z\zeta) \rangle \quad \text{and} \quad \Upsilon_1^*(v_z) = \Upsilon_1(-v_z) = \langle \exp(-jv_z\zeta) \rangle \tag{93}$$

Before investigating the characteristic functions of specific pdf's several properties of the characteristic function should be noted. The

first involves the case where the two random variables of a joint pdf become completely correlated. In this case ζ_1 approaches the value of ζ_2 and thus Eq.(92) simply approaches the expected value of unity. The second case considered is when the two random variable become completely decorrelated. If the random variables become statistically independent while decorrelated the following relationship holds true

$$\text{Lim}_{\rho \to 0} \; \Upsilon_2(v_z,-v_z) = \langle \exp(jv_z\zeta\,) \rangle \langle \exp(-jv_z\zeta\,) \rangle = \Upsilon_1(v_z)\Upsilon_1^*(v_z) \qquad (94)$$

If the density functions are symmetric about zero, all of the pdf's in this thesis are, then

$$\Upsilon_1(v_z)\Upsilon_1^*(v_z) = \Upsilon_1(v_z)^2 \qquad (95)$$

2.1.1 Gaussian and Exponential-type pdf's

The characteristic equation for the bivariate and monovariate Gaussian pdf's are quite easy to derive and can be found in practically any text book that covers characteristic functions [6:99]

$$\Upsilon_2^G = \exp\left[-h^2 v_z^2 (1-\rho)\right] \text{ and } \Upsilon_1^G = \exp\left[-\frac{h^2 v_z^2}{2}\right] \qquad (96)$$

The characteristic functions of the exponential-type pdf were derived by Papa and Lennon and are given as [15:59]

$$\chi_2^{ET} = \left\{1 + \frac{2}{3} h^2 v_z^2 (1-\rho)\right\}^{-3/2} \tag{97}$$

$$\chi_1^{ET} = \left\{1 + \frac{1}{3} h^2 v_z^2\right\}^{-3/2} \tag{98}$$

Graphs of the one and two dimensional characteristic functions for the Gaussian and exponential-type pdf's are shown in Figs. 10 and 11 respectively. The fact that the exponential-type does not split into statistically independent random variables is obvious from the fact that the two dimensional characteristic function does not approach the value of the one dimensional squared in Fig. 11.

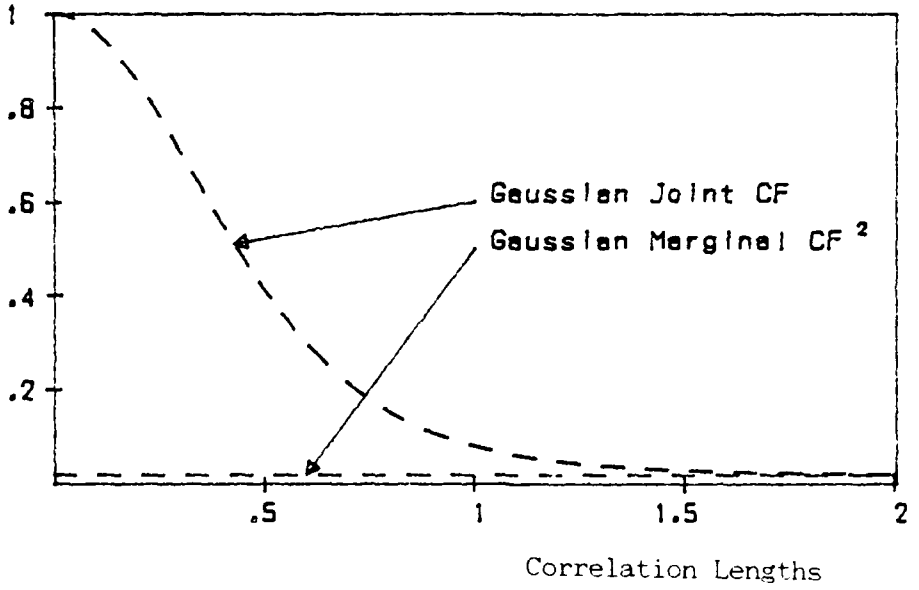

Fig. 10a. Gaussian Joint CF and χ_1^2 as a Function of Correlation Lengths with $h*v_z = 2$

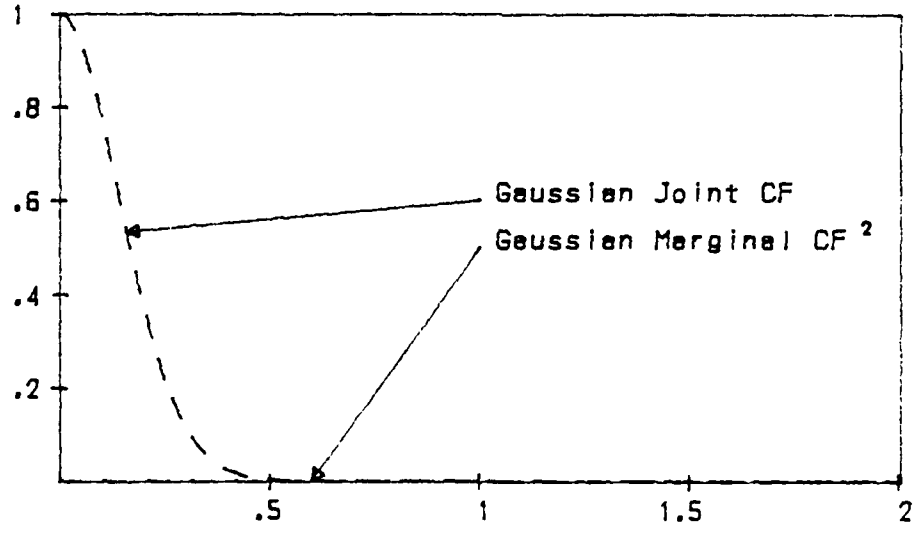

Fig. 10b. Gaussian Joint CF and χ_1^2 as a Function of Correlation Lengths with $h*v_z =$

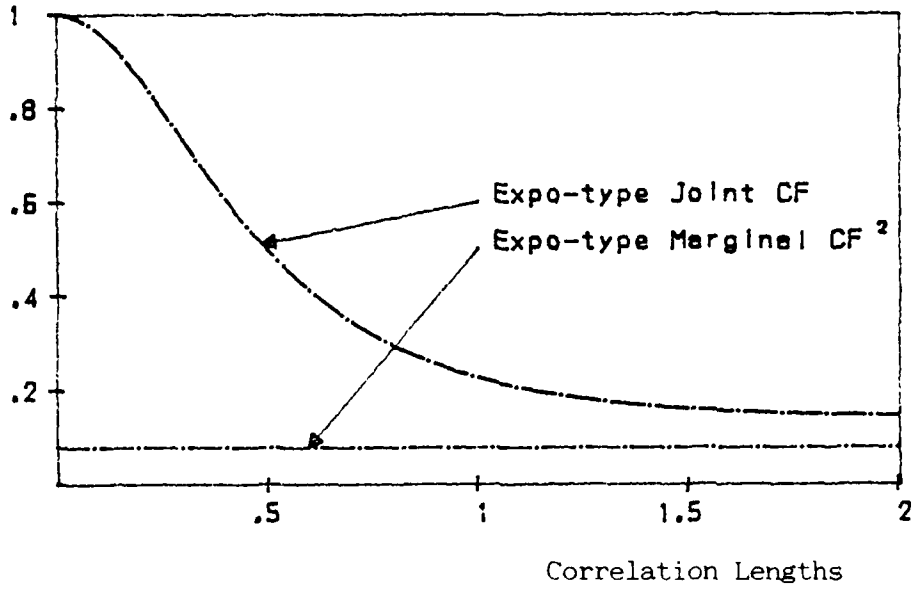

Fig. 11a. Exp-type Joint CF and γ_1^2 as a Function of Correlation Lengths with $h*v_z = 2$

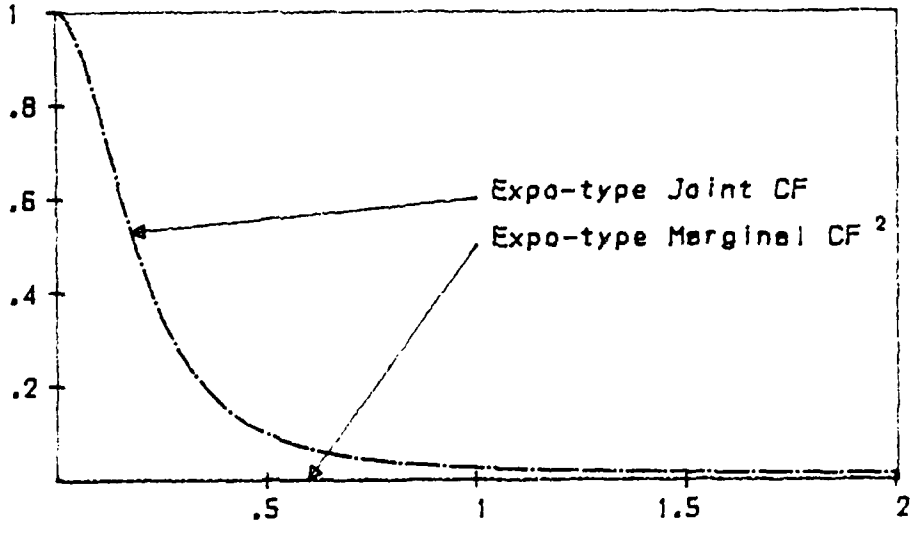

Fig. 11b. Exp-type Joint CF and γ_1^2 as a Function of Correlation Lengths with $h*v_z = 5$

2.1.2 True Exponential pdf

The one dimensional characteristic function for the true exponential is easily calculated to be

$$\chi_1^E = \left[\frac{1}{1 + h^2 v_z^2} \right] \tag{99}$$

Unfortunately, the two dimensional characteristic function is neither as easy to find nor is its final form quite as compact. Because its derivation is lengthy it has been provided in a separate appendix, Appendix A. The solution, arrived at in collaboration with Reif [19] and with the assistance of thesis advisors Pyati and Baker, is given by Eq (A-37) which contains two infinite series.

Obviously, one would prefer to have the solution given in closed form. Appendix B, also derived with those named above, gives a closed form solution for the first series of the total solution. The geometric series identity used to get a closed form solution for the first series cannot be applied to the second series. The most that could be done with the second infinite series was to approximate it by a finite series and a remainder term. This approximation can be found in Appendix C.

Figure 12 was generated by incorporating the contents of Appendixes A through C into the program MAIN2.BAS (see Appendix D) which calculates values of the two dimensional characteristic function. All three characteristic functions are shown together in Fig. 13 using the value $hv_z = 10$.

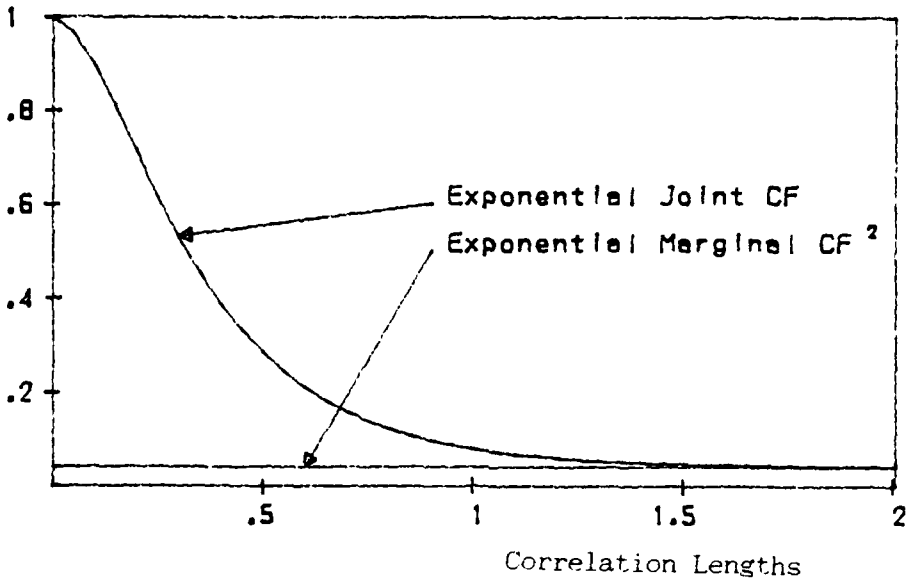

Fig. 12a. Exponential Joint CF and χ_1^2 as a Function of Correlation Lengths with $h*v_z = 2$

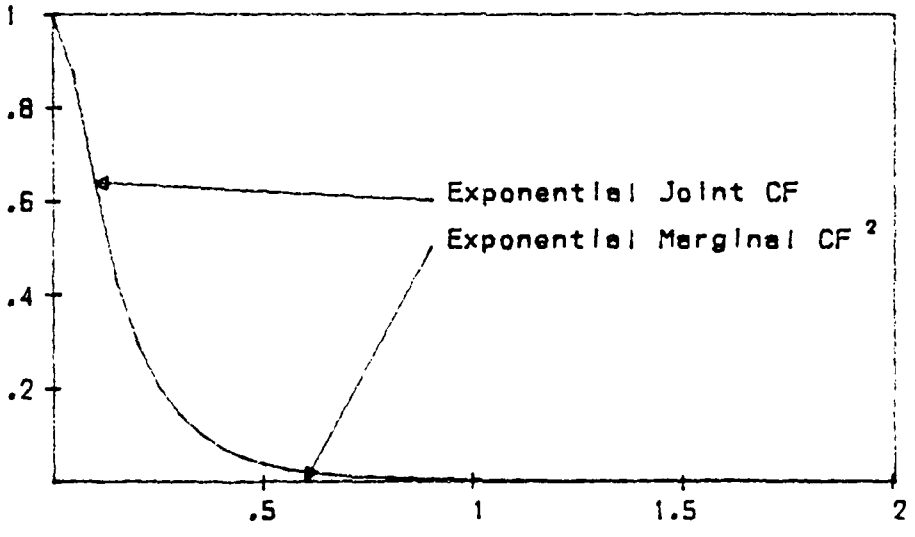

Fig. 12b. Exponential Joint CF and χ_1^2 as a Function of Correlation Lengths with $h*v_z = 5$

2.2 Performing the Final Integration

Having computed the characteristic functions for the pdf's all that remains is to perform the integration of Eq (78). Closed form solutions to Eq (78) have been found in the past for the Gaussian and exponential-type pdf's where the surface is assumed to be very rough using the method of stationary phase. Very rough in this case means that the square of the one dimensional characteristic function is essentially zero and the power is diffusely scattered. From reviewing Figs. 10 through 13, this means that the product $h*v_z$ should be at least 5 for the Gaussian pdf and somewhat larger than 5 for the exponential-type pdf. By assuming this condition, the square of the one dimensional characteristic function need not be subtracted from the two dimensional characteristic function thus making the stationary phase integration much easier. Under this condition, the diffuse scattering contribution to the average RCS per unit area of a surface represented by the joint Gaussian pdf is given by [20:724]

$$\langle RCS \rangle_D^G = \frac{\sec^4(\theta)}{s^2} \exp\left[- \frac{1}{s^2} \tan^2(\theta) \right] \tag{100}$$

where s^2 is the mean squared surface slope given by $4h^2/\ell^2$. ℓ being the correlation length of the surface. (A more detailed explanation of the mean squared surface slope term can be found in Reif [19]).

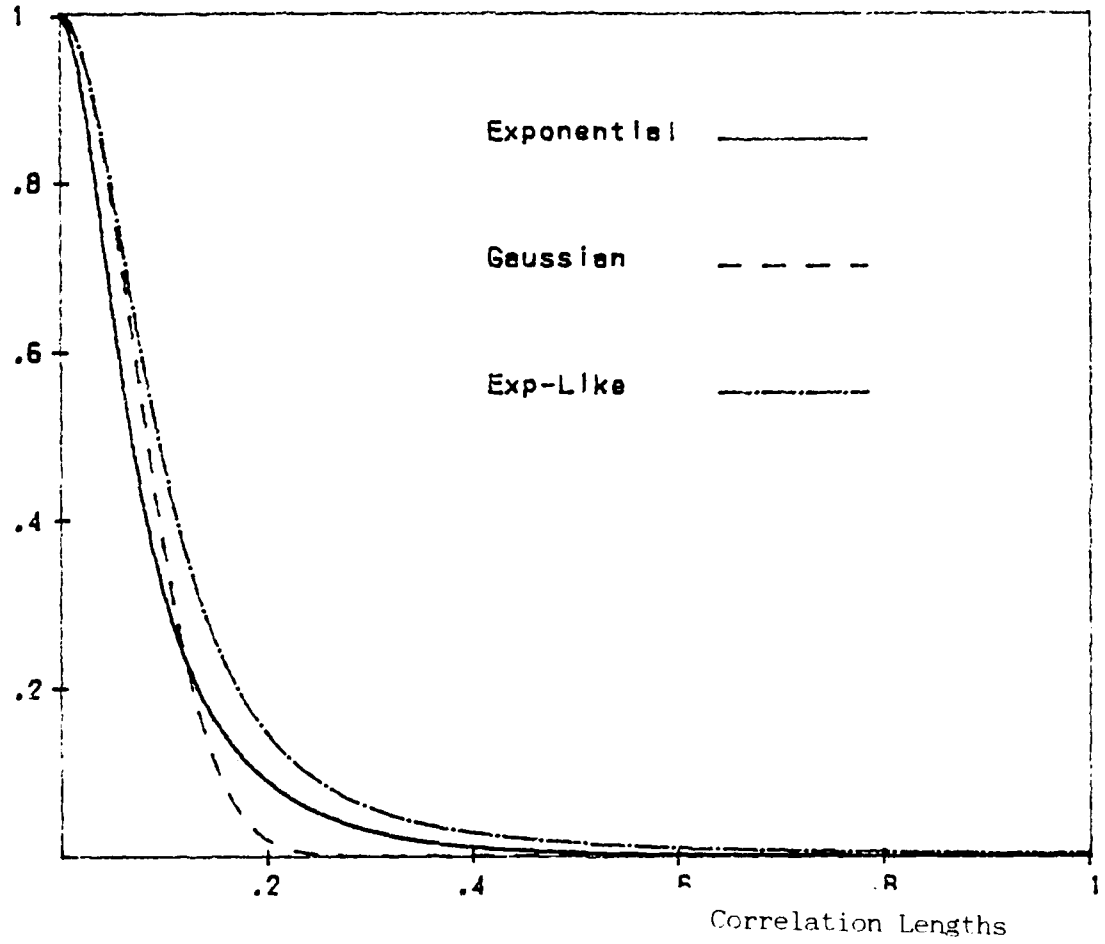

Fig. 13. Characteristic Functions $\chi_2(10,-10)$

For the exponential-type pdf, the diffuse power contribution to the average RCS is given by [20:725]

$$\langle RCS \rangle_D^{ET} = \frac{3\sec^4(\theta)}{s^2} \exp\left[- \frac{\sqrt{6}}{s^2} \tan(\theta) \right] \qquad (101)$$

It should be noted that Eqs (100) and (101) are valid only for very large values of $h*v_z$ since the method of stationary phase (a high frequency asymptotic technique) was used to perform the integrations. This masks the problems associated with the exponential-type jpdf. The associated graphs of Eqs (100) and (101) are given in Figs. 14 and 15 respectively.

A better physical understanding of Figs. 14 and 15 can be obtained from considering a few ray optics arguments. As a plane wave impinges normal to the mean of a randomly rough surface, the rays will be scattered in random directions (diffusely). The rays scattered in any given direction can be attributed to scattering from the specular points for that direction. Increasing the roughness of the surface by increasing h does not change the number or position of the specular points. It does, however, decrease the principle radii of curvature (R_1 and R_2) of those points. Since the RCS of an object using specular point theory is given by RCS = $\pi R_1 R_2$ [10:119] this obviously will decrease the average RCS of the surface. The rougher the surface is, the smaller the radii of curvature these specular points will have. Therefore, an increase in roughness reduces the normal backscatter.

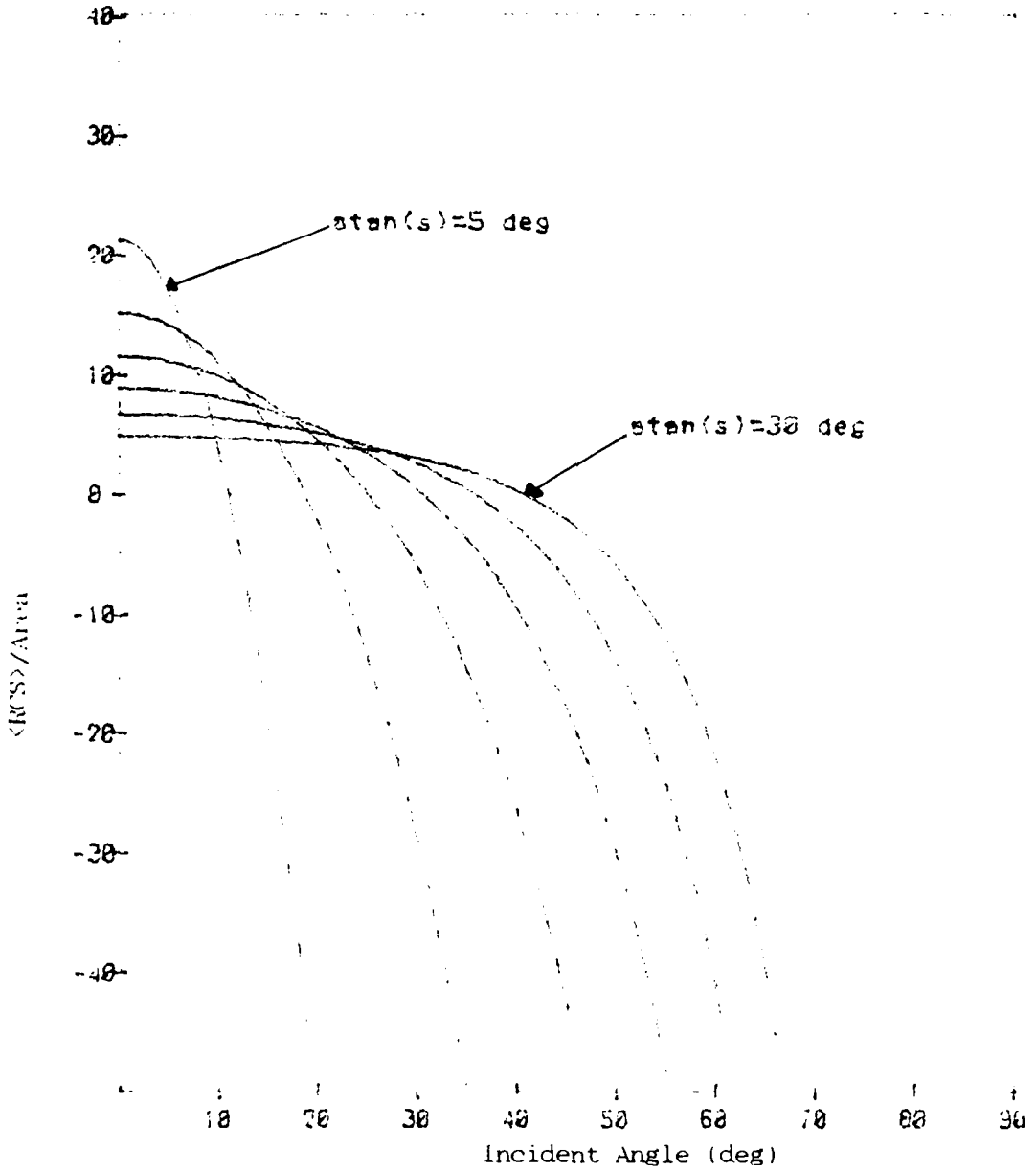

Fig. 14. <RCS>/Area for a Gaussian Surface as a Function of Incident Angle with 5 deg Mean Surface Slope Steps

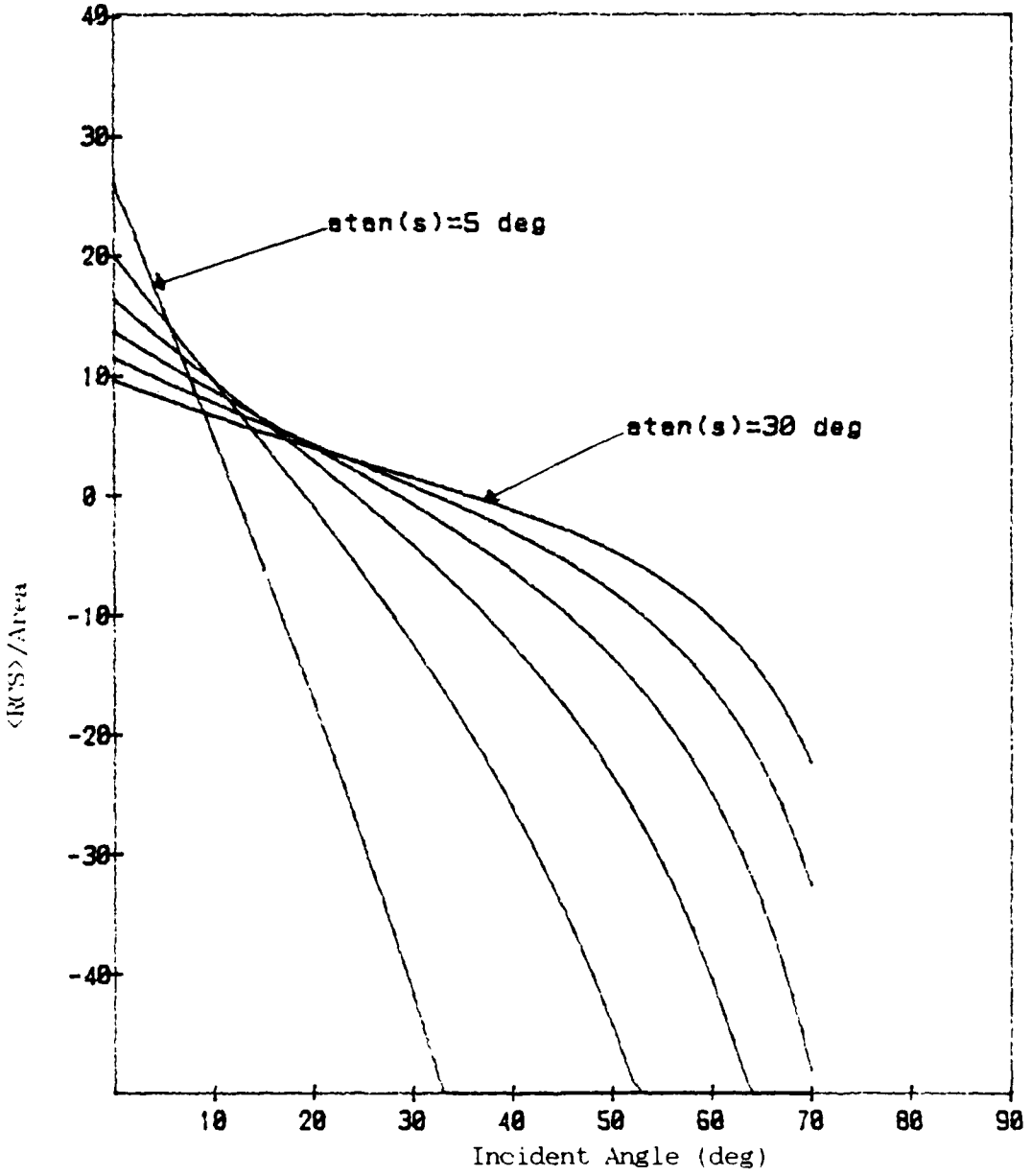

Fig. 15. <RCS>/Area for an Exponential-type Surface as a Function of Incident Angle with 5 deg Mean Surface Slope Steps

As the angle of incidence is increased, the number of specular points is decreased. If the surface is only slightly rough, it is highly unlikely that there will be specular points for angles of incidence other than those near zero. The rougher the surface, the more likely it is that there will be specular points at higher angles of incidence. (It should also be remembered that the rougher the surface is, the greater will be the effects of shadowing which is not accounted for in these figures.) For more on the specular theory of rough surface scattering one can refer to [4], Reif [19] is a good source for the shadowing theory.

Before taking on the task of performing the numerical integration of Eq (78) with data points of the exponential characteristic functions, the behavior of the elements of the integrand should be analyzed with respect to their possible effects on the integration. Keeping in mind what must be done in a numerical integration, it is seen that to reproduce solutions such as those in Figs. 14 and 15, one must successively solve the integral for discrete values of the mean surface slope and at discrete angles of incidence. The variables that change as these parameters change are h, v_z and v_x while the correlation length, ℓ, is kept constant. (The correlation length is set to 1 throughout this thesis.) Two of these variables, h and v_z are arguments of the characteristic functions. Because of the length of time it takes to calculate data points for the exponential characteristic function (To generate the 5001 data points that were eventually used in the integration it took 56 hours.) one must find a way of using only one set of data points from the characteristic function and scaling the other

parameters accordingly. Fortunately, h and v_z only appear as the dimensionless parameter $h*v_z$ within the characteristic function. Therefore, the goal can be accomplished by letting $h*v_z$ equal some constant.

To keep $h*v_z$ constant for any given mean surface slope as the angle of incidence changes, the following must hold:

$$h*v_z = 2k\cos(\theta) = C \tag{102}$$

$$\therefore \quad k = \frac{C}{2h\cos(\theta)} \tag{103}$$

where C is the yet to be determined constant. Fortunately, as can be seen by reviewing Eqs (100) and (101), the $\langle RCS \rangle_D$ is not a function of k as long as k is large enough so that the one dimensional characteristic functions can be ignored. From Fig. 13 it would appear that letting C = 10 is sufficiently large, therefore 10 will be the value used. The use of C = 10 as a high enough number will also be confirmed by the accuracy with which the numerical integration of the <RCS> integral reproduces the stationary phase result for the Gaussian surface.

It is seen from Eq (103) that as the angle of incidence increases, the value of k to be used in the integration increases. This causes the constant portion of the Bessel function argument in Eq (78) to be increased. This in turn increases the frequency of the Bessel function. Figure 16 illustrates this relationship. The fact that it is the increased cancellation between the positive and negative portions of the

high frequency Bessel function that cause the RCS to go to zero emphasizes the necessity to use enough data points in the integration. When the angle of incidence is held constant and the mean surface slope is increased, the result is a decrease in the wave number. The effects of this relationship are shown in Fig. 17.

Since the characteristic functions for the Gaussian and exponential pdf's are not dramatically different, one might assume that the same number of data points required to integrate Eq (78) using the Gaussian CF would be adequate to integrate the exponential. By incrementally increasing the number of data points used to do such an integration, it was found that with $h*v_z = 10$ that 5001 data points evenly spaced from 0 to 1 correlation length (that is, .0002 correlation lengths apart) produced adequate results. These results are shown in Fig. 18. Overlaying this graph and the graph of the stationary phase solution of the integral, it is found that the values are exactly correct until they get down into the -20 dBsm region where they obviously deviate from the stationary phase solution.

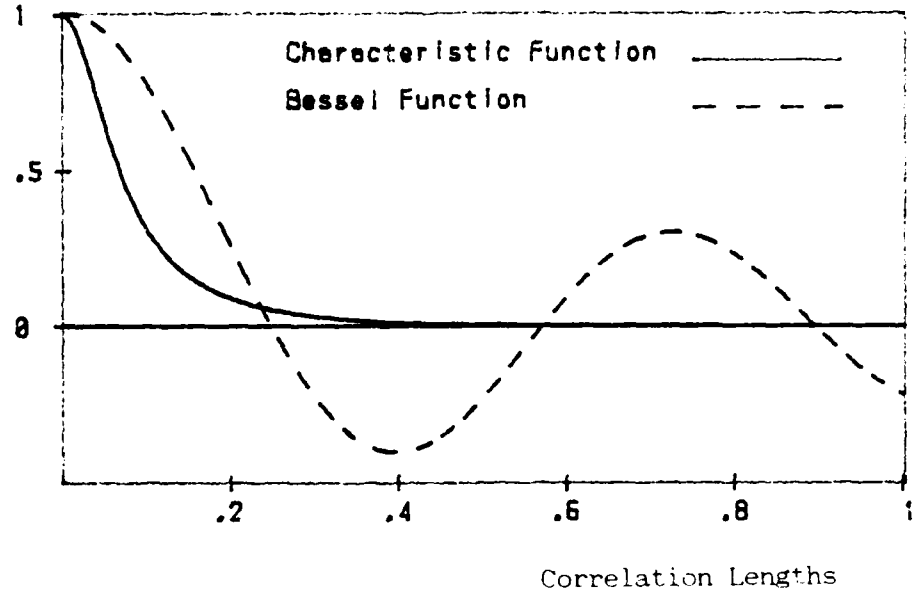

Fig. 16a. Exponential CF, $h*v_z = 10$, atan(s) = 20°

Angle of Incidence = 10°

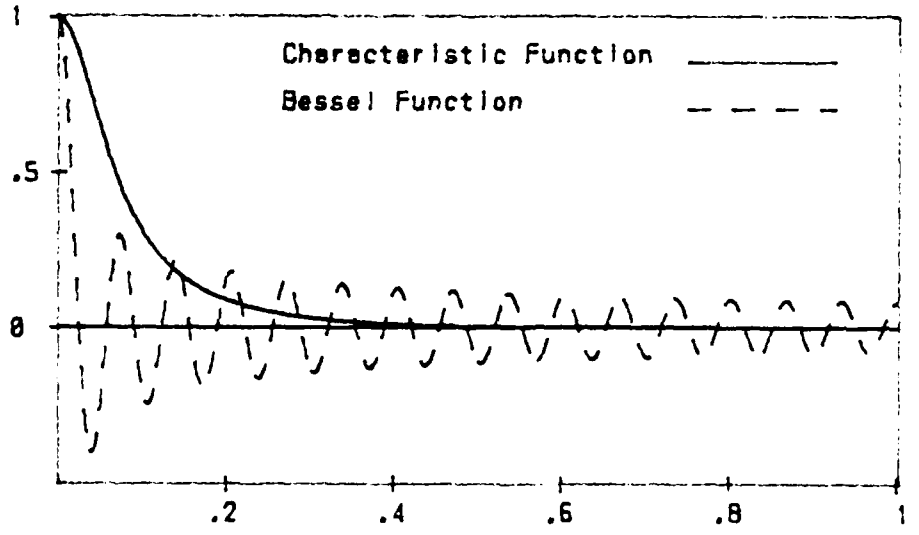

Fig. 16b. Exponential CF, $h*v_z = 10$, atan(s) = 20°

Angle of Incidence = 60°

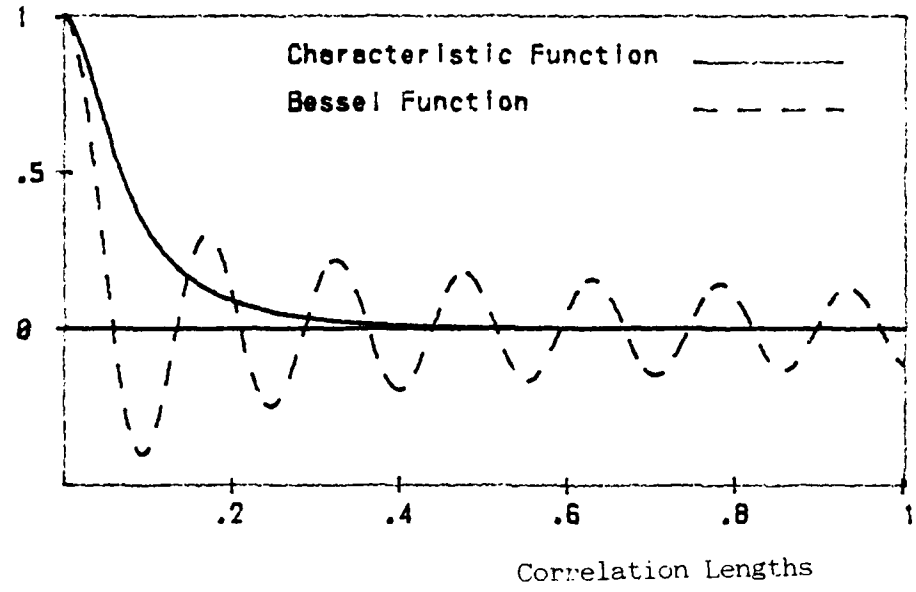

Fig. 17a. Exponential CF, $h*v_z = 10$, atan(s) = 10^o

Angle of Incidence = 20^o

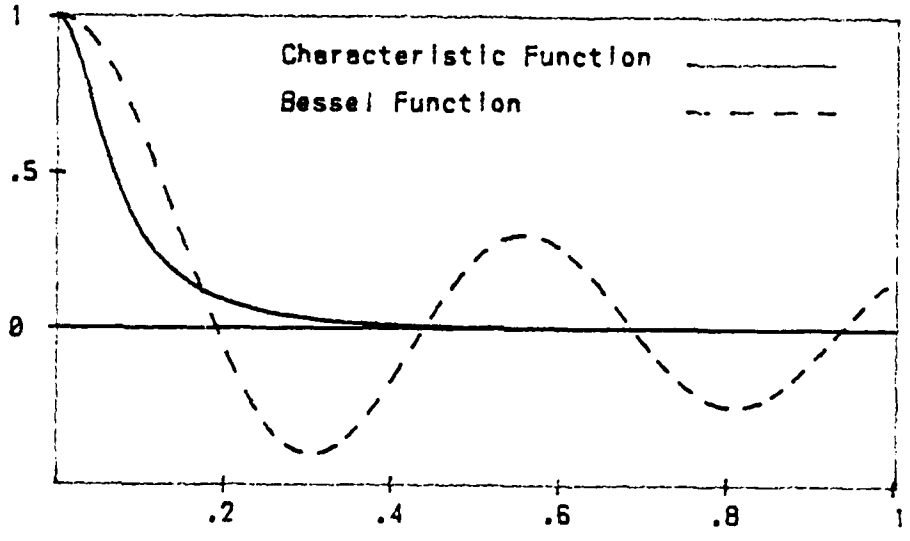

Fig. 17b. Exponential CF, $h*v_z = 10$, atan(s) = 30^o

Angle of Incidence = 20^o

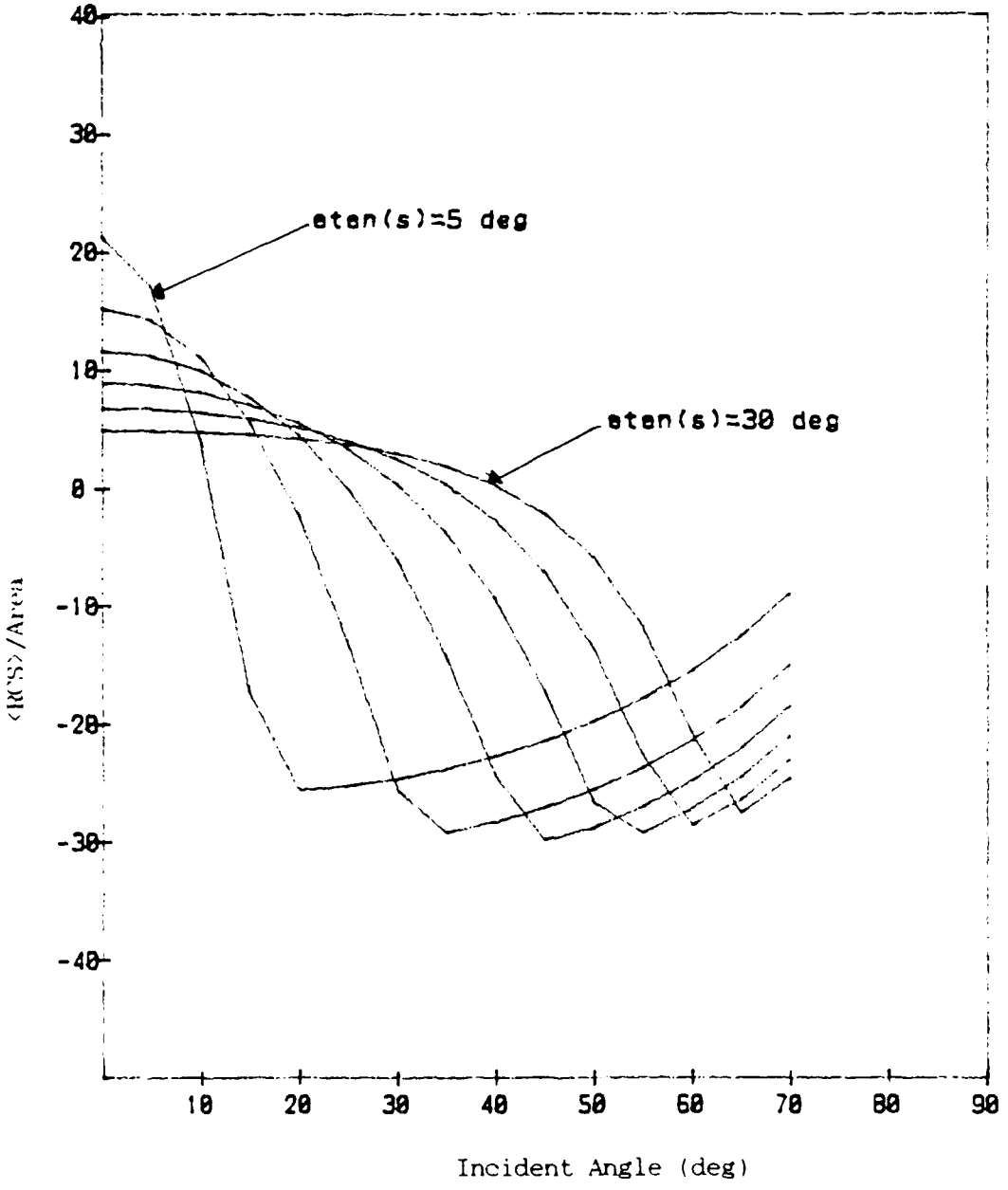

Fig. 18. Numerically Computed <RCS>/Area for a Gaussian Surface as a Function of Incident Angle with 5 deg Mean Surface Slope Steps

Creating the 5001 data points for the integration proved to be no trivial task. As stated earlier, every attempt was made to minimize the number of calculations required to produce this exponential CF data (see Appendixes A-C). Finally, the program MAIN2.BAS was written to crunch the numbers. It was soon realized that running this program on the basic IBM PC, even in compiled TurboBASIC, would place the run time of the program dangerously close to the mean time between failures of the computer. The computer was therefore enhanced with a faster CPU and a numerical coprocessor. This increased the speed of the calculations by a factor of 8 allowing the data file to be built in only 56 hours of continuous run time. After completing the data file, program RCS2.BAS was run to perform the integration using a Simpson's integration scheme. The results of these integrations were then multiplied by $\sec^2(\theta)$ to produce Fig. 19.

Figure 19 gives the average RCS per unit area of a very rough surface represented by the true exponential pdf. It is interesting to note that it does indeed resemble the graph of the exponential-type results in shape. This is the only similarity though, as overlaying the graphs clearly shows that the values are not the same. The RCS of the true exponential surface is lower at normal incidence and falls off much slower than that of either the exponential-like or Gaussian surfaces.. This indicates that the true exponential surface is a rougher surface given the same surface height variance (h^2). In the next section, computer generated surfaces will show this to be true but for now this argument will be supported by simply looking at a comparison of the pdf's.

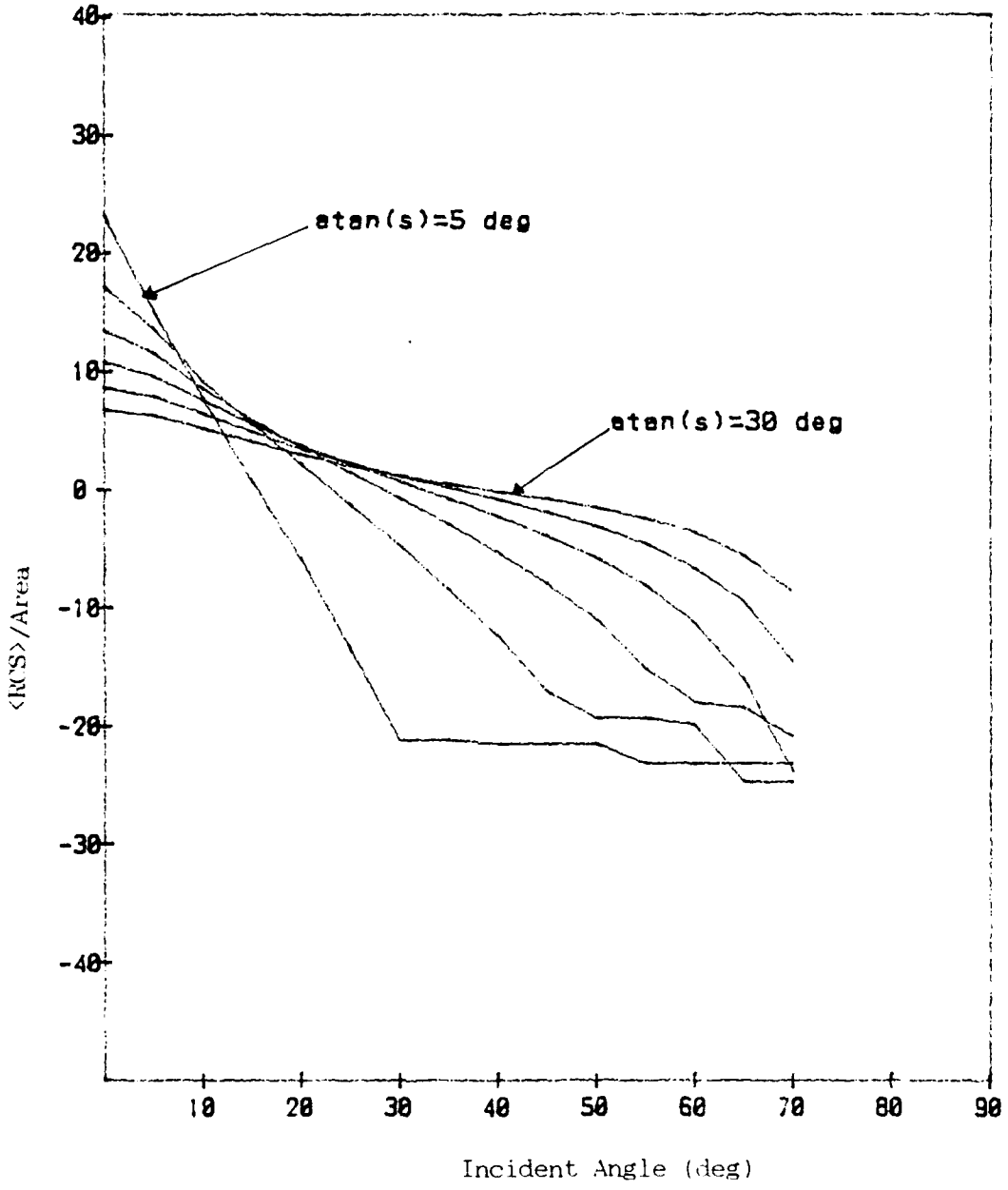

Fig. 19. Numerically Computed <RCS>/Area for an Exponential Surface as a Function of Incident Angle with 5 deg Mean Surface Slope Steps

3. Summary

In this section some of the properties of the Gaussian, exponential-type and the exponential joint probability density functions were investigated along with some of the related properties of their characteristic functions. It was shown that upon decorrelation the Gaussian and exponential random variables become statistically independent. It was also shown that the exponential-type jpdf lacks this property and is therefore not suitable as a rough surface model.

In support of the <RCS> results found for the different jpdf surface representations one can refer to Figures 4, 6 and 8 all of which were generated with the variance set equal to one. Although the scale of the graphs are all different (this was done to maintain constant size for the graphs) it is obvious that the exponential-like and the Gaussian pdf's go to zero much faster than does the exponential. This indicates that the exponential surface will have higher peaks on its surface than will the other surfaces. This in turn will give the exponential surfaces smaller specular points distributed over a larger range of angles. Referring back to the specular point arguments for the way the RCS of a rough surface acts, this supports the findings presented in Figs. 14, 15 and 19.

Part B

Part A of this section dealt with mathematically predicting the average diffuse RCS of a surface given that the surface was represented by specific probability density functions. The only way to check such calculations would seem to be to check them against RCS measurements made on real surfaces that obey such statistics. Most surfaces in nature, however, have many different degrees and types of roughness superimposed upon one another. Therefore, surfaces that conform to a single statistical representation are not easily found. (Two references that address this topic are [13] and [18].) An alternative given in this section to real RCS measurements is computer predicted RCS's of computer generated rough surfaces that meet the proper statistics.

In this section, random rough surfaces that obey Gaussian and exponential statistics will be generated by computer. The RCS of these surfaces will then be calculated for different combinations of mean surface slopes and $h*v_z$. These results will then be graphed and compared with the predicted results from Part A.

1. The Generation of Random Rough Surfaces (Background)

The technique for producing random rough surfaces is borrowed from Harnly and Jensen [9] where it was used to create spatially correlated infrared noise. Harnly and Jensen, developed this technique under the guidance of AFIT faculty member Dr. Peter Maybeck. The only modification to the technique is one of interpretation. That is, instead of creating spatially correlated noise, one is now finding spatially correlated surface heights.

Spatially correlated surface heights can be generated from a vector of uncorrelated surface heights from the equation

$$\bar{Z}(t_i) = {}^{c}\sqrt{\bar{R}}\ \ \bar{W}(t_i) \tag{104}$$

where $\bar{Z}(t_i)$ is a vector of dimension N^2, each element of which represents the surface height at an individual point of a grid numbered as in Fig (20).

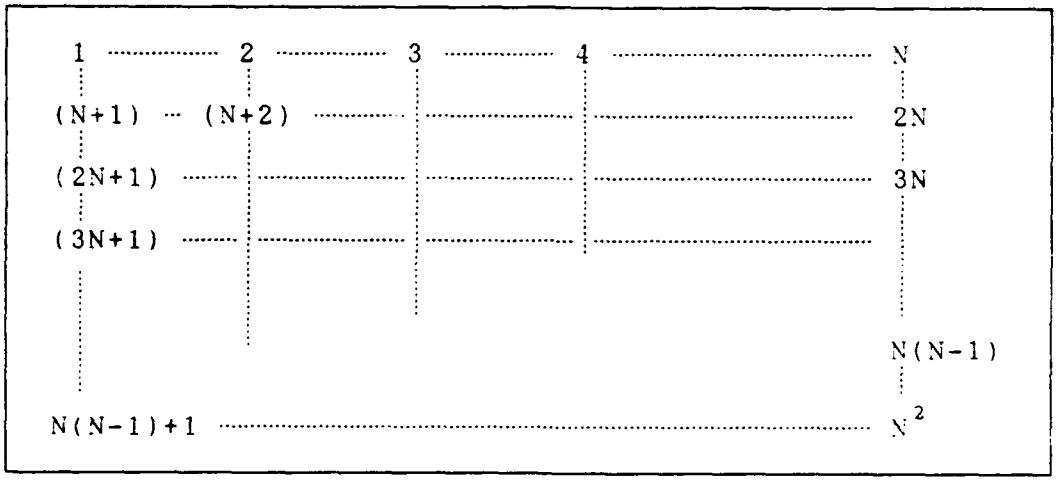

Fig. 20. Grid for Computer Generated Surfaces

$\bar{W}(t_i)$ is an N^2 dimensional vector of uncorrelated surface heights and ${}^{c}\sqrt{\bar{R}}$ is the Cholesky square root of the correlation matrix. The surface heights of two points within the above grid will become statistically independent as the correlation coefficient between the two points goes to zero.

The correlation matrix is simply an $N^2 \times N^2$ matrix, each element of which represents the correlation coefficient between a point (j) and a point (k) where (j) and (k) index from 1 to N^2 [7:366]. The correlation matrix is given by

$$\bar{R} = \begin{bmatrix} 1 & \rho_{1,2} & \rho_{1,3} & \rho_{1,4} & \cdots & \rho_{1,N^2} \\ \rho_{2,1} & 1 & \rho_{2,3} & \cdots & \cdots & \rho_{2,N^2} \\ \rho_{3,1} & \rho_{3,2} & 1 & \cdots & \cdots & \vdots \\ \rho_{4,1} & \cdots & \cdots & 1 & \cdots & \vdots \\ \cdots & \cdots & \cdots & \ddots & \ddots & \vdots \\ \rho_{N^2,1} & \rho_{N^2,2} & \rho_{N^2,3} & \cdots & \cdots & 1 \end{bmatrix} \tag{105}$$

For the purposes of this thesis, a Gaussian correlation coefficient is used. Therefore

$$\rho_{j,k} = \exp\left(-d_{j,k}^2 / \ell^2\right) \tag{106}$$

where $d_{j,k}$ is the distance between points j and k. Obviously, it then follows that $\rho_{j,j} = 1$ and $\rho_{j,k} = \rho_{k,j}$. Also, as the distance between two points gets large, the correlation coefficient will go to zero and the points will be statistically independent. The extreme example of this would be a grid for which even the adjacent points were very far apart. Under this condition the correlation matrix would simply be the identity matrix which has off diagonal terms of zero and diagonal terms equal to one. In such a case Eq (104) simply gives $\bar{Z}(t_1) = \bar{W}(t_1)$.

The elements of the Cholesky square root matrix are generated sequentially, row by row, from the recursion: for i=1,2,...N^2 compute [12:371]

$$\alpha_{ij} = \begin{cases} \dfrac{1}{\alpha_{jj}} \left[\rho_{ij} - \sum_{k=1}^{j-1} \alpha_{ik} * \alpha_{jk} \right] & j = 1,2,3,\ldots,i-1 \quad (107) \\ \sqrt{\rho_{ii} - \sum_{k=1}^{i-1} \alpha_{ik}^2} & j = i \quad (108) \\ 0 & j > i \quad (109) \end{cases}$$

where the α's are the elements of the Cholesky square root matrix and the ρ's are the correlation matrix elements.

As stated, the vector $\bar{W}(t_i)$ is simply N^2 uncorrelated surface heights produced by any valid one dimensional pdf. This is extremely convenient since one dimensional pdf's are easy to come by. Surfaces can then be generated which follow Gaussian statistics, exponential statistics or even uniform or Raleigh statistics if one so desired.

The program that will be used to calculate the RCS of the generated surfaces is written in Fortran and resides on a VAX-11/785 which is owned by AFWAL. Therefore, the programs that generate the surfaces were written in Fortran on the same computer. The following programs were written for this purpose

CORCOEFF: Given the horizontal distance between surface points and the number of points in a row,

this program calculates the total distance between each point and creates a file containing the correlation matrix.

CHOLESKY: Given a correlation matrix file, this program creates the lower triangular Cholesky square root of it and places it in a file.

GESURF: Given a Cholesky square root file, this program creates the $\overline{W}(t_i)$ vector and then the $\overline{Z}(t_i)$ vector which represents the rough surface. The surfaces generated by this program have a surface height variance of one. The variance of these surfaces can be changed by simply multiplying the existing heights by the square root of the variance, h.

Each of these programs is listed in the Appendix D.

The diagonal terms in the Cholesky decomposition algorithm get increasingly smaller as the size of the correlation matrix increases and the horizontal distance between points increases. Roundoff error then comes into play and can cause the term within the square root sign on Eq (108) to become negative which should not happen for the positive definite correlation matrices presented in this thesis. This limits the the size of the surfaces that can be generated. Trial and error showed that square surfaces could be generated that were a total of 4.2 correlation lengths long and had 15 rows and columns of surface heights each separated by .3 correlation lengths. The generated surfaces are shown in Figs. E1 through E20 of Appendix E along with the RCS information for each surface.

2. The RCS Program

The program used to calculate the RCS of the computer generated surfaces, the Radar Cross Section-Basic Scattering Code (RCS-BSC), was provided by AFWAL/AAWP-3. The code itself was written at Ohio State University's Electroscience Laboratory under the supervision of Ronald Marhefka [11]. Although the RCS-BSC has capabilities well beyond that of just providing physical optics predictions for perfectly conducting bodies, only the option which makes these assumptions was used since the calculations in Part A are based upon these assumptions.

Two minor problems had to be overcome before the RCS-BSC could be run against the generated surfaces. First, the RCS-BSC could only handle objects represented by a maximum of 50 plates with a maximum of 40 sides per plate. In addition, the code does not allow plates to be concave. That is, all of the corners of the plates must be in the same plane. The surfaces generated are made up of 196 plates, each with 4 sides, none of which are planar. Therefore RCS-BSC had to be modified to allow objects to be represented by more plates. This was simply a matter of plodding through the program and changing the appropriate dimension statements. Since no more than four sides per plate were needed, it was possible to increase the number of plates the program could handle while decreasing its memory requirement by redimensioning the plate geometry array to 400 × 4. The problem of concaveness was solved by representing each square plate as two triangles since triangles are planar by definition. This would have allowed the redimensioning of the arrays to allow only three sides instead of four but this was not done since computer memory availability was not a

problem and since the redimensioning to allow up to 400 plates had already been accomplished. Since each of the 196 squares was now represented by 2 triangles, 382 of the 400 allowable plates were used.

To finally calculate the RCS of the surfaces, files needed to be generated that set the proper control parameters for RCS-BSC and placed the surface height data in the proper format. Program BUILD.FOR accomplished this chore. In addition, since a single run of RCS-BSC against a surface took 27 CPU minutes on the VAX, batch files had to be written to run the code after hours.

As mentioned, the run time of the program was a concern. Even limiting the RCS calculations to 5 degree increments between 0 and 90^{o} the calculation of a single pattern took 27 CPU minutes. Therefore, only a limited number of surface RCS calculations could be run. The final series of runs consisted of 10 Gaussian surfaces and 10 exponential surfaces. The heights of these surfaces was scaled so that each had mean surface slopes of 5^{o} and 25^{o}. The RCS of each of these surfaces was in turn calculated at 5.46 Ghz and 17 Ghz so that the pattern could be compared as a function of the wavenumber k. The RCS's calculated for each surface are given in the tables associated with each surface in Appendix E.

Having completed all the runs, the RCS's were averaged at the discrete angles of incidence. To average the RCS's of the surfaces, each RCS was first converted to square meters. The average of the RCS's was then calculated in square meters and then transformed into dBsm. Tables II and III give the results of this process along with the physical optics solution for the RCS of a flat plate at each point.

These results are also graphed in Figs. 21 through 24. The RCS's of the flat plates are provided so that one may see that the diffuse scattering does indeed fill the nulls of the coherent pattern and decreases the the peaks of the pattern.

The results of this experiment show excellent agreement with the predicted results. The selected combinations of mean surface slopes and frequency assured that $hk > 5$ for all measurements. Therefore, as stated in Part A, the scattered power should be primarily diffuse and independent of frequency. Comparison of the results shows that frequency independence. In addition, comparison of Figs. (21) through (24) with Figs. (18) and (19) show excellent agreement between the behavior of the average RCS as a function of mean surface slope and incident angle as well as good agreement between the actual RCS values and the predicted RCS values at small angles of incidence.

TABLE II

<RCS>/Area for Gaussian Surfaces (dBsm)

Ang	Gaussian				Flat	
	atan(s)=5		atan(s)=25			
	hk=5	hk=27	hk=16	hk=83	k=114	k=357
0	23.46	22.83	8.45	4.53	36.20	46.08
5	15.39	15.62	8.06	6.84	10.55	5.64
10	7.11	5.00	8.19	5.08	8.73	7.54
15	-1.81	-4.40	4.73	2.44	6.25	6.13
20	-5.73	-10.11	5.02	6.12	3.74	-3.96
25	-6.29	-14.55	4.42	2.49	1.18	-20.52
30	-8.86	-13.96	4.53	1.68	-4.28	-5.54
35	-11.76	-18.11	0.56	0.66	-11.69	-7.33
40	-11.22	-17.26	0.20	1.84	-3.75	-20.65
45	-13.65	-18.83	-3.02	-5.96	-8.26	-5.93
50	-13.44	-17.99	-7.81	-10.40	-17.30	-22.52
55	-18.15	-18.83	-11.53	-17.57	-14.49	-19.59
60	-14.01	-21.62	-16.34	-21.17	-9.85	-10.08
65	-22.19	-24.07	-16.68	-22.04	-37.22	-41.25
70	-18.01	-25.53	-17.36	-24.74	-17.25	-17.77
75	-21.28	-24.42	-22.84	-25.01	-21.47	-19.83
80	-26.70	-19.06	-21.20	-24.09	-28.48	-31.13
85	-26.84	-33.80	-20.46	-19.84	-28.15	-30.60
90	-32.05	-32.58	-17.56	-17.98	-99999	-99999

TABLE III

<RCS>/Area for Exponential Surfaces (dBsm)

Ang	Exponential				Flat	
	atan(s)=5		atan(s)=25			
	hk=5	hk=27	hk=16	hk=83	k=114	k=357
0	20.00	19.45	4.51	7.65	36.20	46.08
5	15.08	13.28	5.12	1.05	10.55	5.64
10	5.89	4.11	6.13	4.50	8.73	7.54
15	-4.59	-6.01	2.63	4.05	6.25	6.13
20	-8.32	-11.13	1.90	1.59	3.74	-3.96
25	-8.47	-14.14	0.59	1.87	1.18	-20.52
30	-13.55	-16.54	1.36	0.71	-4.28	-5.54
35	-16.08	-18.42	2.38	2.21	-11.69	-7.33
40	-16.60	-19.28	-3.03	0.20	-3.75	-20.65
45	-18.16	-23.18	-3.59	-3.06	-8.26	-5.93
50	-18.19	-22.71	-8.42	-10.08	-17.30	-22.52
55	-21.28	-25.32	-15.82	-19.25	-14.49	-19.59
60	-18.36	-23.92	-17.51	-20.75	-9.85	-10.08
65	-22.68	-29.15	-16.41	-24.63	-37.22	-41.25
70	-20.00	-26.81	-21.88	-22.91	-17.25	-17.77
75	-23.00	-28.57	-22.79	-23.12	-21.47	-19.83
80	-28.01	-22.40	-23.33	-27.80	-28.48	-31.13
85	-27.23	-32.65	-19.98	-23.81	-28.15	-30.60
90	-32.82	-30.64	-18.50	-16.06	-99999	-99999

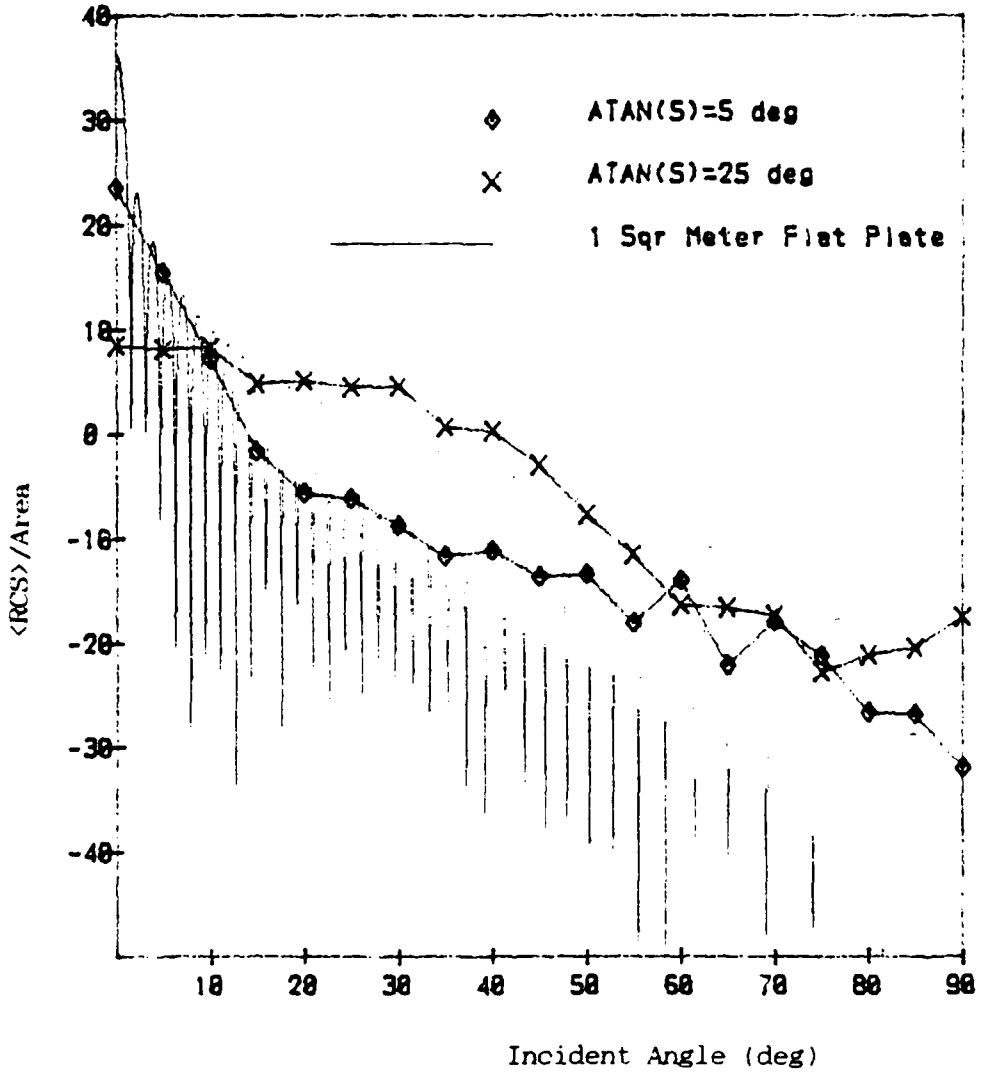

Fig. 21. <RCS>/Area for Computer Generated Gaussian Surfaces at 5.46 Ghz

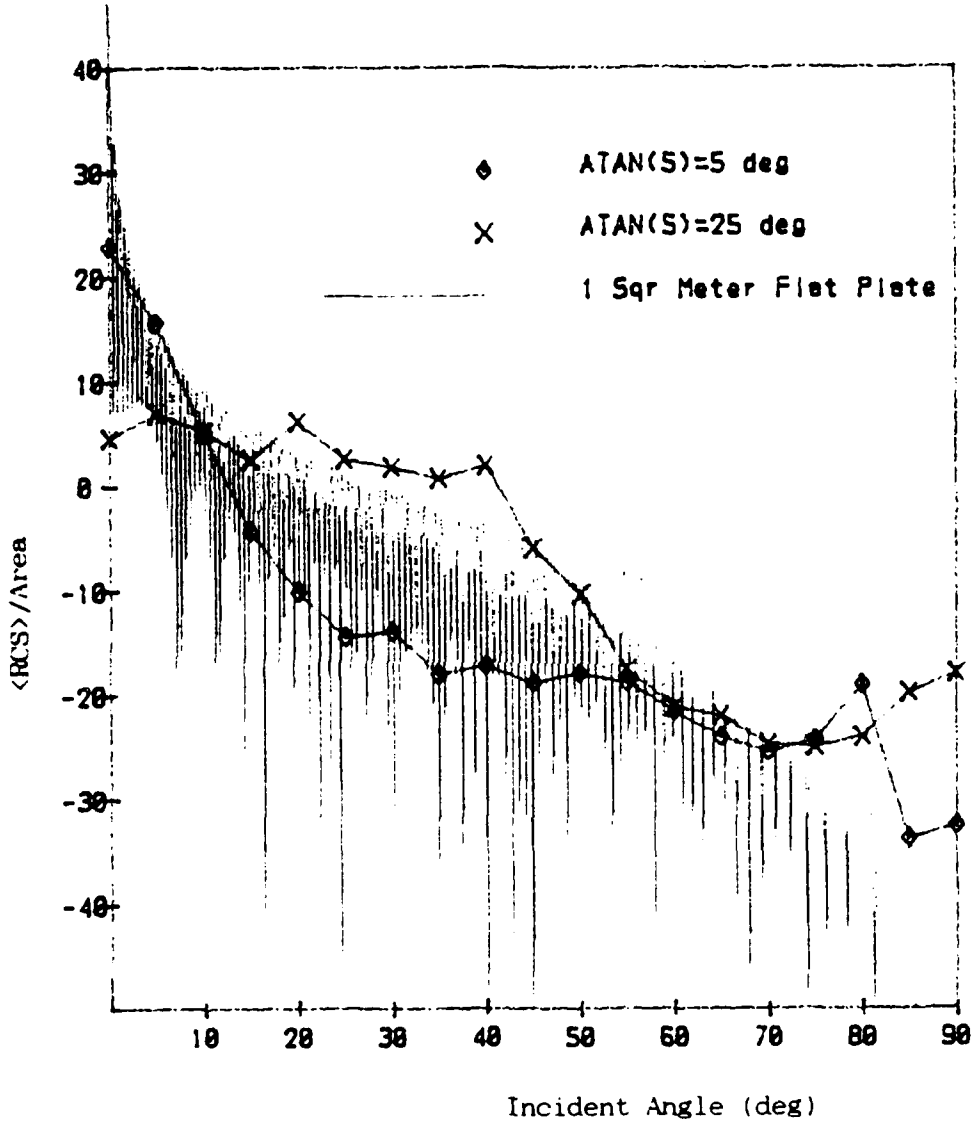

Fig. 22. <RCS>/Area for Computer Generated Gaussian Surfaces at 17.0 Ghz

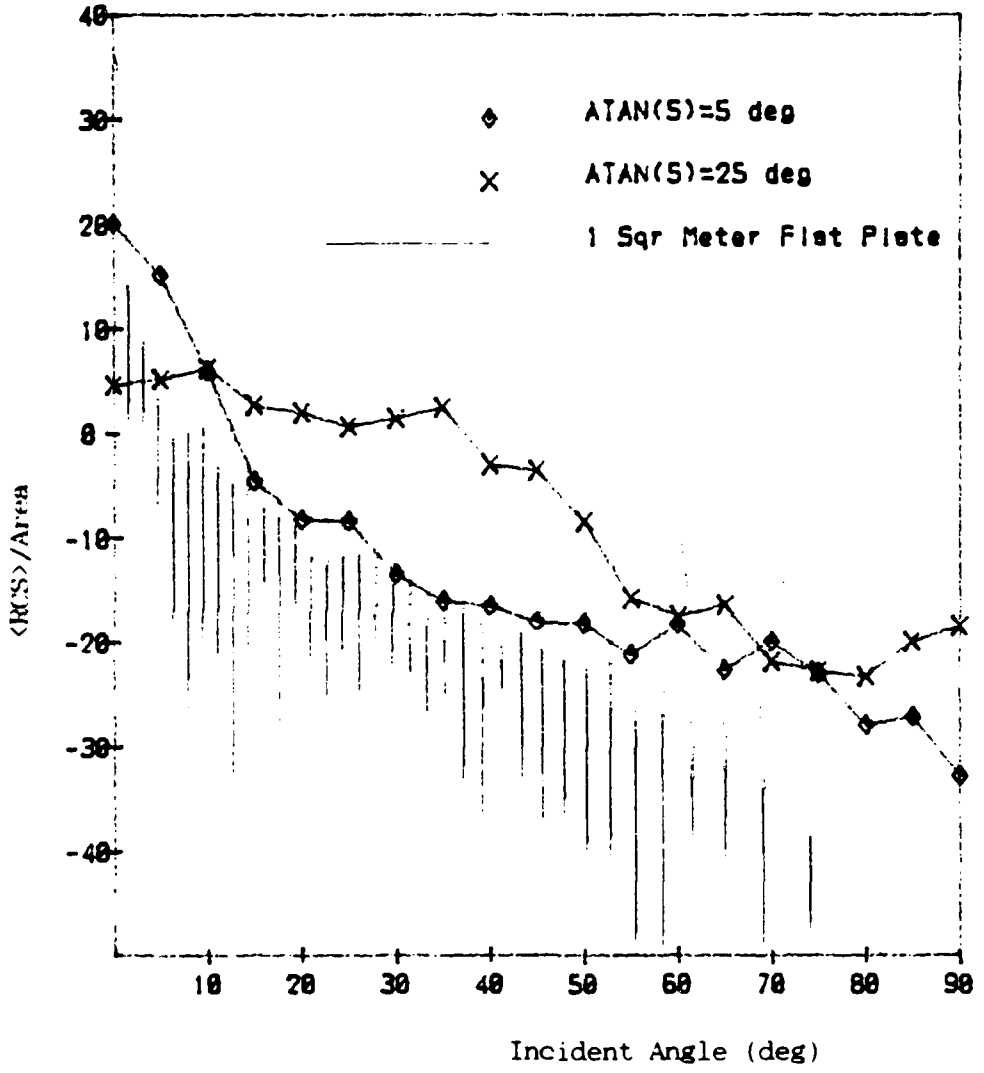

Fig. 23. <RCS>/Area for Computer Generated Exponential Surfaces at 5.46 Ghz

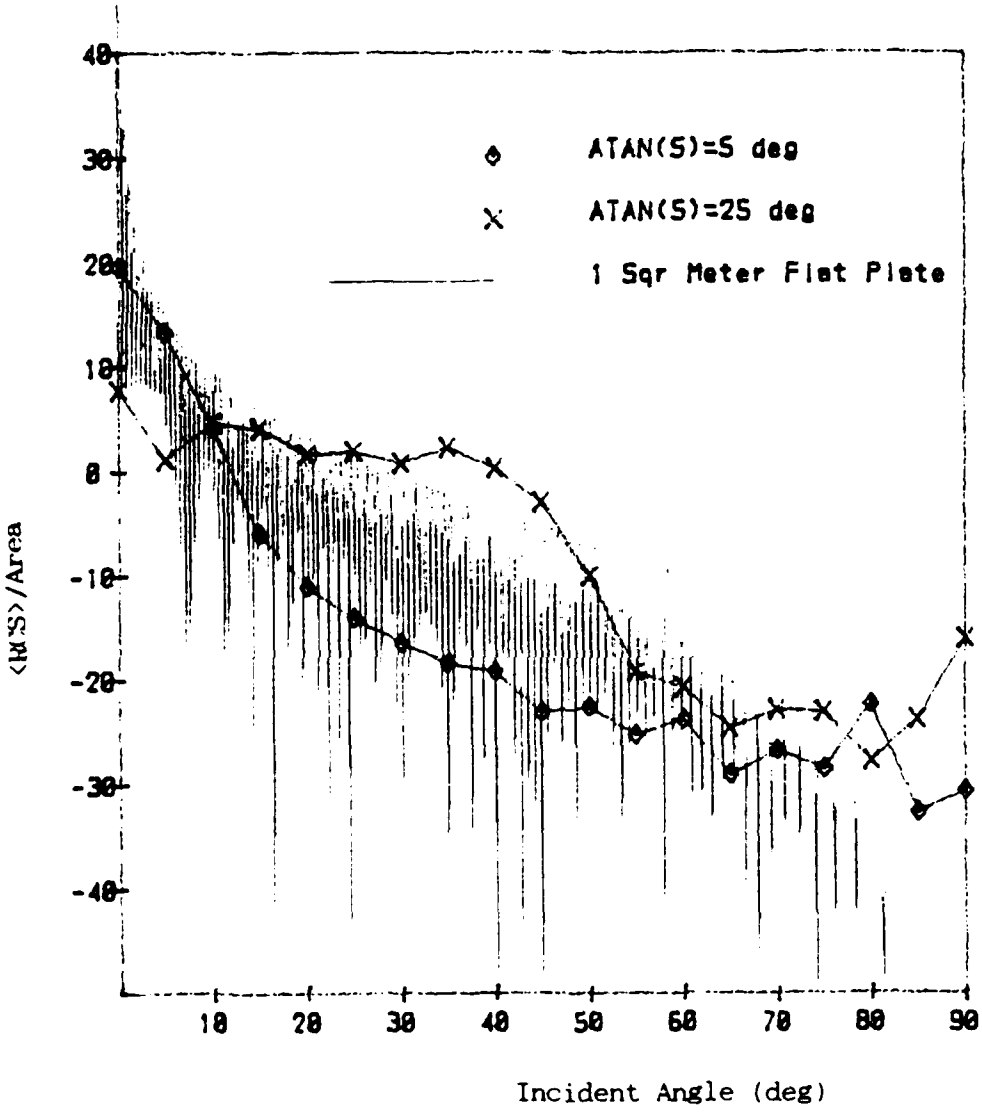

Fig. 24. <RCS>/Area for Computer Generated Exponential Surfaces at 17.0 Ghz

IV. Conclusion and Recommendations

1. Summary of Work Completed

In this thesis it was postulated that any joint probability density function used to model statistically rough surfaces should decorrelate into statistically independent random surface height variables. A joint exponential pdf which met this requirement was then introduced and the diffuse scattering properties of surfaces modeled by it were derived using physical optics and infinite conductivity approximations. This represents the first time the diffuse scattering properties of a true joint exponential pdf have been calculated. The resulting scattering properties of the joint exponential pdf surfaces were then compared to the scattering properties of the joint Gaussian pdf and a joint exponential pdf and were found to be significantly different.

In addition, a technique was introduced whereby one can generate rough surfaces that satisfy virtually any kind of statistics. Then, 10 surfaces each that satisfied Gaussian and exponential statistics with mean surface slopes of 5° and 25° were generated and the high frequency RCS's of these surfaces was calculated. The resulting average RCS's per unit area for the different types of surfaces were shown to be in in good agreement with the RCS's predicted by the more traditional means but to deviate from the traditional predictions off normal angles of incidence.

2. Recommendations for Further Study

Several follow on studies that could be conducted are enumerated below.

(1) The rough surfaces studied in this thesis could be expanded to include rough surfaces that have finite conductivity. The calculations could be done using Eq (79) with the scattering matrix elements defined for the particular surface under study. Introduction of finite conductivities to the surfaces generated by computer in Chapter III, Part B could be easily accomplished.

(2) The effects of different correlation coefficients upon the diffuse scattering properties of the joint exponential pdf could be studied. This would require only slight modification to the integrand of Eq (78) since the characteristic functions are a function of the correlation coefficient. It would also be possible to replace the Gaussian correlation matrix used in Chapter III, Part B with some other type of correlation matrix. This was tried for an exponential correlation function with no apparent problems.

(3) With the introduction of the rough surface generating technique, surfaces that meet other type of statistics could be generated and the RCS's calculated for comparison to the ones studied in this thesis.

(4) Follow on work could be done to show the validity of modeling rough surfaces with joint probability density functions. In this regard, the surface heights of actual terrain and other

rough surfaces of interest could be measured and statistically analyzed. Also, actual Laser and radar cross section measurements could be made and studied for comparison to the predicted results.

(5) Surfaces appearing in nature usually have more than one type of surface roughness. For instance, terrain might have large scale roughness that is properly modeled with a certain joint probability density function while its smaller scale roughness might be more properly modeled by another type of jpdf. On top of the terrain one would possibly find vegetation which might best be modeled by randomly oriented cylinders. Therefore, a study that showed the construction of an entire surface model might be appropriate.

(6) Finally, a study that looked at the total bistatic scattering of different types of rough surfaces could be done. This study should include an integration of the total power scattered diffusely for different scales of roughness. This power could then be subtracted from the total power incident upon the surface. The remaining power would be the coherently scattered power. The total scattered power would be represented by the addition of the diffuse and coherent scattered fields.

Appendix A

Characteristic Function for the Bivariate Exponential PDF

The purpose of this appendix is to show how the characteristic function $\iota_2^E(\zeta_1,\zeta_2;\rho)$ for Pyati's two dimensional exponential pdf, Eq (3), was derived. The characteristic function $\iota_2(v_1,v_2)$ of a two dimensional pdf $P_2(\zeta_1,\zeta_2)$ is defined as [6:189]

$$\iota_2(v_1,v_2) = \int_{-\infty}^{\infty}\int_{-\infty}^{\infty} P_2(\zeta_1,\zeta_2)\, \exp\left[jv_1\zeta_1 + jv_2\zeta_2\right] d\zeta_1 d\zeta_2 \qquad \text{(A-1)}$$

To find the characteristic function of Dr Pyati's two dimensional exponential pdf, replace $P_2(\zeta_1,\zeta_2)$ in Eq (A-1) with Eq (3) and solve. The integrals that need to be solved to obtain the characteristic function are shown in Eq (A-2).

In Eq (A-2), ζ_1 and ζ_2 symbolize two random surface heights which are functions of x and y. ζ_1 and ζ_2 are separated by a distance r and where $\rho = \rho(r)$ is the surface-height correlation function. I_α is a modified Bessel function of the first kind of order α. Also, sgn(x) is the signum function of x.

$$\gamma_2^E(v_1,v_2;\rho) = \int_{-\infty}^{\infty}\int_{-\infty}^{\infty} \frac{1}{4h^2(1-\rho^2)} \exp\left\{-\left[\frac{|\zeta_1| + |\zeta_2|}{h(1-\rho^2)}\right]\right\}$$

$$\times\left\{I_o\left[\frac{2\rho\left[|\zeta_1|\,|\zeta_2|\right]^{1/2}}{h(1-\rho^2)}\right] + \frac{8}{\pi^2}\,\mathrm{sgn}(\zeta_1)\,\mathrm{sgn}(\zeta_2)\right.$$

$$\left.\times\sum_{n=0}^{\infty}\frac{1}{(2n+1)^2} I_{2n+1}\left[\frac{2\rho\left[|\zeta_1|\,|\zeta_2|\right]^{1/2}}{h(1-\rho^2)}\right]\right\}$$

$$\times \exp\left[\, j\,(v_1\zeta_1 + v_2\zeta_2)\,\right]\, d\zeta_1\, d\zeta_2 \qquad \text{(A-2)}$$

At first glance, it appears impossible to obtain a closed form solution for Eq (A-2). However. after much trial and error, a valid solution was obtained.

The first step in solving Eq (A-2) is to remove the dependence of the integral upon the absolute value functions and the signum functions. This can be done by using the following relationships.

$$|\zeta_{1,2}| = -\zeta_{1,2} \quad \text{for} \quad -\infty < \zeta_{1,2} < 0$$

$$= \zeta_{1,2} \quad \text{for} \quad 0 < \zeta_{1,2} < \infty \qquad \text{(A-3)}$$

$$\text{sgn}(\zeta_{1,2}) = -1 \quad \text{for} \quad -\infty < \zeta_{1,2} < 0$$

$$= +1 \quad \text{for} \quad 0 < \zeta_{1,2} < \infty \qquad \text{(A-4)}$$

Using equations (A-3) and (A-4) the above Fourier transform integral, Eq (A-2), can be written as the sum of four integrals.

$$\mathfrak{t}_2^E(v_1, v_2) = I_1 + I_2 + I_3 + I_4 \qquad \text{(A-5)}$$

The values of I_1 through I_4 are given on the next two pages. Also, a substitution of $c = h(1-\rho^2)$ is used for brevity.

$$I_1 = \int_{-\infty}^{0}\int_{-\infty}^{0} \frac{1}{4hc} \exp\left[\frac{\zeta_1 + \zeta_2}{c}\right] \left\{ I_o\left[\frac{2\rho\left(\zeta_1\zeta_2\right)^{1/2}}{c}\right] \right.$$

$$\left. + \frac{8}{\pi^2} \sum_{n=o}^{\infty} \frac{1}{(2n+1)^2} I_{2n+1}\left[\frac{2\rho\left(\zeta_1\zeta_2\right)^{1/2}}{c}\right] \right\}$$

$$\times \exp\left[j \left(v_1\zeta_1 + v_2\zeta_2\right) \right] d\zeta_1 d\zeta_2 \qquad \text{(A-6)}$$

$$I_2 = \int_{-\infty}^{0}\int_{0}^{\infty} \frac{1}{4hc} \exp\left[\frac{-\zeta_1 + \zeta_2}{c}\right] \left\{ I_o\left[\frac{2\rho\left(-\zeta_1\zeta_2\right)^{1/2}}{c}\right] \right.$$

$$\left. - \frac{8}{\pi^2} \sum_{n=o}^{\infty} \frac{1}{(2n+1)^2} I_{2n+1}\left[\frac{2\rho\left(-\zeta_1\zeta_2\right)^{1/2}}{c}\right] \right\}$$

$$\times \exp\left[j \left(v_1\zeta_1 + v_2\zeta_2\right) \right] d\zeta_1 d\zeta_2 \qquad \text{(A-7)}$$

$$I_3 = \int_0^{\infty} \int_{-\infty}^{0} \frac{1}{4hc} \exp\left[\frac{\zeta_1 - \zeta_2}{c}\right] \times \left\{ I_o\left[\frac{2\rho\left(-\zeta_1\zeta_2\right)^{1/2}}{c}\right] \right.$$

$$\left. - \frac{8}{\pi^2} \sum_{n=o}^{\infty} \frac{1}{(2n+1)^2} I_{2n+1}\left[\frac{2\rho\left(-\zeta_1\zeta_2\right)^{1/2}}{c}\right] \right\}$$

$$\times \exp\left[j \left(v_1\zeta_1 + v_2\zeta_2 \right) \right] d\zeta_1 \, d\zeta_2 \qquad \text{(A-8)}$$

$$I_4 = \int_0^{\infty} \int_{0}^{\infty} \frac{1}{4hc} \exp\left[\frac{-\zeta_1 - \zeta_2}{c}\right] \times \left\{ I_o\left[\frac{2\rho\left(\zeta_1\zeta_2\right)^{1/2}}{c}\right] \right.$$

$$\left. + \frac{8}{\pi^2} \sum_{n=o}^{\infty} \frac{1}{(2n+1)^2} I_{2n+1}\left[\frac{2\rho\left(\zeta_1\zeta_2\right)^{1/2}}{c}\right] \right\}$$

$$\times \exp\left[j \left(v_1\zeta_1 + v_2\zeta_2 \right) \right] d\zeta_1 \, d\zeta_2 \qquad \text{(A-9)}$$

These integrals need to be arranged into a form that can be integrated or for which an integral is known. One form that works was (see Appendix A.1) is given by

$$\int_0^\infty x^{p-1} e^{-ax} \cos(mx)\, dx = \frac{\Gamma(p) \cos(p\theta)}{(a^2 + m^2)^{p/2}} \qquad \text{(A-10)}$$

$$\int_0^\infty x^{p-1} e^{-ax} \sin(mx)\, dx = \frac{\Gamma(p) \sin(p\theta)}{(a^2 + m^2)^{p/2}} \qquad \text{(A-11)}$$

$$\theta = \tan^{-1}\left[\frac{m}{a}\right] = \cos^{-1}\left[\frac{1}{(a^2 + m^2)^{1/2}}\right] \qquad \text{(A-12)}$$

Several manipulations must be performed to get integrals one through four into the above form. The first step is to make all the limits of integration to be from zero to infinity. This is done in two steps, first making all integrals start at zero, then changing any negative infinities to positive by changing the sign of the appropriate variable. These changes are shown on the next four pages.

Step 1: Change order of limits.

$$I_1 = \int_0^{-\infty}\int_0^{-\infty} \frac{1}{4hc} \exp\left[\frac{\zeta_1 + \zeta_2}{c}\right] \cdot \left\{ I_o\left[\frac{2\rho(\zeta_1\zeta_2)^{1/2}}{c}\right] + \frac{8}{\pi^2}\sum_{n=o}^{\infty}\frac{1}{(2n+1)^2} I_{2n+1}\left[\frac{2\rho(\zeta_1\zeta_2)^{1/2}}{c}\right]\right\}$$

$$\cdot \exp\left[j\left(v_1\zeta_1 + v_2\zeta_2\right)\right] d\zeta_1\, d\zeta_2 \qquad \text{(A-13)}$$

$$I_2 = -\int_0^{-\infty}\int_0^{\infty} \frac{1}{4hc} \exp\left[\frac{-\zeta_1 + \zeta_2}{c}\right] \cdot \left\{ I_o\left[\frac{2\rho(-\zeta_1\zeta_2)^{1/2}}{c}\right] - \frac{8}{\pi^2}\sum_{n=o}^{\infty}\frac{1}{(2n+1)^2} I_{2n+1}\left[\frac{2\rho(-\zeta_1\zeta_2)^{1/2}}{c}\right]\right\}$$

$$\cdot \exp\left[j\left(v_1\zeta_1 + v_2\zeta_2\right)\right] d\zeta_1 d\zeta_2 \qquad \text{(A-14)}$$

$$I_3 = -\int_0^{\infty}\int_0^{-\infty} \frac{1}{4hc} \exp\left[\frac{\zeta_1 - \zeta_2}{c}\right] \cdot \left\{ I_o\left[\frac{2\rho\left(-\zeta_1\zeta_2\right)^{1/2}}{c}\right] \right.$$

$$\left. - \frac{8}{\pi^2} \sum_{n=o}^{\infty} \frac{1}{(2n+1)^2} I_{2n+1}\left[\frac{2\rho\left(-\zeta_1\zeta_2\right)^{1/2}}{c}\right] \right\}$$

$$\cdot \exp\left[j\left(v_1\zeta_1 + v_2\zeta_2\right)\right] d\zeta_1 d\zeta_2 \qquad \text{(A-15)}$$

$$I_4 = \int_0^{\infty}\int_0^{\infty} \frac{1}{4hc} \exp\left[\frac{-\zeta_1 - \zeta_2}{c}\right] \cdot \left\{ I_o\left[\frac{2\rho\left(\zeta_1\zeta_2\right)^{1/2}}{c}\right] \right.$$

$$\left. + \frac{8}{\pi^2} \sum_{n=o}^{\infty} \frac{1}{(2n+1)^2} I_{2n+1}\left[\frac{2\rho\left(\zeta_1\zeta_2\right)^{1/2}}{c}\right] \right\}$$

$$\cdot \exp\left[j\left(v_1\zeta_1 + v_2\zeta_2\right)\right] d\zeta_1\, d\zeta_2 \qquad \text{(A-16)}$$

Step 2: Make all limits positive.

$$I_1 = \int_0^{\infty}\int_0^{\infty} \frac{1}{4hc} \exp\left[\frac{-\zeta_1 - \zeta_2}{c}\right] \times \left\{ I_o\left[\frac{2\rho\left(\zeta_1\zeta_2\right)^{1/2}}{c}\right] \right.$$

$$\left. + \frac{8}{\pi^2} \sum_{n=o}^{\infty} \frac{1}{(2n+1)^2} I_{2n+1}\left[\frac{2\rho\left(\zeta_1\zeta_2\right)^{1/2}}{c}\right] \right\}$$

$$\times \exp\left[j\left(-v_1\zeta_1 - v_2\zeta_2\right)\right] \, d\zeta_1 \, d\zeta_2 \qquad \text{(A-17)}$$

$$I_2 = \int_0^{\infty}\int_0^{\infty} \frac{1}{4hc} \exp\left[\frac{-\zeta_1 - \zeta_2}{c}\right] \times \left\{ I_o\left[\frac{2\rho\left(\zeta_1\zeta_2\right)^{1/2}}{c}\right] \right.$$

$$\left. - \frac{8}{\pi^2} \sum_{n=o}^{\infty} \frac{1}{(2n+1)^2} I_{2n+1}\left[\frac{2\rho\left(\zeta_1\zeta_2\right)^{1/2}}{c}\right] \right\}$$

$$\times \exp\left[j\left(v_1\zeta_1 - v_2\zeta_2\right)\right] \, d\zeta_1 \, d\zeta_2 \qquad \text{(A-18)}$$

$$I_3 = \int_0^\infty \int_0^\infty \frac{1}{4hc} \exp\left[\frac{-\zeta_1 - \zeta_2}{c}\right] \times \left\{ I_o\left[\frac{2\rho\left(\zeta_1\zeta_2\right)^{1/2}}{c}\right] \right.$$

$$\left. - \frac{8}{\pi^2} \sum_{n=o}^{\infty} \frac{1}{(2n+1)^2} I_{2n+1}\left[\frac{2\rho\left(\zeta_1\zeta_2\right)^{1/2}}{c}\right] \right\}$$

$$\times \exp\left[j\left(-v_1\zeta_1 + v_2\zeta_2\right)\right] d\zeta_1\, d\zeta_2 \qquad \text{(A-19)}$$

$$I_4 = \int_0^\infty \int_0^\infty \frac{1}{4hc} \exp\left[\frac{-\zeta_1 - \zeta_2}{c}\right] \times \left\{ I_o\left[\frac{2\rho\left(\zeta_1\zeta_2\right)^{1/2}}{c}\right] \right.$$

$$\left. + \frac{8}{\pi^2} \sum_{n=o}^{\infty} \frac{1}{(2n+1)^2} I_{2n+1}\left[\frac{2\rho\left(\zeta_1\zeta_2\right)^{1/2}}{c}\right] \right\}$$

$$\exp\left[j\left(v_1\zeta_1 + v_2\zeta_2\right)\right] d\zeta_1\, d\zeta_2 \qquad \text{(A-20)}$$

These integrals can be simplified by noting that they are really the sum of two integrands. Thus, if the simplifications listed below are made, the integrals can be written in a workable form.

$$A = I_o \left[\frac{2\rho \left(\zeta_1 \zeta_2 \right)^{1/2}}{c} \right] \tag{A-21}$$

$$B = \frac{8}{\pi^2} \sum_{n=o}^{\infty} \frac{1}{(2n + 1)^2} I_{2n+1} \left[\frac{2\rho \left(\zeta_1 \zeta_2 \right)^{1/2}}{c} \right] \tag{A-22}$$

$$D = \frac{1}{4hc} \exp \left[\frac{-\zeta_1 - \zeta_2}{c} \right] \tag{A-23}$$

With the use of these substitutions and equations (A-17) through (A-20), the integral Eq (A-5) becomes

$$\begin{aligned} \zeta_2^E = & \int_0^x \int_0^x D\,(A + B) \exp \left[j\left(-v_1\zeta_1 - v_2\zeta_2\right) \right] d\zeta_1 d\zeta_2 \\ & + \int_0^x \int_0^x D\,(A - B) \exp \left[j\left(-v_1\zeta_1 + v_2\zeta_2\right) \right] d\zeta_1 d\zeta_2 \\ & + \int_0^x \int_0^x D\,(A - B) \exp \left[j\left(+v_1\zeta_1 - v_2\zeta_2\right) \right] d\zeta_1 d\zeta_2 \\ & + \int_0^x \int_0^x D\,(A + B) \exp \left[j\left(+v_1\zeta_1 + v_2\zeta_2\right) \right] d\zeta_1 d\zeta_2 \end{aligned} \tag{A-24}$$

Grouping like terms, Eq (A-24) can be rewritten as

$$t_2^E = \int_0^x \int_0^x D\,(A + B) \left\{ \exp\left[j\left(v_1\zeta_1 + v_2\zeta_2\right)\right] + \exp\left[-j\left(v_1\zeta_1 + v_2\zeta_2\right)\right]\right\} d\zeta_1 d\zeta_2 + \int_0^\infty \int_0^\infty D\,(A - B) \left\{ \exp\left[j\left(v_1\zeta_1 - v_2\zeta_2\right)\right] + \exp\left[-j\left(v_1\zeta_1 - v_2\zeta_2\right)\right]\right\} d\zeta_1 d\zeta_2 \qquad (A\text{-}25)$$

Using Euler's identity $\exp(jx) + \exp(-jx) = 2\cos(x)$, Eq (A-25) can be written in the form

$$t_2^E = 2\int_0^\infty \int_0^\infty D\,(A + B)\cos\left(v_1\zeta_1 + v_2\zeta_2\right) + 2\int_0^\infty \int_0^\infty D\,(A - B)\cos\left(v_1\zeta_1 - v_2\zeta_2\right) \qquad (A\text{-}26)$$

Equation (A-26) with the use of a the trigonometric identity for the addition and subtraction of angles, which states $\cos(\alpha \mp \beta) = \cos\alpha \cos\beta \mp \sin\alpha \sin\beta$, can be written as

$$\begin{aligned} \gamma_2^E = \; & 2 \int_0^x \int_0^x D\,(A + B) \left\{ \cos(v_1\zeta_1)\cos(v_2\zeta_2) \right. \\ & \left. - \sin(v_1\zeta_1)\sin(v_2\zeta_2) \right\} \\ & + 2 \int_0^\infty \int_0^\infty D\,(A - B) \left\{ \cos(v_1\zeta_1)\cos(v_2\zeta_2) \right. \\ & \left. + \sin(v_1\zeta_1)\sin(v_2\zeta_2) \right\} \end{aligned} \tag{A-27}$$

Expansion of Eq (A-27) simplifies to

$$\begin{aligned} \gamma_2^E = \; & 4 \int_0^\infty \int_0^\infty D \left[A \cos(v_1\zeta_1)\cos(v_2\zeta_2) \right] d\zeta_1 d\zeta_2 \\ & - 4 \int_0^\infty \int_0^\infty D \left[B \sin(v_1\zeta_1)\sin(v_2\zeta_2) \right] d\zeta_1 d\zeta_2 \end{aligned} \tag{A-28}$$

Now the following substitutions $\xi = \zeta_1/c$ and $\eta = \zeta_2/c$ are made and the Bessel function is replaced with its series equivalent Eq (A-29) found in [1:375].

$$I_\nu(z) = \left[\frac{z}{2} \right]^\nu \sum_{k=0}^{\infty} \frac{(z^2/4)^k}{k!\,\Gamma(\nu+k+1)} \tag{A-29}$$

When ν and k are integers, $\Gamma(\nu+k+1) = (\nu+k)!$ [1:255] and Eq (A-29) reduces to Eq (A-30).

$$I_\nu(z) = \left[\frac{z}{2}\right]^\nu \sum_{k=0}^{\infty} \frac{(z^2/4)^k}{k!\ (\nu+k)!} \tag{A-30}$$

Eq (A-30) and the $\xi$and η substitution are used to transform the variables A, B, and D, given in Eq (A-21) through (A-23), into the following equations.

$$A = I_o\ (2\rho\ \xi^{1/2}\eta^{1/2})$$

$$= \sum_{k=0}^{\infty} \frac{(\rho^2\xi\eta)^k}{k!^2} \tag{A-31}$$

$$B = \frac{8}{\pi^2} \sum_{n=0}^{\infty} \frac{I_{2n+1}(2\rho\ \xi^{1/2}\eta^{1/2})}{(2n+1)^2}$$

$$= \frac{8}{\pi^2} \sum_{k=0}^{\infty} \sum_{n=0}^{\infty} \frac{(\rho\ \xi^{1/2}\eta^{1/2})^{2n+1}\ (\rho^2\xi\eta)^k}{(2n+1)^2\ \ k!\ (2n+1+k)!} \tag{A-32}$$

$$D = \frac{1}{4hc} \exp(-\xi - \eta) \tag{A-33}$$

Substituting Eq (A-31) through (A-33) into Eq (A-28) allows theintegral to be written as

$$\gamma_2^E = \frac{c}{h} \sum_{k=0}^{\infty} \left\{ \frac{\rho^{2k}}{k!^2} \int_0^{\infty} \exp(-\xi)\, \xi^k \cos(cv_1 \xi)\, d\xi \right.$$

$$\left. \cdot \int_0^{\infty} \exp(-\eta)\, \eta^k \cos(cv_2 \eta)\, d\eta \right\}$$

$$- \frac{8c}{\pi^2 h} \sum_{n=0}^{\infty} \sum_{k=0}^{\infty} \frac{\rho^{2n+1+2k}}{(2n+1)^2\, k!\, (2n+1+k)!}$$

$$\cdot \int_0^{\infty} \exp(-\xi)\, \xi^{n+k+1/2} \sin(cv_1 \xi)\, d\xi$$

$$\cdot \int_0^{\infty} \exp(-\eta)\, \eta^{n+k+1/2} \sin(cv_2 \eta)\, d\eta \qquad \text{(A-34)}$$

Eq (A-34) now has its integrals in the form of equations (A-10) and (A-11) for which solutions are known. Therefore, the characteristic function Υ_2^E for Pyati's two- dimensional exponential pdf has the following solution.

$$\Upsilon_2^E = \frac{c}{h} \sum_{k=0}^{\infty} \frac{\rho^{2k} \; \Gamma^2(k+1) \; \cos\left[(k+1)\theta_1\right] \; \cos\left[(k+1)\theta_2\right]}{k!^2 \left[1 + (cv_1)^2\right]^{(k+1)/2} \left[1 + (cv_2)^2\right]^{(k+1)/2}}$$

$$- \frac{8c}{\pi^2 h} \sum_{n=0}^{\infty} \sum_{k=0}^{\infty} \frac{\rho^{2n+1+2k}}{(2n+1)^2 \; k! \; (2n+1+k)!}$$

$$\cdot \frac{\Gamma^2(n+k+1.5) \; \sin\left[(n+k+1.5)\theta_1\right] \; \sin\left[(n+k+1.5)\theta_2\right]}{\left[1+(cv_1)^2\right]^{(n+k+1.5)/2} \left[1+(cv_2)^2\right]^{(n+k+1.5)/2}} \qquad \text{(A-35)}$$

Where θ_1 and θ_2 are given as

$$\theta_{1,2} = \tan^{-1}\left[cv_{1,2}\right]$$

$$= \cos^{-1}\left[\frac{1}{(1 + c^2 v_{1,2}^2)^{1/2}}\right]$$

$$= \sin^{-1}\left[\frac{(1-\rho^2)hv_{1,2}}{(1 + c^2 v_{1,2}^2)^{1/2}}\right] \qquad \text{(A-36)}$$

Finally, letting the arguments be $v_1 = -v_2 = v_z$

$$\gamma_2^E(v_z,-v_z;\rho) = (1-\rho^2)\sum_{k=0}^{\infty}\frac{\rho^{2k}\cos^2[(k+1)\theta]}{\left[1+((1-\rho^2)hv_z)^2\right]^{(k+1)}}$$

$$+\frac{8}{\pi^2}(1-\rho^2)\sum_{n=0}^{\infty}\sum_{k=0}^{\infty}\frac{\rho^{2n+1+2k}}{(2n+1)^2\,k!\,(2n+1+k)!}$$

$$\cdot\frac{\Gamma^2(n+k+1.5)\sin^2[(n+k+1.5)\theta]}{\left[1+((1-\rho^2)hv_z)^2\right]^{(n+k+1.5)}} \qquad \text{(A-37)}$$

$$\theta = \tan^{-1}\left[\frac{v}{cv}\right] = \cos^{-1}\left[\frac{1}{\left(1+((1-\rho^2)hv_z)^2\right)^{1/2}}\right]$$

$$= \sin^{-1}\left[\frac{(1-\rho^2)hv}{\left(1+((1-\rho^2)hv_z)^2\right)^{1/2}}\right] \qquad \text{(A-38)}$$

Appendix A.1

Solution of Integrals from Appendix A

This appendix derives the integral identities that were used in Appendix A to find the characteristic function for the exponential pdf. The integrals, Eqs (A-10) and (A-11), are rewritten here as Eqs (A1-1) and (A1-2) respectively

$$\int_0^\infty x^{p-1} e^{-ax} \cos(mx) dx \tag{A1-1}$$

$$\int_0^\infty x^{p-1} e^{-ax} \sin(mx) dx \tag{A1-2}$$

The solution to these integrals can be found by solving the complex integral

$$\int_0^\infty x^{p-1} e^{-ax} e^{jmx} dx \tag{A1-3}$$

and noting that Eq (A1-1) is simply the real part of Eq (A1-3) and Eq (A1-2) is the imaginary part. Therefore, the real and imaginary parts of the solution will correspond to the solution of Eq (A1-1) and Eq (A1-2) respectively.

By making a substitutionthe integral can be rewritten

$$\int_0^{\infty} x^{p-1}\, e^{-sx}\, dx \qquad \text{(A1-4)}$$

with $s = (a-mj)$

This is then followed up with another change of variables to get

$$s^{-p} \int_0^{\infty} t^{p-1}\, e^{-t}\, dt = s^{-p}\, \Gamma(p) = \frac{\Gamma(p)}{(a-mj)^p} \qquad \text{(A1-5)}$$

$$sx = t \quad \therefore \quad dx = dt/s$$

$$x^{p-1} = \frac{t^{p-1}}{s^{p-1}}$$

The integral can now be put in its final form by representing (a-mj) as $\text{sqr}(a^2+m^2)\exp(-jp\theta)$ with

$$\theta = \tan^{-1}\left(\frac{m}{a}\right) = \cos^{-1}\left[\frac{1}{(a^2+m^2)^{1/2}}\right] \qquad \text{(A1-6)}$$

Then

$$\int_0^{\infty} x^{p-1} e^{-ax} \cos(mx)\, dx = \frac{\Gamma(p) \cos(p\theta)}{(a^2 + m^2)^{p/2}} \qquad \text{(A1-7)}$$

$$\int_0^{\infty} x^{p-1} e^{-ax} \sin(mx)\, dx = \frac{\Gamma(p) \sin(p\theta)}{(a^2 + m^2)^{p/2}} \qquad \text{(A1-8)}$$

Appendix B

A Closed Form Solution for the First Series of the Characteristic Function

The purpose of this appendix is to show how a closed form solution for the first series of Eq (A-35) is derived. The first series of Eq (A-35) is repeated in this appendix as Eq (B-1). This solution was arrived at in conjunction with Reif [19].

$$N_1 = (1-\rho^2)\sum_{k=0}^{\infty}\left\{\frac{\rho^{2k}\cos((k+1)\theta_1)}{\left[1+((1-\rho^2)hv_1)^2\right]^{(k+1)/2}} - \frac{\cos((k+1)\theta_2)}{\left[1+((1-\rho^2)hv_2)^2\right]^{(k+1)/2}}\right\} \tag{B-1}$$

$$\theta_1 = \tan^{-1}\left[(1-\rho^2)hv_1\right] = \cos^{-1}\left[\frac{1}{\left[1+\left((1-\rho^2)hv_1\right)^2\right]^{1/2}}\right]$$

$$= \sin^{-1}\left[\frac{(1-\rho^2)hv_1}{\left[1+\left((1-\rho^2)hv_1\right)^2\right]^{1/2}}\right] \tag{B-2}$$

To obtain the variable θ_2, just replace v_1 with v_2 in Eq (B-2). Then, using Euler's identity for a cosine, the cosine term, $\cos\left[(k+1)\theta_1\right]$, is written as Eq (B-3). The same is done for the $\cos\left[(k+1)\theta_2\right]$ term by replacing θ_1 with θ_2.

$$\cos((k+1)\theta_1) = \frac{\exp\left[j(k+1)\theta_1\right] + \exp\left[-j(k+1)\theta_1\right]}{2} \qquad \text{(B-3)}$$

Also, to reduce Eq (B-1) to a workable form, the following substitutions will be used.

$$A = \left[1 + \left[(1-\rho^2)hv_1\right]^2\right]^{1/2} \qquad \text{(B-4)}$$

$$B = \left[1 + \left[(1-\rho^2)hv_2\right]^2\right]^{1/2} \qquad \text{(B-5)}$$

The use of equations (B-3) through (B-5) allows equation (B-1) to be written as

$$N_1 = \frac{(1-\rho^2)}{4AB} \sum_{k=0}^{\infty} \frac{\rho^{2k}}{A^k B^k} \left\{ \left[\exp\left[j(k+1)\theta_1\right] + \exp\left[-j(k+1)\theta_1\right]\right] \cdot \left[\exp\left[j(k+1)\theta_2\right] + \exp\left[-j(k+1)\theta_2\right]\right] \right\} \qquad \text{(B-6)}$$

Expanding Eq (B-6) by multiplying terms to remove the brackets yields

$$X_1 = \frac{(1-\rho^2)}{4\mathbb{A}\mathbb{B}} \sum_{k=0}^{\infty} \frac{\rho^{2k}}{\mathbb{A}^k \mathbb{B}^k} \Big\{ \exp\left[j(\theta_1+\theta_2)\right] \exp\left[jk(\theta_1+\theta_1)\right]$$

$$+ \exp\left[j(\theta_1-\theta_2)\right] \exp\left[jk(\theta_1-\theta_2)\right]$$

$$+ \exp\left[-j(\theta_1-\theta_2)\right] \exp\left[-jk(\theta_1-\theta_2)\right]$$

$$+ \exp\left[-j(\theta_1+\theta_2)\right] \exp\left[-jk(\theta_1+\theta_2)\right] \Big\} \qquad \text{(B-7)}$$

Using the geometric series identity, $\sum_{k=0}^{\infty} X^k = \frac{1}{1-X}$ which is valid when $|X| < 1$, [MH:107] equation (B-7) can be written as Eq (B-8). Equation (B-8) is now in a close form since the summation sign has been removed.

$$X_1 = \frac{(1-\rho^2)}{4} \Big\{ \frac{\exp\left[j(\theta_1+\theta_2)\right]}{\mathbb{A}\mathbb{B} - \rho^2 \exp\left[j(\theta_1+\theta_2)\right]}$$

$$+ \frac{\exp\left[j(\theta_1-\theta_2)\right]}{\mathbb{A}\mathbb{B} - \rho^2 \exp\left[j(\theta_1-\theta_2)\right]} + \frac{\exp\left[-j(\theta_1-\theta_2)\right]}{\mathbb{A}\mathbb{B} - \rho^2 \exp\left[-j(\theta_1-\theta_2)\right]}$$

$$+ \frac{\exp\left[-j(\theta_1+\theta_2)\right]}{\mathbb{A}\mathbb{B} - \rho^2 \exp\left[-j(\theta_1+\theta_2)\right]} \Big\} \qquad \text{(B-8)}$$

Euler's indentities

$$\exp(jx) = \cos(x) + j\sin(x)$$

and

$$\exp(-jx) = \cos(x) - j\sin(x)$$

are used with the substitutions of the terms

$$M = \cos(\theta_1+\theta_2)$$

$$N = \sin(\theta_1+\theta_2)$$

$$P = \cos(\theta_1-\theta_2)$$

and

$$S = \sin(\theta_1-\theta_2)$$

to obtain

$$X_1 = \frac{(1-\rho^2)}{4}\left\{\frac{M + jN}{2E - \rho^2 M - j\rho^2 N} + \frac{P + jS}{2E - \rho^2 P - j\rho^2 S}\right.$$

$$\left. + \frac{P - jS}{2E - \rho^2 P + j\rho^2 S} + \frac{M - jN}{2E - \rho^2 M + j\rho^2 N}\right\}$$

Manipulating Eq (B-9) by multiplying each term's numerator and denominator by the conjugate of its denominator yields

$$N_1 = \frac{(1-\rho^2)}{4}\left\{\frac{2AB\mathbb{M} - 2\rho^2\mathbb{M}^2-2\rho^2\mathbb{N}^2}{A^2B^2 - 2AB\rho^2\mathbb{M} + \rho^4\mathbb{M}^2+\rho^4\mathbb{N}^2}\right.$$

$$\left. + \frac{2AB\mathbb{P} - 2\rho^2\mathbb{P}^2-2\rho^2\mathbb{S}^2}{A^2B^2 - 2AB\rho^2\mathbb{R} + \rho^4\mathbb{R}^2+\rho^4\mathbb{S}^2}\right\} \qquad \text{(B-10)}$$

Since

$$\mathbb{M}^2 + \mathbb{N}^2 = \cos^2(\theta_1+\theta_2) + \sin^2(\theta_1+\theta_2) = 1$$

and

$$\mathbb{R}^2 + \mathbb{S}^2 = \cos^2(\theta_1-\theta_2) + \sin^2(\theta_1-\theta_2) = 1$$

Eq (B-10) can be reduced to Eq (B-11).

$$N_1 = \frac{(1-\rho^2)}{2}\left\{\frac{AB\mathbb{M} - \rho^2}{A^2B^2 - 2AB\rho^2\mathbb{M} + \rho^4}\right.$$

$$\left. + \frac{AB\mathbb{R} - \rho^2}{A^2B^2 - 2AB\rho^2\mathbb{R} + \rho^4}\right\} \qquad \text{(B-11)}$$

In Eq (B-12) and (B-13), the trigonometric identity for the cosine of the sum of two angles is used to expand M and P in terms of sine and cosine of θ. Also, Eq (B-2), Eq (B-4) and Eq (B-5) are used to evaluate the sine and cosine of θ.

$$M = \cos(\theta_1+\theta_2) = \cos\theta_1\cos\theta_2 - \sin\theta_1\sin\theta_2 \qquad \text{(B-12)}$$

$$P = \cos(\theta_1-\theta_2) = \cos\theta_1\cos\theta_2 + \sin\theta_1\sin\theta_2 \qquad \text{(B-13)}$$

$$\cos\theta_1 = \cos(\cos^{-1}(1/A)) = 1/A \qquad \text{(B-14)}$$

$$\cos\theta_2 = \cos(\cos^{-1}(1/B)) = 1/B \qquad \text{(B-15)}$$

$$\sin\theta_1 = \sin\left[\sin^{-1}\left[\frac{(1-\rho^2)hv_1}{A}\right]\right] = \frac{(1-\rho^2)hv_1}{A} \qquad \text{(B-16)}$$

$$\sin\theta_2 = \sin\left[\sin^{-1}\left[\frac{(1-\rho^2)hv_2}{B}\right]\right] = \frac{(1-\rho^2)hv_2}{B} \qquad \text{(B-17)}$$

Equations (B-12) through (B-17) are used to write new equation for M and P. These terms are now void of sine and cosine terms.

$$M = \frac{1 - (1-\rho^2)hv_1\ (1-\rho^2)hv_2}{AB} = \frac{1 - (1-\rho^2)^2h^2v_1v_2}{AB} \qquad \text{(B-18)}$$

$$P = \frac{1 + (1-\rho^2)hv_1\ (1-\rho^2)hv_2}{AB} = \frac{1 + (1-\rho^2)^2h^2v_1v_2}{AB} \qquad \text{(B-19)}$$

.Substituting equations (B-18) and (B-19) into Eq (B-11) yeilds Eq (B-20). The values for A^2B^2 are given in Eq (B-21).

$$X_1 = \frac{(1-\rho^2)}{2}\left\{\frac{1 - (1-\rho^2)^2h^2v_1v_2 - \rho^2}{A^2B^2 - 2\rho^2\left[1-(1-\rho^2)^2h^2v_1v_2\right] + \rho^4}\right.$$

$$\left.\frac{1 + (1-\rho^2)^2h^2v_1v_2 - \rho^2}{A^2B^2 - 2\rho^2\left[1+(1-\rho^2)^2h^2v_1v_2\right] + \rho^4}\right\} \qquad \text{(B-20)}$$

with

$$A^2B^2 = \left[1+ ((1-\rho^2)hv_1)^2\right]\left[1 + ((1-\rho^2)hv_2)^2\right] \qquad \text{(B-21)}$$

Combining Eq (B-20) and (B-21) and factoring like terms reduces the final equation to a close form solution for the first series of Eq (B-1).

$$X_1 = \frac{1}{2}\left\{\frac{1 - (1-\rho^2)h^2v_1v_2}{(1-\rho^2)^2h^4v_1^2v_1^2 + h^2v_1^2 + h^2v_2^2 + 2\rho^2h^2v_1v_2 + 1}\right.$$

$$\left.+ \frac{1 + (1-\rho^2)h^2v_1v_2}{(1-\rho^2)^2h^4v_1^2v_1^2 + h^2v_1^2 + h^2v_2^2 - 2\rho^2h^2v_1v_2 + 1}\right\} \qquad \text{(B-22)}$$

When $v_1 = -v_2 = v$ Eq (B-22) becomes

$$X_1 = \frac{1}{2}\left\{ \frac{1 + (1-\rho^2)h^2v^2}{(1-\rho^2)^2h^4v^4 + 2h^2v^2 - 2\rho^2h^2v^2 + 1} + \frac{1 - (1-\rho^2)h^2v^2}{(1-\rho^2)^2h^4v^4 + 2h^2v^2 + 2\rho^2h^2v^2 + 1} \right\} \qquad \text{(B-23)}$$

Substituting in the extreme limits of ρ one finds that

$$X_1\Big|_{\rho=0} = \left[\frac{1}{1 + h^2v^2} \right]^2 \qquad \text{(B-24)}$$

$$X_1\Big|_{\rho=1} = \frac{1 + 2h^2v^2}{1 + 4h^2v^2} \qquad \text{(B-25)}$$

which aids in confirming the validity for the following reasons. First, at ρ=0 the exponential jpdf reduces to the square of marginal exponential pdf (see Eq (89)). Therefore, the characteristic function at ρ=0 becomes the square of the the marginal exponential characteristic function (Eq 99). As ρ gets larger the second part of the joint pdf becomes increasingly significant. Therefore, this first series, which represents the fourier transform of only the first part of Eq (3) should only give a portion of the total solution. Since the total joint characteristic function should give a value of one at ρ=1, the value of only the first part of the total solution should be something less than one. Equation (B-25) obviously meets this condition.

Appendix C

The Truncation of the Second Series of the Joint Exponential Characteristic Function

The purpose of this appendix is to show the method by which the second series of the the characteristic function for the joint exponential pdf,Eq (A-37), is reduced for the purposes of numerical calculations. The series is repeated hear as Eq (C-1).

$$\frac{8\rho(1-\rho^2)}{\pi^2}\sum_{n=0}^{x}\frac{\rho^{2n}}{(2n+1)^2}\sum_{k=0}^{x}\frac{\Gamma^2(n+k+1+.5)}{k!\,(2n+1+k)!}\frac{\rho^{2k}\quad \sin^2[(n+k+1+.5)\theta]}{(1+((1-\rho^2)hv_z)^2)^{(n+k+1+.5)}} \qquad (C\text{-}1)$$

$$\theta = \tan^{-1}\left[\frac{v_z}{}\right] = \sin^{-1}\left[\frac{(1-\rho^2)hv_z}{(1+((1-\rho^2)hv_z)^2)^{1/2}}\right] \qquad (C\text{-}2)$$

Although the ratio of the gamma function and the factorial terms is not equal to one in this series, it approaches one for values of k n. Therefore, for k sufficiently large compared to n, the ratio of the gamma function to the factorial terms is replaced with one for the remaining terms. When the ratio is assumed equal to one, the geometric series identity used in Appendix B can be utilized.

The determination of exactly where to alter the series and make the approximation that

$$\frac{\Gamma^2(n+k+1+.5)}{k!\ (2n+1+k)!} \approx 1 \qquad \text{(C-3)}$$

is of course arbitrary. One basis upon which to make such a decision is to decide how close to one the the left side of Eq (C-3) should actually be and then determine the number of terms required to reach that point. Using a Stirling's formula for the evaluation of the Gamma and factorial terms [1:257] a program was written that produced the data in Table (C-I). Table C-I lists the value of k required for the ratio to reach minimum values of .98 and .99 respectively for values of n ranging from 0 to 20. The values of k were incremented in steps of 100 and only the even numbered n values are given for purposes of brevity. The documented program is listed in the software appendix under the title GAMRAT.BAS.

TABLE C-I

Number of k Terms Required to Reach .98 and .99

n	.98 k	.99 k
0	100	100
2	400	700
4	1000	2000
6	2100	4000
8	3400	4700
10	4600	6900
12	6100	8900
14	7700	11300
16	9100	12300
18	11200	13800
20	13900	15900

The series can now be summed up to as many k terms as required and then a remainder term, calculated by setting the left side of Eq (C-3) equal to one, should be added. This remainder term is found as follows.

After summing m terms, and using Eq (C-3), the series on k is

$$K = \sum_{k=m}^{\infty} \frac{\rho^{2k} \sin^2[(n+k+1+.5)\theta]}{(1 + ((1-\rho^2)hv)^2)^{(n+k+1+.5)}} \qquad (C-4)$$

To use the geometric expansion identity, the lower index of the summation must be zero. This is accomplished by letting q = k-m and thus k = q+m. Then Eq (C-4) becomes

$$\frac{\rho^{2m}}{(1+\gamma^2)^{(n+m+1.5)}} \sum_{q=0}^{\infty} \frac{\rho^{2q} \sin^2[(n+q+m+1+.5)\theta]}{(1+\gamma^2)^q} \qquad (C-5)$$

where $\gamma = ((1-\rho^2)hv)^2$. Dealing only with the summation now, Euler's identity can be used to expand the sine term, the series thus becomes

$$K = \sum_{q=0}^{\infty} \frac{\rho^{2q}(\exp(j(n+q+m+1+.5)\theta)-\exp(-j(n+q+m+1+.5)\theta))^2}{(2j)^2 \quad (1+\gamma^2)^q} \qquad (C-6)$$

Expanding Eq (C-6), the summation can be written

$$\frac{1}{4}\sum_{q=0}^{\infty} 2\left[\frac{\rho^2}{(1+\gamma^2)}\right]^q - \left[\frac{\rho^2 e^{2j\theta}}{(1+\gamma^2)}\right]^q \exp(2j\theta(m+n+1.5)) - \left[\frac{\rho^2 e^{-2j\theta}}{(1+\gamma^2)}\right]^q \exp(-2j\theta(m+n+1.5)) \qquad (C\text{-}7)$$

Letting

$$\frac{\rho^2}{(1+\gamma^2)} = \Xi \quad \text{and} \quad \sigma = \theta(m+n+1.5) \qquad (C\text{-}8)$$

the application og the geometric expansion identity brings the series remainder to

$$\frac{1}{4}\left[\frac{2}{1-\Xi} - \frac{e^{2j\sigma}}{1-\Xi e^{2j\theta}} - \frac{e^{-2j\sigma}}{1-\Xi e^{-2j\theta}}\right]. \qquad (C\text{-}9)$$

From this point on the manipulations are not unlike those in Appendix B. Rather than presenting the algebraic gobbledygook the final solution is just presented in Eq (C-10).

$$K = \frac{\rho^{2m}}{2(1+\gamma^2)^{(n+m+1.5)}}\left[\frac{1}{1+\Xi} + \frac{\Xi\sin(\sigma)}{\Delta^2+\Xi^2} - \frac{\Delta\cos(\sigma)}{\Delta^2+\Xi^2}\right] \qquad (C\text{-}10)$$

$$\Xi = \frac{\rho^2}{(1+\gamma^2)} \qquad \sigma = \theta(m+n+1.5) \qquad \Delta = 1-\Xi\cos(2\theta)$$

$$\gamma = ((1-\rho^2)hv)^2 \qquad B = \Xi\sin(2\theta)$$

This result is used in the program MAIN2.BAS which computes values of the exponential characteristic function.

Appendix D

Software

This appendix contains the source code for some of the programs that were written in direct support of of this thesis. Those programs written in support of Part A of the analysis chapter are written primarily in BASIC and were run under compiled TurboBasic . Those programs written in support of Part B are in Fortran and were compiled and run on the Vax 11/785 that was provided by AFWAL. Each program has its own documentation and abstract; the titles of the programs are listed below.

EXPOPDF.BAS: Calculates values for the exponential joint probability density function.

MAIN.BAS: Computes values for the joint exponential characteristic function.

GAMRAT.BAS: Determines the ratio of the gamma and factorial terms in the second series of the exponential joint CF.

RCS2.BAS: Performs the numerical integration to get the <RCS>/Area for exponential surfaces.

CORCOEFF.FOR: Builds a correlation matrix.

CHOLESKY.FOR: Finds the Cholesky square root of the correlation matrix.

GESURF.FOR: Generates random rough surfaces for different statistics.

BUILD.FOR: Buils the data file for use by the RCS-Basic Scattering Code program.

```
10  sub EXPOPDF(v,p,z1,z2,w) static
'*************************************************************
'*                                                           *
'*  Sub: EXPOPDF.BAS                                         *
'*                                                           *
'*  Purpose:  Calculates the value of the exponential        *
'*    pdf proposed by Dr. Pyati.                             *
'*                                                           *
'*  Input Parameters:                                        *
'*    h = RMS surface height                                 *
'*    p = correlation coefficient                            *
'*   z1 = height at a point 1                                *
'*   z2 = height at a point 2                                *
'*                                                           *
'*  Output Parameters:                                       *
'*    w = probabilty of getting z2 and z1                    *
'*                                                           *
'*************************************************************
     pi = 4*atn(1)
   ' Calculate values for the sugnum functions and take absolute
   ' values of z1 and z2
     sgnz1 = 1 : sgnz2 = 1
     if z1 < 0 then  sgnz1 = -1  end if
     if z1 = 0 then  sgnz1 =  0  end if
     if z2 < 0 then  sgnz2 = -1  end if
     if z2 = 0 then  sgnz2 =  0  end if
     z1 = abs(z1) : z2 = abs(z2)

   ' Calculate the first term
     term1 = exp(-(z1+z2)/(h*(1-p^2)))/(4*h^2*(1-p^2))

  '  Compute the zeroth ordered Bessel function
30   a = 0 : x = sqr(z1*z2)*2*p/(h*(1-p^2)) : xx = x
40   call modbesl(a,xx,term2) ' the modified bessel function

   ' Sum only the first 15 terms of the infinite seires of Bessel
   ' functions
50   sum = 0
60   for n = 0 to 15
70      a = 2*n+1 : xx = x
80      call modbesl(a,xx,bessy)
90      tm = bessy/a^2
100     sum = sum+tm
110     if sum = oldsum then
120        goto 500
130     end if
140     oldsum = sum
150  next n
500  term3 = sum*(8/pi^2)*sgnz1*sgnz2

    ' Combine the terms to get the total solution
510  w = term1*(term2+term3)
     end sub
```

```
sub modbesl(a,x,bj) static
'''''''''''''''''''''''''''''''''''''''''''''''''''''''''''''
'                                                           '
'  Sub: MODBESL                                             '
'                                                           '
'  Purpose:  Returns the value of the modified bessel       '
'     function I                                            '
'                                                           '
'  Parameters:                                              '
'   a = order of the bessel function                        '
'   x = point at which bessel is to be calculated           '
'  bj = returned value of the bessel function               '
'                                                           '
'''''''''''''''''''''''''''''''''''''''''''''''''''''''''''''

if a = 0 then ' Compute by polynomial approximation
   if abs(x) < 3.75 or abs(x) = 3.75 then
      t = x/3.75
      bj = 1 + 3.5156229*t^2 + 3.0899424*t^4
      bj = bj + 1.2067492*t^6 + .2659732*t^8
      bj = bj + .0360768*t^10 + .0045813*t^12
      goto done
   end if
   if x > 3.75 then
      t = x/3.75
      bj = .3894228+ .01328592/t + .00225319/t^2 -
      bj = bj -.00157565/t^3 + .00916281/t^4
      bj = bj - .02057706/t^5 + .02635537/t^6
      bj = bj - .01647633/t^7 + .00392377/t^8
      bj = bj/(sqr(x)*exp(-x))
      goto done
   end if
end if

if a = 1 then ' Compute by polynomial approximation
   if abs(x) < 3.75 or abs(x) = 3.75 then
      t = x/3.75
      bj = 1/2 + .87890594*t^2 + .54918869*t^4
      bj = bj +.15084934*t^6 + .02658733*t^8
      bj = bj + .00301532*t^10 + .00032411*t^12
      bj = x*bj
      goto done
   end if
   if x > 3.75 then
      t = x/3.75
      bj = .39894228 - .3988024/t - .00362018/t^2
      bj = bj + .00163801/t^3 - .01031555/t^4
      bj = bj + .02282967/t^5 - .02895312/t^6
      bj = bj + .01787654/t^7 - .00420059/t^8
      bj = bj/(sqr(x)*exp(-x))
      goto done
   end if
end if
```

```
'(sub MODBESL.BAS cont.)
'   Use infinite series representation
    for m = 0 to 10000
        gosub NEWTERM
        bj = bj + term
        if TERM < 1E-15 then
           goto done
        end if
    next m

NEWTERM:
      numer = (x/2)^(2*m + a)
      for n = 1 to m
          numer = numer / n
      next n
      for n = 1 to (m+a)
          numer = numer / n
      next n
      '
      return

999   done:
         end sub
```

```
'*************************************************************
'                                                            *
'  Prgm:GAMRAT.BAS                                           *
'                                                            *
'  Purpose:  This program calculates the ratio of the        *
'     gamma function term to the factorial terms in the      *
'     part of the exponential CF that was not put into       *
'     closed form.  As set up, this program will output      *
'     the value of k needed for the ratio to be at least     *
'     .99.  This data is then used in the program that       *
'     calculates the CF (MAIN2.BAS).                         *
'                                                            *
'     Algorithm:  The program uses Stirling's formula        *
'        [Abramowitz & Stegun: 257] to represent the         *
'        values of the gamma functions and factorial         *
'        terms.  Logaritmic calculations are utilized to     *
'        avoid overflow problems.                            *
'                                                            *
'*************************************************************
for n = 0 to 20 step 1
    for k = 0 to 100000 step 100
       u1 = log(n+k+1.5) : um =(1+1/(12*(n+k+1.5)))+(1/(288*(n+k+1.5)^2))
       um = log(um)
       v1 = log(k+1) : v2 = log(k+2*n+2)
       vm1 =(1+1/(12*(k+1)))+1/(288*(k+1)^2) : vm1 = log(vm1)
       vm2 =(1+1/(12*(2*n+k+2)))+1/(288*(2*n+k+2)^2) : vm2 = log(vm2)
       term = (2*n+2*k+2)*u1+2*um-k*(v1+v2)-2*n*v2-v1/2-1.5*v2-vm1-vm2
       if exp(term)>.99 then
           print using "              n = ####    k = ######    ratio =
           ##.#########";n,k,exp(term)
           goto 100
        end if
     next k
100 next n
```

```
'*****************************************************************
'*                                                               *
'*  Prgm: MAIN2.BAS                                              *
'*                                                               *
'*  Purpose: Creates the values of the joint characteristic      *
'*     function of the exponential PDF.  For correlation         *
'*     coefficient very near 1, this program takes a long        *
'*     time to calculate a single data point.  As the            *
'*     correlation coefficient decreases, the infinte series     *
'*     in the solution becomes less significant since it is      *
'*     multiplied by the correlation coefficient raised to a     *
'*     high power.  Therefore, the program speeds up as it       *
'*     progresses.  However, this program still took 56 hours    *
'*     to complete using compiled TurboBASIC™ and the 8087       *
'*     numerical coprocessor in the IBM PC.                      *
'*                                                               *
'*  Algorithm:  As with GAMRAT.BAS, Stirling's formula is used   *
'*     for the gamma functions and factorial terms while         *
'*     logarithmic calculations are used to avoid overflow.      *
'*     Otherwise, this program is simply a straight forward      *
'*     implementation of the formulas derived in Appendixes      *
'*     A through C.                                              *
'*                                                               *
'*  Input  Files:  None                                          *
'*  Output Files:  E:\THESIS\EXPO.DAT                            *
'*                                                               *
'*****************************************************************
' Use double precision variables to reduce error.
  defdbl a-h,o-z : defi t i-n

' Setup parameters for the run of 5001 data points spaced .0002
' correlation lengths apart with h*vz = 10
  pi=4*atn(1)
  v = 10.0        ' Value of Vz
  space = .0002   ' Spacing between data points
  h=1.0           ' RMS value of the surface heights
  npoints = 5001  ' Total number of points to calculate

' Open a random access file to store the data points in
  fout$="e:\thesis\expo.dat"
  open fout$ as #1 len=8
  field #1, 8 as cval$

' Increment from 0 correlation lengths to 1 correlation length in
' steps of .0002 cor. lens.
  for ntow = 0 to npoints
      tow = ntow*space
      p = exp(-tow^2)  'Gaussian Cor Coefficient
      gosub charfun    'Calc the CF
      '  Provide feedback to the user
      print using " t=#.####  p=#.######   char=#.######";tow,p,char
      ' put the data in the file
      lset cval$=mkd$(char) : put #1
```

```
    next ntow
    close #1
    end
500 charfun:
    ''''''''''''''''''''''''''''''''''''''''''''''''''''''''''''''''''''''''''''''''
    '  Sub CHARFUN                                                                  '
    '                                                                               '
    '  Purpose: Evaluates the sums of the firts and second                          '
    '    series of the characteristic function solution                             '
    '                                                                               '
    '  Input Parameters:                                                            '
    '    h = RMS value of the surface heights                                       '
    '    v = Absolute vale of Vz                                                    '
    '    p = Correlation Coefficient                                                '
    '                                                                               '
    '  Returned Parameters:                                                         '
    '    char = Value of the characteristic function                                '
    '                                                                               '
    ''''''''''''''''''''''''''''''''''''''''''''''''''''''''''''''''''''''''''''''''
    '
    '  These are the 99% cutoff values where the ratio
    '  of the gamma and factorial terms becomes > .99
    '  (see Appendix C) and program GAMRAT.BAS
    dim maxk(20)
    maxk(0) =100  :   maxk(1) =200
    maxk(2) =400  :   maxk(3) =600
    maxk(4) =1000 :   maxk(5) =1500
    maxk(6) =2100 :   maxk(7) =2800
    maxk(8) =3400 :   maxk(9) =4200
    maxk(10)=4600 :   maxk(11)=5000
    maxk(12)=6100 :   maxk(13)=6600
    maxk(14)=7700 :   maxk(15)=8300
    maxk(16)=9100 :   maxk(17)=10600
    maxk(18)=11200:   maxk(19)=12000
    maxk(20)=13900

     sum2 = 0 ' Initialize variable
     if p = 0 then goto 900 ' Only the closed form portion is relevant
     if p = 1 then
         char = 1
         goto 999
     end if

     '  The portion of the solution which is left in summation form
     '  (see Appendix C) is calculated first.  The outer summation
     '  is truncated after 21 terms whereas the inner series is
     '  truncated based upon the ration of the gamma and factorial
     '  terms for a given (n).  A remainder term is then added to
     '  compensate for the truncation of the inner series.
     '  Set up parameters that are constant within the loops
     c = (1-p^2)*h*v
     t = atn(c)
     pl = log(p) : cl = log(1+c^2) :am=8*(1-p^2)/pi^2
```

```
     for n = 0 to 20  ' Truncate the series at 20
        anl = 2*log(2*n+1)
        termk = 0
        for k = 0 to (maxk(n)-1)
510        u1 = log(n+k+1.5)
515        um = log(1+1/(12.0*(n+k+1.5)))
520        v1 = log(k+1)
525        v2 = log(k+2+2.0*n)
530        vm1 = log(1+1/(12.0*(k+1)))
535        vm2 = log(1+1/(12.0*(2.0*n+k+2)))
540        u=(2.0*n+2.0*k+2)*u1+2*um1-(k+.5)*v1
           u=u-(k+2.0*n+1.5)*v2-vm1-vm2
545        st = (sin((n+k+1.5)*t))^2
550        if st = 0 then goto 790
560        tnum = p1*(2.0*n+2.0*k+1)+u
565        tden = anl+c1*(n+k+1.5)
           term = am*exp(tnum-tden)
           if term < 1E-40 then goto 795 ' to small to matter
           term = term*st
           termk = termk + term
790     next k
        gosub remainder  ' Add in the compensation for the truncation
795     sum2 = sum2 + termk + remain
800  next n
900  gosub sumone ' Get the closed form part of the solution
     char = sum1 + sum2
999  return

1100 sumone:
     ''''''''''''''''''''''''''''''''''''''''''''''''''''''''''''
     '                                                          '
     '  Sub: SUMONE                                             '
     '                                                          '
     '  Purpose: Calculate the first series which has           '
     '  a closed form solution (see Appendix B).                '
     '                                                          '
     '  Algorithm: Implements Eq B.24                           '
     '                                                          '
     '  Input Parameters:                                       '
     '    h = RMS value of the surface heights                  '
     '    v = Vz                                                '
     '    p = Correlation Coefficient                           '
     '                                                          '
     '  Output Paramteres:                                      '
     '    sum1 = Summation of the first series                  '
     '                                                          '
     ''''''''''''''''''''''''''''''''''''''''''''''''''''''''''''
     s1  = 1 + h^2*v^2*(1+p^2)
     s12 = 1-h^6*v^6*(p^6-3*p^4+3*p^2-1)
     s12 = s12-h^4*v^4*(p^4+2*p^2-3)+h^2*v^2*(p^2+3)
     sum1= s1/s12
     return
```

```
1200  remainder:
      '''''''''''''''''''''''''''''''''''''''''''''''''''''''
      '                                                     '
      '  Sub: REMAINDER                                     '
      '                                                     '
      '  Purpose:  The second series of the solution has    '
      '    been truncated at the point where the ratio of   '
      '    the Gamma functions and the factorial terms is   '
      '    at least .99.  This routine calculates the       '
      '    remainder of that term of the series with the    '
      '    assumption that the gamma and factorial terms    '
      '    completely concel.                               '
      '                                                     '
      '  Algorithm: Implements Eq C.10                      '
      '                                                     '
      '  Input Parameters:                                  '
      '    h = RMS value of the surface heights             '
      '    v = Vz                                           '
      '    p = Correlation Coefficient                      '
      '    t = theta angle (see Sub CharFun)                '
      '    c = shorthand   (see Sub CharFun)                '
      '    maxk(n) and n = (see Sub CharFun)                '
      '    pl, anl and cl= (see Sub CharFun)                '
      '                                                     '
      '  Output Paramteres:                                 '
      '    remain = the remainder                           '
      '                                                     '
      '''''''''''''''''''''''''''''''''''''''''''''''''''''''
      '
      sigma = 2*(maxk(n)+n+1.5)*t
      a = 1-p^2*cos(2*t)/(1+c^2) : al = log(a)
      b = p^2*sin(2*t)/(1+c^2)   : bl = log(b)
      albl = log(a^2+b^2)
      el = log(1-p^2/(1+c^2))
      pl2 = log(1-p^2)
      rl = pl*(2*(maxk(n)+n)+1)-anl+pl2-cl*(maxk(n)+n+1.5)
      rm1 = rl-el
      rm2 = rl+bl-albl
      rm3 = rl+al-albl
      remain=(exp(rm1)+sin(sigma)*exp(rm2)cos(sigma)*exp(rm3))
      remain = remain*4/pi^2
      return
```

```
'*****************************************************************
'*                                                               *
'*  Prgm: RCS2.BAS                                               *
'*                                                               *
'*  Purpose:  Calculates the values of the normalized            *
'*    RCS of the exponentially rough surface.                    *
'*                                                               *
'*  Algorithm:  Integrates Eq (87)  using a Simpson's            *
'*    approximation routine and the 5001 data points of the      *
'*    eponential CF generated by MAIN2.BAS                       *
'*    The Bessel function is calculated using a polynomial       *
'*    approximation taken from [Abramowitz & Stegun:369]         *
'*                                                               *
'*  Input  Files: E:\THESIS\EXPO.DAT                             *
'*                                                               *
'*  Output Files: E:\THESIS\JEXPO.DAT                            *
'*                                                               *
'*****************************************************************

   defdbl a-h,o-z
   defint i-n
   ' expo will hold the data points for the exponential CF
   ' value will hold the integrand value at the 5001 discrete
   ' points
   ' result will hold the vaule of the integral for the 15
   ' different angles and the 6 values of atan(s)
   dim value(5001),result(15,6),expo(5001)
   pi=4*atn(1)

   ' This section takes care of the initialization of the
   ' arrays that are used in the bessel function
   ' subroutine rather than reintializing the arrays
   ' each of the 5001 times the routine is called.
   dim ja#(7),jb#(7),jc#(7)
   ' Data for calcualtion of Bessel(x) for x<=3
   ja#(0) = 1.00
   ja#(1) = -2.2499997  :  ja#(2) = 1.2656208
   ja#(3) = -.3163866   :  ja#(4) = .044447900
   ja#(5) = -.0039444   :  ja#(6) = .0002100
   ' Data for calcualtion of Bessel(x) for x>3
   jc#(0) =  .79788456  :  jc#(1) = -.00000077
   jc#(2) = -.00552740  :  jc#(3) = -.00009512
   jc#(4) =  .00137237  :  jc#(5) = -.00072805
   jc#=(6) = .00014476
   jb#(0) = 3.00        : jb#(1) = -.78539816
   jb#(2) = -.04166397  : jb#(3) = -.00003954
   jb#(4) = .00262573   : jb#(5) = -.00054125
   jb#(6) = -.00029333 : jb#(7) = .00013558

   open "E:\THESIS\EXPO.DAT" as #1 len=8
   field #1, 8 as cval$
   print "Getting data from data file."
   for n=1 to 5001
```

```
   get #1 : expo(n)=cvd(cval$)
next n
close #1
(RCS2.BAS cont.)

space=.0002
h=1.0:vz=10.0
x1 = 1/(1+h^2*vz^2)  ' One dimensional Char Func
for ang% = 0% to 70% step 5%
   nang = nang+1% ' counter for result(nang,nslope)
   rang = pi*ang%/180  '
   for m = 5% to 30% step 5%
      nslope=nslope+1 ' Slope index counter
      ' Scale the wavenumber (ck) according to the angle of
      ' incidence and teh mean surface slope
      ck = 10/(tan(m*pi/180)*cos(rang))
      vx = 2*ck*sin(rang)  '
      for n = 1 to 5001
         tow=(n-1)*space
         arg = vx*tow   ' Bessel argument
         if (arg<3 or arg=3) then
            gosub BESLLOW
         else
            gosub BESLHI
         end if
         value(n) = tow*j0#*(expo(n)-x1^2)*2*ck^2
      next n
      locate 1,1:print ang%,m
      npoints=5001
      call simpson(value(),npoints,space,result(nang,nslope))
   next m
next ang%

 ' Transfer data to a file
 open "E:\THESIS\JEXPO.DAT" for output as #2
 for nslope=1 to 6
    for nang = 1 to 15
       print #2,nslope*5.0,(nang1)*5.0,result(nang,nslope)
    next nang
 next nslope
 end
```

```
''''''''''''''''''''''''''''''''''''''''''''''''''''''''''''''''''''''''''''''''
'                                                                               '
'  Zeroth order Bessel function polynomial                                      '
'  approximations.  Taken from Abromowitz and Stegun.                           '
'                                                                               '
'  Input Parameters:                                                            '
'    Coefficient Arrays = Filled in main prgm                                   '
'    arg = argument of the bessel function                                      '
'                                                                               '
'  Returned Parameters:                                                         '
'    j0# = Value of the bessel function                                         '
'                                                                               '
''''''''''''''''''''''''''''''''''''''''''''''''''''''''''''''''''''''''''''''''

BESLLOW:
   j0#=0.0
   for nbl% = 0 to 6
      j0# = j0# + ja#(nbl%)*(arg/3)^(2*nbl%)
   next nbl%
   return

BESLHI:
    theta#=0.0:f0#=0.0
    for nbl% = 0 to 7
       theta# = theta# + jb#(nbl%)*(3/arg)^(nbl%-1)
    next nbl%

    for nbl% = 0 to 6
       f0# = f0# + jc#(nbl%)*(3/arg)^nbl%
    next nbl%
    j0# = arg^(-1/2)*f0#*cos(theta#)
    return

sub simpson(f#(1),n%,h#,result#) static
''''''''''''''''''''''''''''''''''''''''''''''''''''''''''''''''''''''''''''''''
'                                                                               '
'  Sub: SIMPSON                                                                 '
'                                                                               '
'  Purpose:  Performs a Simpson's approxomation                                 '
'    Integration.  Algorithm taken from 'Applied                                '
'    Numerical Analysis by Curtis F. Gerald.                                    '
'                                                                               '
'  Input Parameters:                                                            '
'   f#(1) = a one dimensional array of data points                              '
'   n% = the number of data points in the array                                 '
'   h# = the spacing between the data points                                    '
'                                                                               '
'  Returned Parameters:                                                         '
'   result# = the approximated value of the integral                            '
'                                                                               '
''''''''''''''''''''''''''''''''''''''''''''''''''''''''''''''''''''''''''''''''
   local i%,npanel%,nbegin%,nhalf%
```

```
    ' Check to see if the number of panels is even
    npanel% = n% - 1
    nhalf% = int(npanel%/2)
    nbegin% = 1
    result% = 0

    if npanel% - 2*nhalf% = 0 then
       goto EVEN
    end if

    ' Number of panels is odd. Use 3/8 rule on first three
    ' panels and 1/3 rule on the rest of the panels.
    result# = 3*h#/8* ( f#(1) + 3*f#(2) + 3*f#(3) + f#(4) )
    nbegin% = 4

EVEN:       '
    ' Apply 1/3 rule, add in first ,second, and last
    ' values.
    rtemp#= h#/3 * ( f#(nbegin) + 4*f#(nbegin+1) + f#(n) )
    result# = result# + rtemp#
    nbegin% = nbegin# + 2
    if nbegin% = n% then
       goto DONE
    end if

    ' The pattern after nbegin+2 is repetitive.
    (RCS2.BAS subprogram SIMPSON cont.)

    ' Get nend, the place to stop.
    nend% = n%-2
    for i% = nbegin% to nend% step 2
        result# = result# + h#/3 * ( 2*f#(i) + 4*f#(i+1) )
    next i%
    '
DONE:
    end sub
```

```
C*****************************************************************
C                                                                 *
C  Prgm: CorCoeff.FOR                                             *
C                                                                 *
C  Purpose: Fortran program to create a file containing           *
C   the values of the correlation matrix.                         *
C                                                                 *
C  Algoritm:  Corrleation is a function of the distance           *
C    (d) between two points.  (d) is calculated by finding        *
C    the horizontal (b) and the vertical (a) distance             *
C    between two points and then solving the right                *
C    triangel equation to find the hypotenues (d).                *
C    Following this, the Gaussian Correlation coefficient         *
C    equation is applied.                                         *
C                                                                 *
C*****************************************************************

      parameter(n=15,n2=225,space=.3)
      virtual coeff(n2,n2)
      real*16 coeff,a,b,d
      integer corrow,corcol,refrow,refcol

C     Create lower triangle of corr. matrix (symetric matrix)
      do 33 i=1,n2
C        calculate the row point (i) is in (reference Fig.(21))
         corrow = (((i-1)/n)+1)
C        claculate the column point (i) is in
         corcol = i-((corrow-1)*n)
         write(6,*) i
         do 31 j=1,i
C           calculate the row point (j) is in
            refrow = (((j-1)/n)+1)
C           calculate the column point (j) is in
            refcol = j - ((refrow-1)*n)
C           the vertical distance (a)
            a = (corrow-refrow)*space
C           the horizontal distance (b)
            b = (corcol-refcol)*space
            d = sqrt(a**2+b**2)
            coeff(i,j) = exp(-d**2)
31       continue
33    continue
      open(unit=11,name='corg3.dat',status='NEW')
      do 43 i = 1,n2
         write(6,*) i
         do 41 j=1,i
            write(11,*) coeff(i,j)
41       continue
43    continue
      close(unit=11)
      stop
      end
```

```
C*****************************************************************
C                                                                *
C   Prgm:CHOLESKY.FOR                                            *
C                                                                *
C   Purpose:  Finds the Cholesky square root of the              *
C     correlation matrix.                                        *
C                                                                *
C   Algorithm:  Implements Eqs (xx) through (xx).                *
C                                                                *
C   Input Files: The correlation matrix file created by          *
C     CORCOEFF.FOR                                               *
C   Output Files:  The lower half of the Cholesky matrix.        *
C                                                                *
C*****************************************************************

        parameter(n2=225)
        virtual cor(n2,n2),cho(n2,n2)
        real*16 cor,cho,sum
        open(unit=11,name='corg3.dat',status='OLD')
C       Input the correlation matrix (lower triangle)
        do 33 i=1,n2
           write(6,*) i
           do 31 j=1,i
              read(11,*) cor(i,j)
31         continue
33      continue
        close(unit=11)
C       decompose into Cholesky sqrt.
        do 43 k=1,n2
           do 41 i=1,(k-1)
              sum = 0.0
              do 40 j=1,(i-1)
                 sum = sum+cho(i,j)*cho(k,j)
40            continue
              cho(k,i)=(cor(k,i)-sum)/cho(i,i)
41         continue
           sum = 0.0
           do 42 j=1,(k-1)
              sum = sum+cho(k,j)**2
42         continue
           cho(k,k) = sqrt(cor(k,k)-sum)
43      continue
C       Ouput data to a file
        open(unit=11,name='chog3.dat',status='NEW')
        do 53 k=1,n2
           do 51 i = 1,k
              write(11,*) cho(k,i)
51         continue
           write(6,*) k
53      continue
        close(unit=11)
        stop
        end
```

```
C*****************************************************************
C                                                                *
C  Prgm: GESURF.FOR                                              *
C                                                                *
C  Purpose:  Generate the data which represents the rough        *
C    surface.                                                    *
C                                                                *
C  Algorithm:  Implements Eq (xx) to generate a set of           *
C    correlated data points, each of which represents the        *
C    surface height at a given point.  There are two basic       *
C    parts of this program.  The first part generates the        *
C    vectors of uncorrelated Gaussian and exponential surface    *
C    heights using a Monte-Carlo technique.  The second part     *
C    multiplies this vector by the Cholesky sqrt of the          *
C    correlation matrix to get the vector of correlated          *
C    surface heights.                                            *
C                                                                *
C  Input Files: The Cholesky sqrt file generated by CHOLESKY     *
C  Output Files:  A Gaussian and an exponential surface file.    *
C                                                                *
C*****************************************************************
      parameter(n2=225)
      virtual cho(n2,n2)
      dimension g(n2),e(n2),sg(n2),se(n2)
      integer*4 seed
      real*8 u1,u2,api,gval,eval
      character*11 infile,gfile,efile
      write(6,10)
10    format(1x,'inputting cholesky data file ')
11    format(1x,'input output gaussian file name')
12    format(1x,'input output exponential file name')
C     get data from the Cholesky sqrt file.
      open(unit=11,name='chog3.dat',status='OLD')
      do 34 i=1,n2
         do 33 j=1,i
            read(11,*) cho(i,j)
33       continue
34    continue
      close(unit=11)
35    continue
C     Assign name for the Gaussian surface file
      write(6,11)
      read(5,*) gfile
C     Assign name for the exponential surface file
      write(6,12)
      read(5,*) efile
      write(6,40)
C     Input a random number generator seed to make this a unique
C     set of surfaces
40    format(1x,'input seed')
      read(5,*) seed
      api = 4*atan(1.0)
      kount = 1
```

(Prgm GESURF.FOR cont.)

```
C       Monte-Carlo methos of generating uncorrelated Gaussian
C       surface heights.  The maximum height possible of being
C       generated is 5 standard deviations.  The variance is set
C       to 1
50      u1 = ran(seed)
        u1 = (u1-.5)*10.0
        u2 = ran(seed)
        gval=exp(-u1**2/2.0)/sqrt(2.0*api)
        if (u2 .lt. gval) then
           g(kount) = u1
           kount = kount+1
        end if
        if (kount .le. n2) go to 50

C       Create the uncorrelated exponential data by Monte-Carlo
        kount = 1
60      u1 = ran(seed)
        u1 = (u1-.5)*10.0
        u2 = ran(seed)
        eval = exp(-sqrt(u1**2))/2.0
        if (u2 .lt. eval) then
           e(kount) = u1
           kount = kount+1
        end if
        if (kount .le. n2) go to 60
C       open the output files
        open(unit=11,name=gfile,status='NEW')
        open(unit=12,name=efile,status='NEW')
C       perform the matric /vector multiplication and output data
        do 74 i = 1,n2
           sg(i) = 0.0
           se(i) = 0.0
           do 73 j = 1,i
              sg(i) = sg(i)+g(j)*cho(i,j)
              se(i) = se(i)+e(j)*cho(i,j)
c             write(6,*) cho(i,j)
73         continue
           write(11,*) sg(i)
           write(12,*) se(i)
74      continue
        close(unit=11)
        close(unit=12)
C       loop back to create another surface if desired.
80      format(' Input a 1 if go again, -1 to stop.')
        write(6,80)
        read(6,*) nagain
        if (nagain .EQ. 1) then
           go to 35
        end if
        stop
        end
```

```
C*****************************************************************
C                                                                *
C   Prgm: BUILD.FOR                                              *
C                                                                *
C   Purpose:  Builds a data file on the format required by       *
C     the Radar Cross Section-Basic Scattering Code from         *
C     the surface files created by GESURF.                       *
C                                                                *
C   Algorithm:  Outputs the proper control codes and             *
C     parameters to have the RCS-BSC operate in the perfect      *
C     conductor, physical optics mode and at the proper          *
C     frequency.  Also, outputs the scaled surface data as       *
C     392 flat triangle so that there are no convex/concave      *
C     surfaces.                                                  *
C                                                                *
C   Input files: A surface file created by GESURF                *
C   Output files:  A data file for input to RCS-BSC              *
C                                                                *
C*****************************************************************

      parameter(nblock=14)
      dimension z(15,15),plate(392,3,3)
      space=1.0/(nblock*1.0)
      api=4*atan(1.0)

C     Input the mean surface slope required.
      write(6,4)
      read(5,*) s
4     format(' Input the atn(s) angle')

C     Calculate the scale factor to multiply the heights by.
C     Use the equation atan(s)=2h/l and the fact that the
C     surfaces were generated with h=1.  Thus h=atan(s)*l/(2).
C     Since there are a total of (14*.3) correlation lenghts in
C     each direction of the surface, a single correlation length
C     is equal to 1/(14*.3) units.  Therefore, the scale factor
C     becomes
      scale=tan(s*api/180.0)/(28.*.3)

C     Open a surface data file and read in data.
5     format(' Opened .dat')
      open(unit=11,name='G8.dat',status='OLD')
      write(6,5)
      do 30 i=1,15
         do 20 j=1,15
            read(11,*) z(i,j)
c           write(6,*) z(i,j)
20       continue
30    continue
      close(unit=11)
```

(Prgm BUILD.FOR cont.)

```
C       Calculate the x,y and z coordinates of each corner of the
C       triangle to be input to the program as an individual plate.
        do 50 n=1,nblock
           write(6,*) n
           do 40 m=1,nblock
              nop=(n-1)*2*nblock+(2*m)-1
              plate(nop,1,1)=(m-1)*space
              plate(nop,1,2)=(n-1)*space
              plate(nop,1,3)=z(n,m)*scale
              plate(nop,2,1)=m*space
              plate(nop,2,2)=(n-1)*space
              plate(nop,2,3)=z(n,m+1)*scale
              plate(nop,3,1)=m*space
              plate(nop,3,2)=n*space
              plate(nop,3,3)=z(n+1,m+1)*scale

C             Calculate total surface area of the surface
              delx=(plate(nop,2,1)-plate(nop,1,1))**2
              delz=(plate(nop,2,3)-plate(nop,1,3))**2
              xlen=sqrt(delx+delz)
              dely=(plate(nop,2,2)-plate(nop,3,2))**2
              delz=(plate(nop,2,3)-plate(nop,3,3))**2
              ylen=sqrt(dely+delz)
              area=area+(xlen*ylen)/2
              nop=nop+1
              plate(nop,2,1)=(m-1)*space
              plate(nop,2,2)=n*space
              plate(nop,2,3)=z(n+1,m)*scale
              do 39 nk=1,3
                 plate(nop,1,nk)=plate((nop-1),1,nk)
                 plate(nop,3,nk)=plate((nop-1),3,nk)
39            continue
              delx=(plate(nop,2,1)-plate(nop,3,1))**2
              delz=(plate(nop,2,3)-plate(nop,2,3))**2
              xlen=sqrt(delx+delz)
              dely=(plate(nop,1,2)-plate(nop,2,2))**2
              delz=(plate(nop,1,3)-plate(nop,2,3))**2
              ylen=sqrt(dely+delz)
              area=area+(xlen*ylen)/2
40         continue
50      continue
        write(6,75) area
75      format('    Area = ',f10.7)

C       Output to RCS-BSC file
C       while setting parameters
        open(unit=11,name='G8RCS.DAT',status='NEW',carriagecontrol='NONE')
100     format( f10.8,',',f10.8,',',f10.8)
105     format('PG:')
107     format('3')
110     format('TO:')
```

```
115     format('F,F,F,F')
120     format('F,F,F')
125     format('F')
        (Prgm BUILD.FOR cont.)

126     format('T,F,F,F,F,F')
127     format('F,F,F')
128     format('F,F,F,F')
C        (Prgm BUILD.FOR cont.)
130     format('UN:')
135     format('1')
140     format('PD:')
145     format('0.0,0.0,90.0,0.0')
150     format('F,90.0')
155     format('-90,90,5')
160     format('BK:')
165     format('0.0')
170     format('PP:')
175     format('T')
176     format('T,3.,3.')
177     format('0.,90.,10.')
178     format('0.,30.,10.')
180     format('LP:')
185     format('T')
190     format('FR:')
195     format('5.46')
c       last one is frequency Ghz
        write(11,110)
        write(11,115)
        write(11,120)
        write(11,125)
        write(11,126)
        write(11,127)
        write(11,128)
        write(11,130)
        write(11,135)
        write(11,140)
        write(11,145)
        write(11,150)
        write(11,155)
        write(11,160)
        write(11,165)
        write(11,170)
        write(11,175)
        write(11,176)
        write(11,177)
        write(11,178)
        write(11,180)
        write(11,185)
        write(11,190)
        write(11,195)
200     continue
```

```
(Prgm BUILD.FOR cont.)

C       Ouput (x,y,z) of triangle points
        do 250 i=1,2*nblock*nblock
           write(11,105)
           write(11,107)
           do 220 j=1,3
              write(11,100) plate(i,j,1),plate(i,j,2),plate(i,j,3)
220        continue
250     continue
300     format('XQ:')
305     format('EN:')
        write(11,300)
        write(11,305)
        close(unit=11)
        stop
        end
```

Appendix E

Computer Generated Rough Surfaces and

their Computed Radar Cross Sections

This appendix contains the graphs of the computer generated Gaussian and exponential surfaces along with tables of the computed RCS values. The tables contain the predicted RCS's for each accompanying figure at discrete angles from normal incidence (0°) to edge on incidence (90°). The RCS's are tabulated for two different frequencies, 5.76 Ghz and 17 Ghz, and for two different values of mean surface slope (atan(2h/l)). Therefore, there are four sets of RCS's values associated with each surface. The combination of a 5.76 Ghz frequency and a mean surface slope of 5° results in a Rayleigh parameter of hk=5. A mean surface slope of 25° at 5.76 Ghz results in hk=16. When the frequency is increased to 17 Ghz, hk=27 at 5° and hk=83 at 25°. Each table also includes the physical optics RCS values for a perfectly flat plate at the two frequencies for comparison. All computations assume perfect conductivity. Figure E.21 is added to contrast surfaces with a mean slopes of $5^{\circ}$and 25°.

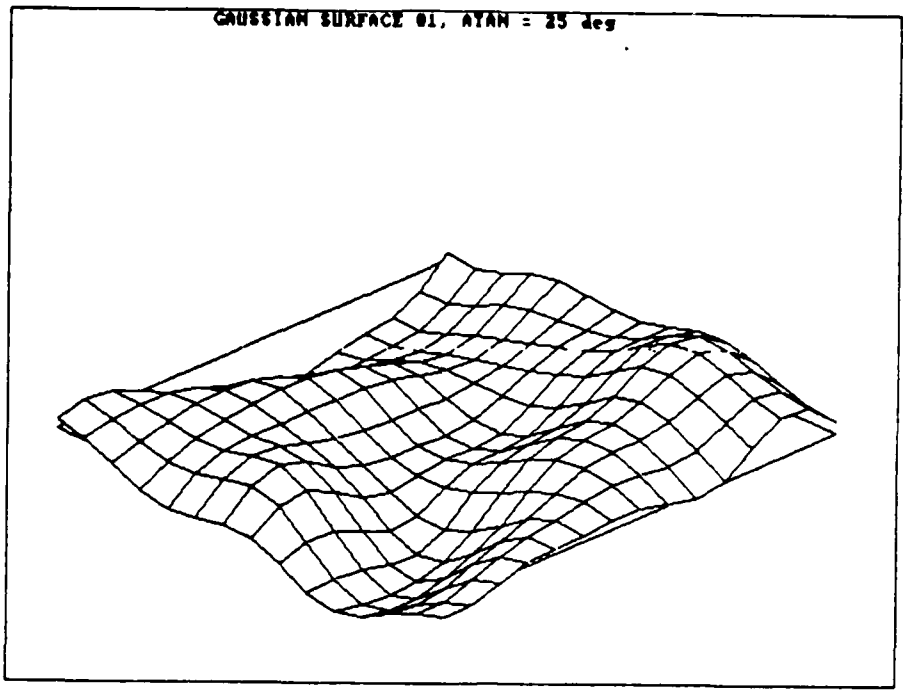

TABLE E.1

<RCS>/Area in dBsm

Ang	Gaussian #01 atan(s)=5 hk=5	Gaussian #01 atan(s)=5 hk=27	Gaussian #01 atan(s)=25 hk=16	Gaussian #01 atan(s)=25 hk=83	Flat k=114	Flat k=357
0	14.79	19.42	0.34	-11.07	36.20	46.08
5	16.21	16.50	1.82	4.47	10.55	5.64
10	6.71	5.84	13.91	1.86	8.73	7.54
15	-4.93	-11.18	-9.37	0.59	6.25	6.13
20	-14.31	-14.21	11.28	7.71	3.74	-3.96
25	-10.70	-25.35	6.27	5.27	1.18	-20.52
30	-9.72	-13.11	1.63	4.79	-4.28	-5.54
35	-9.15	-18.38	-0.74	3.60	-11.69	-7.33
40	-12.61	-15.28	-6.35	-11.73	-3.75	-20.65
45	-15.09	-17.21	-15.94	-11.28	-8.26	-5.93
50	-23.09	-25.19	-18.03	-29.15	-17.30	-22.52
55	-17.29	-20.73	-20.53	-25.09	-14.49	-19.59
60	-16.43	-33.70	-15.54	-25.06	-9.85	-10.08
65	-17.58	-19.27	-21.13	-16.52	-37.22	-41.25
70	-15.28	-23.18	-17.70	-35.32	-17.25	-17.77
75	-18.57	-26.54	-21.99	-21.46	-21.47	-19.83
80	-31.81	-21.51	-27.85	-23.77	-28.48	-31.13
85	-26.11	-28.05	-24.32	-16.06	-28.15	-30.60
90	-36.35	-28.44	-21.81	-13.91	-99999	-99999

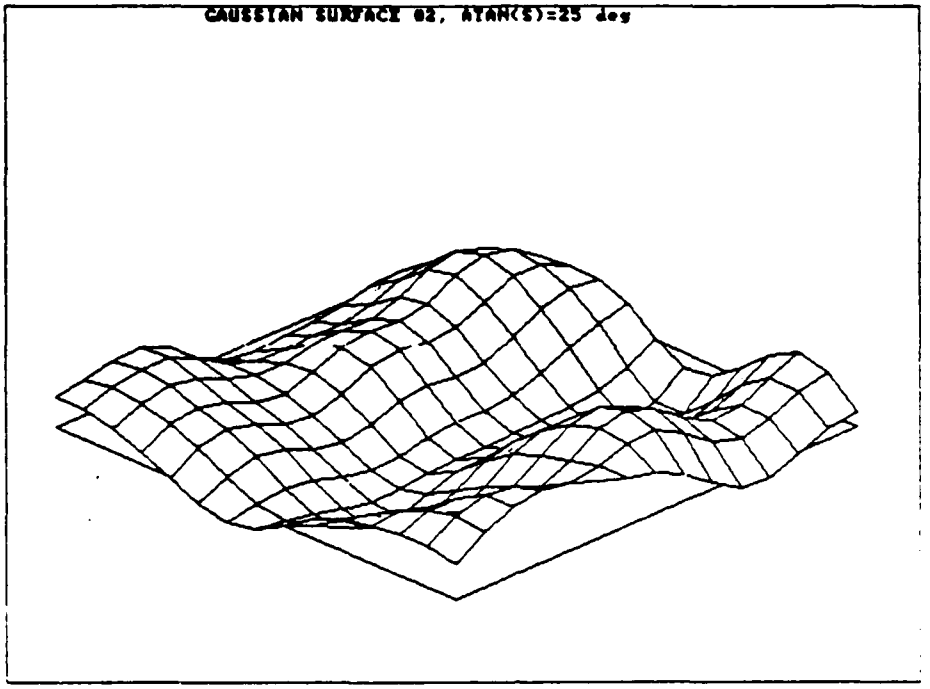

TABLE E.2

<RCS>/Area in dBsm

Ang	Gaussian #02 atan(s)=5 hk=5	Gaussian #02 atan(s)=5 hk=27	Gaussian #02 atan(s)=25 hk=16	Gaussian #02 atan(s)=25 hk=83	Flat k=114	Flat k=357
0	18.34	16.55	6.35	6.29	36.20	46.08
5	19.91	19.99	0.61	4.24	10.55	5.64
10	5.92	2.36	-4.31	6.90	8.73	7.54
15	-2.65	-7.35	1.86	5.46	6.25	6.13
20	-5.51	-13.23	6.15	3.64	3.74	-3.96
25	-3.76	-15.72	9.80	-7.68	1.18	-20.52
30	-18.99	-18.87	7.68	5.44	-4.28	-5.54
35	-13.03	-14.50	5.32	-0.20	-11.69	-7.33
40	-17.51	-18.49	-0.12	-2.19	-3.75	-20.65
45	-15.03	-20.61	-3.92	-6.94	-8.26	-5.93
50	-12.45	-15.85	-14.56	-13.76	-17.30	-22.52
55	-24.07	-18.95	-17.84	-17.11	-14.49	-19.59
60	-15.01	-17.95	-15.65	-17.44	-9.85	-10.08
65	-23.49	-31.51	-12.46	-26.00	-37.22	-41.25
70	-16.67	-23.73	-21.20	-20.25	-17.25	-17.77
75	-19.96	-24.77	-22.06	-28.97	-21.47	-19.83
80	-25.53	-17.39	-21.03	-26.48	-28.48	-31.13
85	-25.42	-33.98	-15.95	-20.98	-28.15	-30.60
90	-30.03	-30.19	-15.44	-15.39	-99999	-99999

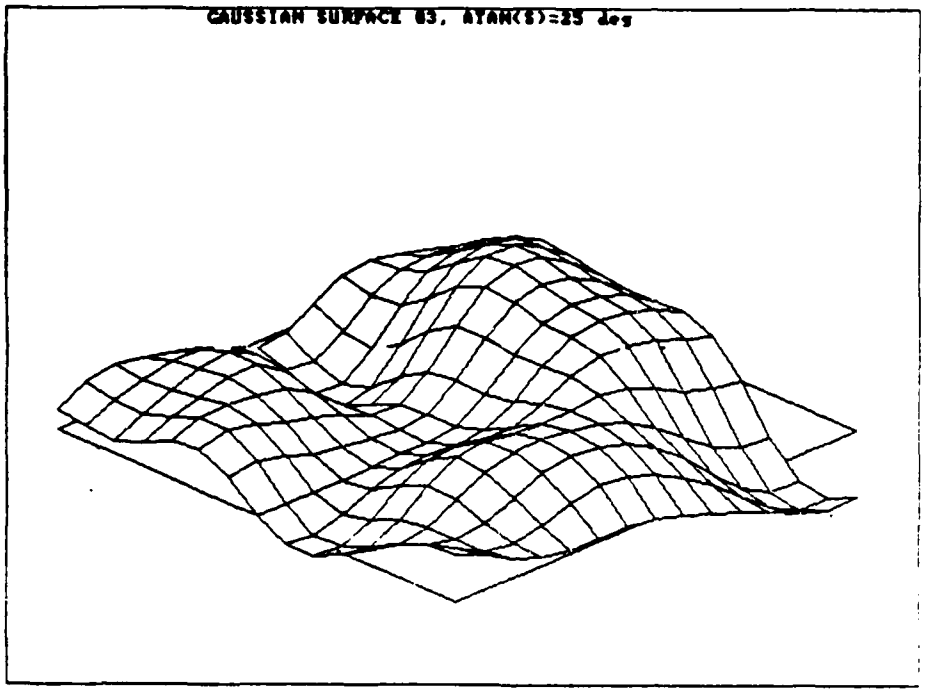

TABLE E.3

<RCS>/Area in dBsm

	Gaussian #03				Flat	
	atan(s)=5		atan(s)=25			
Ang	hk=5	hk=27	hk=16	hk=83	k=114	k=357
0	11.36	16.36	7.52	4.46	36.20	46.08
5	11.13	13.57	8.22	-9.48	10.55	5.64
10	-1.98	-1.14	1.97	3.31	8.73	7.54
15	-14.04	-0.23	5.14	-1.41	6.25	6.13
20	-8.16	-12.31	-11.63	4.58	3.74	-3.96
25	-7.25	-25.38	-12.57	-10.20	1.18	-20.52
30	-11.17	-15.83	5.46	3.44	-4.28	-5.54
35	-11.18	-18.82	-10.50	5.07	-11.69	-7.33
40	-12.96	-26.90	2.77	3.90	-3.75	-20.65
45	-11.00	-16.14	2.31	-8.51	-8.26	-5.93
50	-9.97	-28.52	-10.17	-5.38	-17.30	-22.52
55	-17.78	-27.09	-7.01	-13.40	-14.49	-19.59
60	-14.69	-24.54	-9.24	-22.26	-9.85	-10.08
65	-20.23	-25.69	-11.40	-17.07	-37.22	-41.25
70	-25.89	-25.34	-18.13	-26.89	-17.25	-17.77
75	-27.65	-22.78	-23.57	-31.47	-21.47	-19.83
80	-23.97	-18.21	-17.67	-26.36	-28.48	-31.13
85	-25.86	-31.91	-22.03	-20.60	-28.15	-30.60
90	-29.62	-30.44	-15.47	-16.10	-99999	-99999

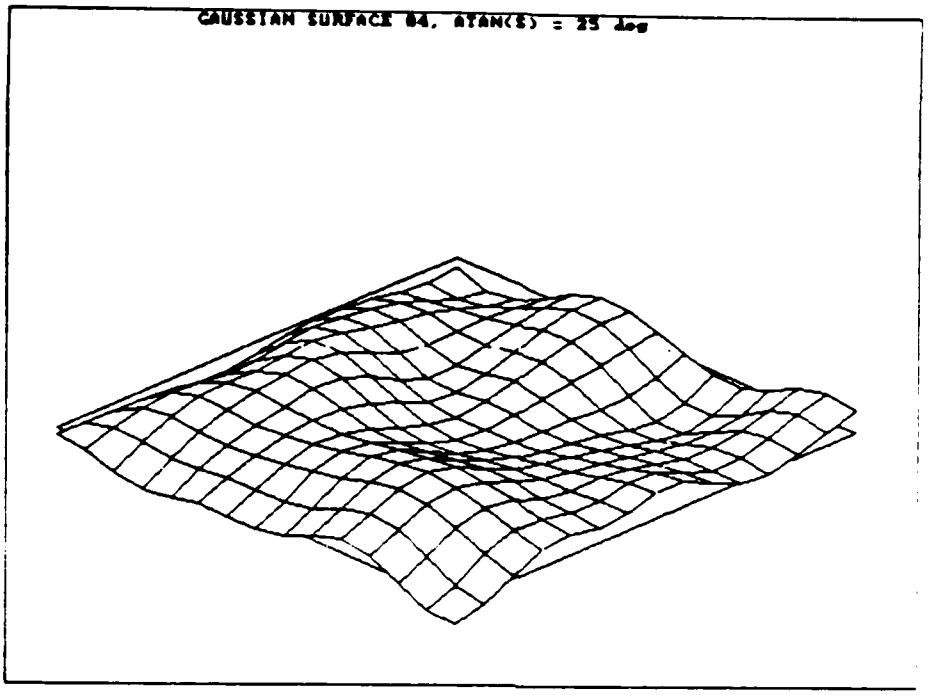

TABLE E.4

<RCS>/Area in dBsm

Ang	Gaussian atan(s)=5 hk=5	Gaussian atan(s)=5 hk=27	Gaussian atan(s)=25 hk=16	Gaussian atan(s)=25 hk=83	Flat k=114	Flat k=357
0	29.28	26.90	6.23	8.47	36.20	46.08
5	8.24	8.37	6.70	6.18	10.55	5.64
10	7.22	1.05	9.28	1.28	8.73	7.54
15	2.45	0.36	2.54	4.41	6.25	6.13
20	1.38	-12.13	1.21	-3.19	3.74	-3.96
25	-1.99	-11.65	-3.19	-8.51	1.18	-20.32
30	-2.42	-8.28	-17.92	-12.52	-4.28	-5.54
35	-13.85	-16.43	-11.01	-24.25	-11.69	-7.33
40	-5.64	-12.12	-21.15	-31.19	-3.75	-20.65
45	-17.91	-18.32	-21.72	-24.22	-8.26	-5.93
50	-44.50	-12.72	-21.90	-22.14	-17.30	-22.52
55	-39.19	-12.96	-19.43	-26.90	-14.49	-19.59
60	-12.85	-19.52	-22.33	-19.81	-9.85	-10.08
65	-21.31	-21.97	-28.96	-26.43	-37.22	-41.25
70	-16.25	-25.03	-23.97	-24.24	-17.25	-17.77
75	-20.42	-20.70	-25.69	-25.63	-21.47	-19.83
80	-29.43	-21.02	-24.09	-28.07	-28.48	-31.13
85	-29.56	-41.32	-27.34	-17.05	-28.15	-30.60
90	-36.28	-34.10	-20.60	-18.70	-99999	-99999

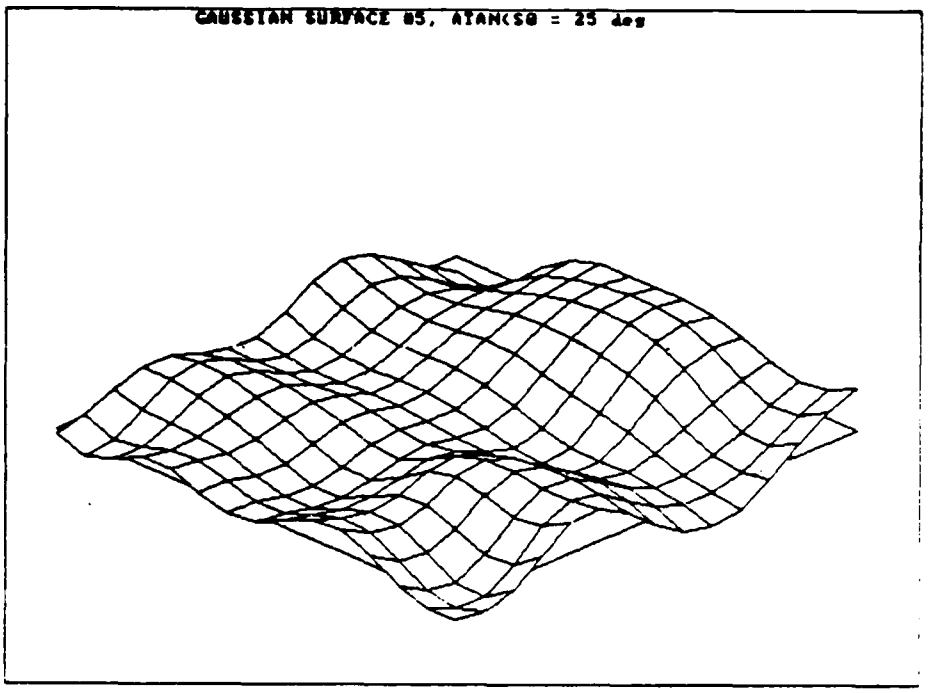

TABLE E.5

<RCS>/Area in dBsm

Ang	Gaussian =05 atan(s)=5 hk=5	Gaussian =05 atan(s)=5 hk=27	Gaussian =05 atan(s)=25 hk=16	Gaussian =05 atan(s)=25 hk=83	Flat k=114	Flat k=557
0	24.99	26.30	11.56	5.55	36.20	46.08
5	10.01	-6.05	0.57	5.54	10.55	5.64
10	-12.67	-10.83	13.33	8.82	8.73	7.54
15	-4.07	-12.19	6.34	6.21	6.25	6.13
20	-14.18	-16.63	0.79	-19.23	3.74	-3.96
25	-10.61	-16.40	-6.52	-6.10	1.18	-20.52
30	-8.94	-16.05	-5.34	-12.85	-4.28	-5.54
35	-9.79	-23.31	-20.27	-23.71	-11.69	-7.33
40	-12.15	-20.79	-16.71	-20.42	-3.75	-20.65
45	-10.13	-24.87	-26.73	-20.01	-8.26	-5.93
50	-12.11	-29.71	-21.40	-26.18	-17.30	-22.52
55	-11.99	-22.62	-21.08	-23.48	-14.49	-19.59
60	-13.87	-18.45	-28.22	-25.56	-9.85	-10.08
65	-25.13	-39.13	-22.75	-32.95	-37.22	-41.25
70	-21.51	-38.38	-26.55	-37.09	-17.25	-17.77
75	-24.91	-23.10	-24.74	-29.82	-21.47	-19.83
80	-24.85	-21.16	-23.48	-24.08	-28.48	-31.13
85	-27.83	-43.52	-27.68	-25.39	-28.15	-30.60
90	-28.82	-35.44	-14.12	-21.19	-99999	-99999

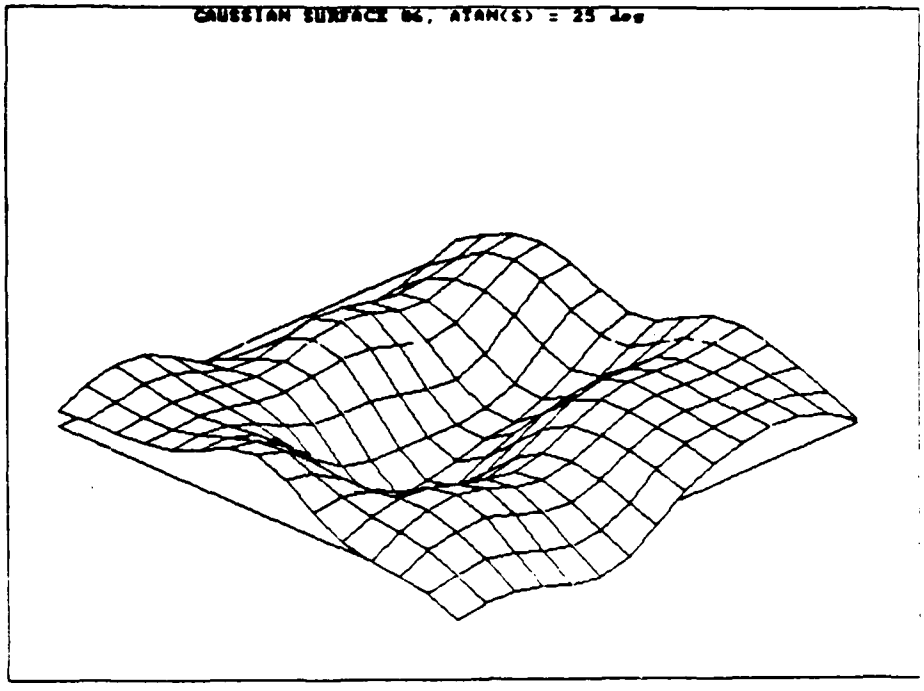

TABLE E.6

<RCS>/Area in dBsm

	Gaussian #06				Flat	
	atan(s)=5		atan(s)=25			
Ang	hk=5	hk=27	hk=16	hk=83	k=114	k=357
0	25.92	18.99	12.53	3.96	36.20	46.08
5	19.97	-0.36	14.17	6.11	10.55	5.64
10	12.57	6.32	1.16	3.12	8.73	7.54
15	-6.07	-2.79	6.18	-5.52	6.25	6.13
20	-17.46	-3.51	3.94	-6.24	3.74	-3.96
25	-4.20	-10.59	2.97	4.13	1.18	-20.52
30	-18.59	-17.00	10.61	3.31	-4.28	-5.54
35	-16.40	-28.88	-3.72	3.72	-11.69	-7.33
40	-19.56	-21.80	5.50	2.46	-3.75	-20.65
45	-13.90	-17.54	-2.31	2.71	-8.26	-5.93
50	-10.32	-17.80	0.81	-7.37	-17.30	-22.52
55	-20.02	-17.70	-13.40	-12.51	-14.49	-19.59
60	-14.29	-31.50	-14.42	-16.74	-9.85	-10.08
65	-26.45	-21.42	-19.43	-25.33	-37.22	-41.25
70	-21.99	-29.42	-11.25	-22.68	-17.25	-17.77
75	-24.50	-28.51	-19.07	-30.77	-21.47	-19.83
80	-24.44	-16.25	-38.53	-18.06	-28.48	-31.13
85	-28.04	-38.50	-20.80	-24.66	-28.15	-30.60
90	-32.53	-46.83	-17.99	-32.30	-99999	-99999

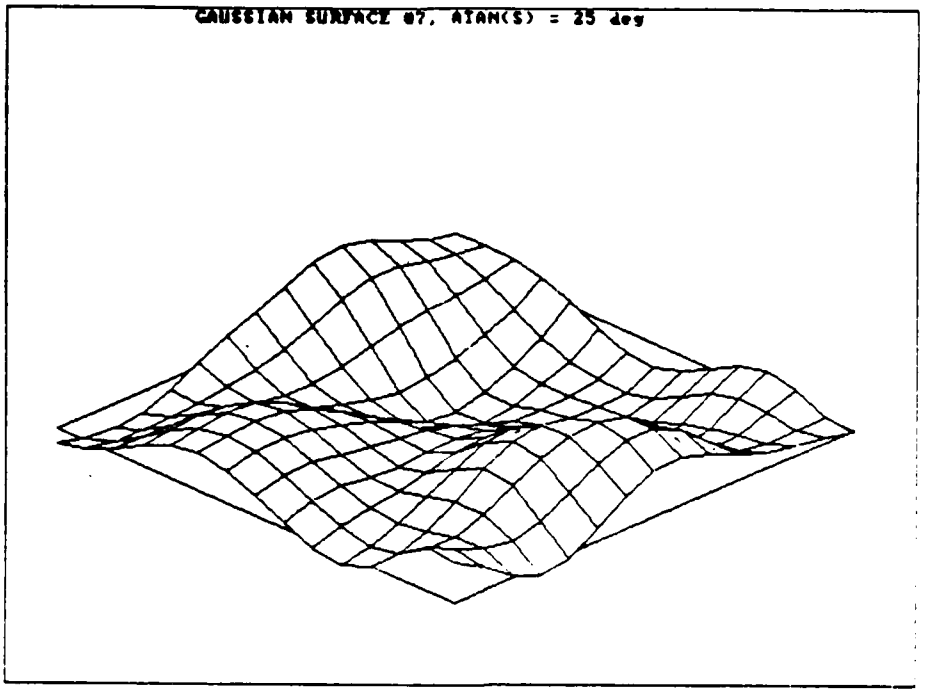

TABLE E.7

<RCS>/Area in dBsm

	Gaussian #07				Flat	
	atan(s)=5		atan(s)=25			
Ang	hk=5	hk=27	hk=16	hk=83	k=114	k=357
0	11.81	23.90	0.68	-2.85	36.20	46.08
5	8.19	16.76	6.26	-0.27	10.55	5.64
10	8.15	7.23	2.17	-2.39	8.73	7.54
15	-6.15	-19.06	9.80	-5.65	6.25	6.13
20	-16.13	-10.15	-1.41	2.69	3.74	-3.96
25	-13.25	-12.20	6.02	-13.37	1.18	-20.52
30	-17.07	-26.28	-3.07	-9.23	-4.28	-5.54
35	-10.24	-23.90	5.78	-4.13	-11.69	-7.33
40	-15.45	-20.80	-3.77	2.17	-3.75	-20.65
45	-11.71	-20.54	-3.93	-14.91	-8.26	-5.93
50	-14.76	-16.66	-13.94	-24.50	-17.30	-22.52
55	-17.35	-20.82	-10.54	-28.69	-14.49	-19.59
60	-12.83	-21.67	-24.64	-30.06	-9.85	-10.08
65	-24.39	-28.84	-15.50	-25.62	-37.22	-41.25
70	-18.46	-30.99	-24.60	-23.80	-17.25	-17.77
75	-21.38	-24.93	-28.55	-31.28	-21.47	-19.83
80	-26.40	-20.11	-36.55	-30.87	-28.48	-31.13
85	-25.11	-35.64	-18.45	-25.65	-28.15	-30.60
90	-29.28	-32.28	-15.01	-17.73	-99999	-99999

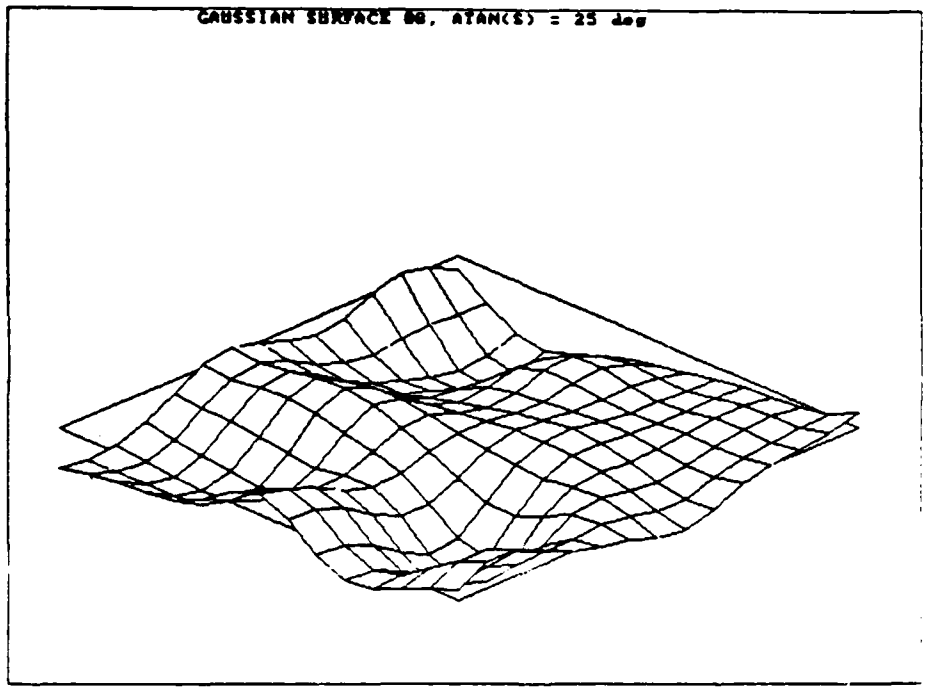

TABLE E.8

<RCS>/Area in dBsm

	Gaussian #08				Flat	
	atan(s)=5		atan(s)=25			
Ang	hk=5	hk=27	hk=16	hk=83	k=114	k=357
0	26.20	21.81	9.54	3.08	36.20	46.08
5	12.20	7.08	1.19	12.16	10.55	5.64
10	10.57	11.41	1.87	9.72	8.73	7.54
15	4.46	-3.26	-3.69	3.71	6.25	6.13
20	-2.07	-11.98	-5.98	3.93	3.74	-3.96
25	-3.20	-19.01	0.38	8.41	1.18	-20.52
30	-8.41	-14.08	3.23	-2.86	-4.28	-5.54
35	-21.74	-20.29	4.19	2.00	-11.69	-7.33
40	-6.99	-19.97	4.80	.38	-3.75	-20.65
45	-15.49	-18.86	2.60	- .16	-8.26	-5.93
50	-17.01	-17.48	-6.13	-..47	-17.30	-22.52
55	-24.15	-17.38	-5.18	-14.24	-14.49	-19.59
60	-11.86	-21.23	-23.22	-19.62	-9.85	-10.08
65	-22.94	-24.58	-15.66	-25.00	-37.22	-41.25
70	-16.68	-22.36	-13.14	-26.75	-17.25	-17.77
75	-19.81	-22.14	-21.61	-25.56	-21.47	-19.83
80	-26.64	-19.18	-15.24	-22.22	-28.48	-31.13
85	-26.16	-47.67	-18.27	-16.03	-28.15	-30.60
90	-36.09	-32.19	-22.03	-17.68	-99999	-99999

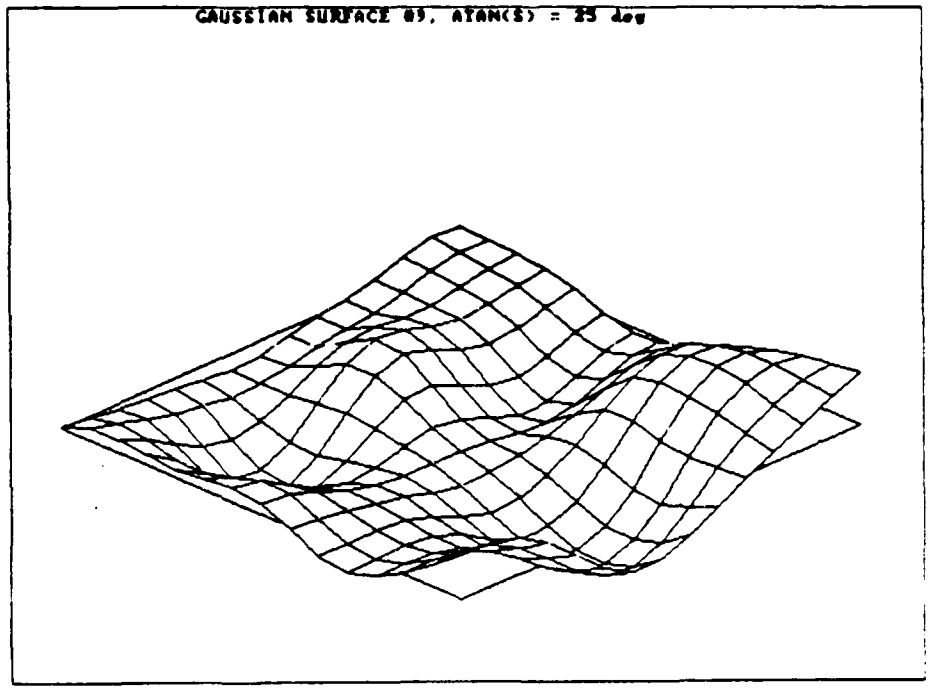

TABLE E.9

<RCS>/Area in dBsm

Ang	Gaussian #09 atan(s)=5 hk=5	Gaussian #09 atan(s)=5 hk=27	Gaussian #09 atan(s)=25 hk=16	Gaussian #09 atan(s)=25 hk=83	Flat k=114	Flat k=357
0	15.36	16.07	-2.16	4.04	36.20	46.08
5	12.95	13.82	11.56	11.27	10.55	5.64
10	-3.28	-11.40	1.16	1.95	8.73	7.54
15	-9.25	-10.04	0.67	2.37	6.25	6.13
20	-13.72	-9.65	0.47	13.71	3.74	-3.96
25	-16.53	-14.57	1.14	0.09	1.18	-20.52
30	-6.89	-11.06	-3.66	-6.44	-4.28	-5.54
35	-9.62	-16.86	-9.94	-15.75	-11.69	-7.33
40	-13.80	-13.98	-8.14	-13.44	-3.75	-20.65
45	-14.76	-16.86	-14.88	-18.30	-8.26	-5.93
50	-12.21	-21.22	-24.96	-25.19	-17.30	-22.52
55	-19.70	-25.41	-23.39	-25.34	-14.49	-19.59
60	-13.55	-24.75	-24.36	-36.52	-9.85	-10.08
65	-26.59	-24.80	-25.55	-22.05	-37.22	-41.25
70	-19.02	-28.84	-27.01	-27.07	-17.25	-17.77
75	-22.60	-29.77	-33.11	-23.16	-21.47	-19.83
80	-30.43	-20.38	-22.67	-33.56	-28.48	-31.13
85	-30.39	-36.02	-33.05	-39.75	-28.15	-30.60
90	-34.78	-43.17	-20.36	-28.79	-99999	-99999

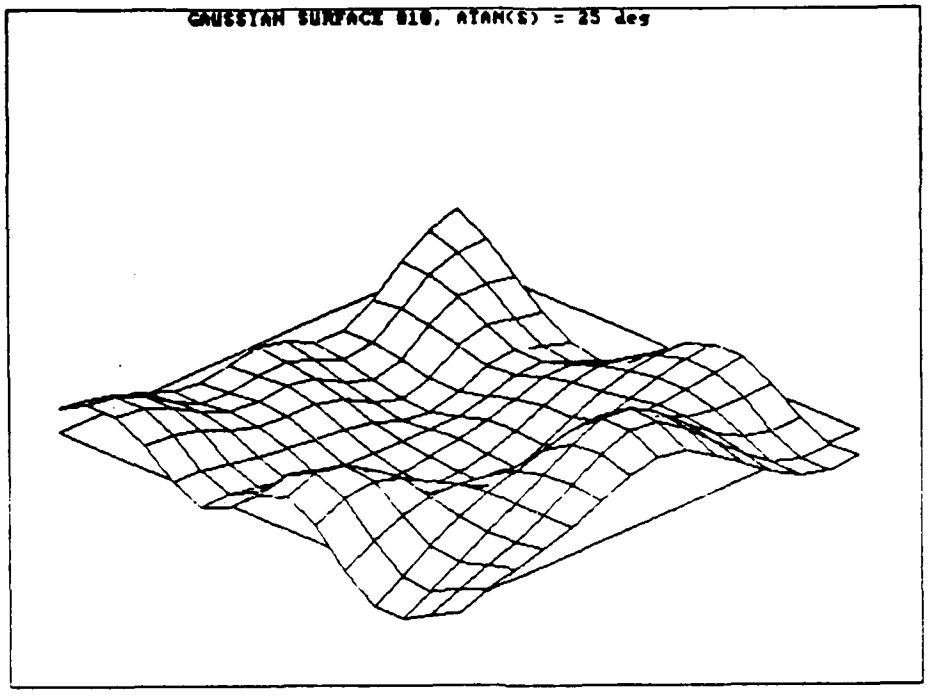

TABLE E.10

<RCS>/Area in dBsm

Ang	Gaussian =10 atan(s)=5 hk=5	Gaussian =10 atan(s)=5 hk=27	Gaussian =10 atan(s)=25 hk=16	Gaussian =10 atan(s)=25 hk=83	Flat k=114	Flat k=357
0	19.38	24.88	10.69	4.81	36.20	46.08
5	15.34	20.54	4.47	-7.37	10.55	5.64
10	-4.92	-3.17	5.47	0.32	8.73	7.54
15	-8.52	-7.78	5.35	-2.39	6.25	6.13
20	-10.80	-14.66	8.50	1.00	3.74	-3.96
25	-22.40	-14.94	6.78	4.98	1.18	-20.52
30	-16.85	-29.63	4.35	4.62	-4.28	-5.54
35	-13.97	-15.45	-22.71	-0.87	-11.69	-7.33
40	-17.89	-21.25	-7.07	-23.54	-3.75	-20.65
45	-21.54	-30.89	-29.34	-33.15	-8.26	-5.93
50	-16.54	-19.83	-25.23	-16.39	-17.30	-22.52
55	-21.14	-22.65	-17.69	-27.08	-14.49	-19.59
60	-17.69	-22.93	-26.05	-25.69	-9.85	-10.08
65	-22.76	-26.75	-27.32	-35.36	-37.22	-41.25
70	-17.25	-24.37	-20.61	-23.81	-17.25	-17.77
75	-20.14	-39.39	-21.05	-20.26	-21.47	-19.83
80	-32.68	-18.68	-22.89	-27.32	-28.48	-31.13
85	-26.87	-31.20	-18.86	-20.67	-28.15	-30.60
90	-42.33	-35.37	-28.70	-20.78	-99999	-99999

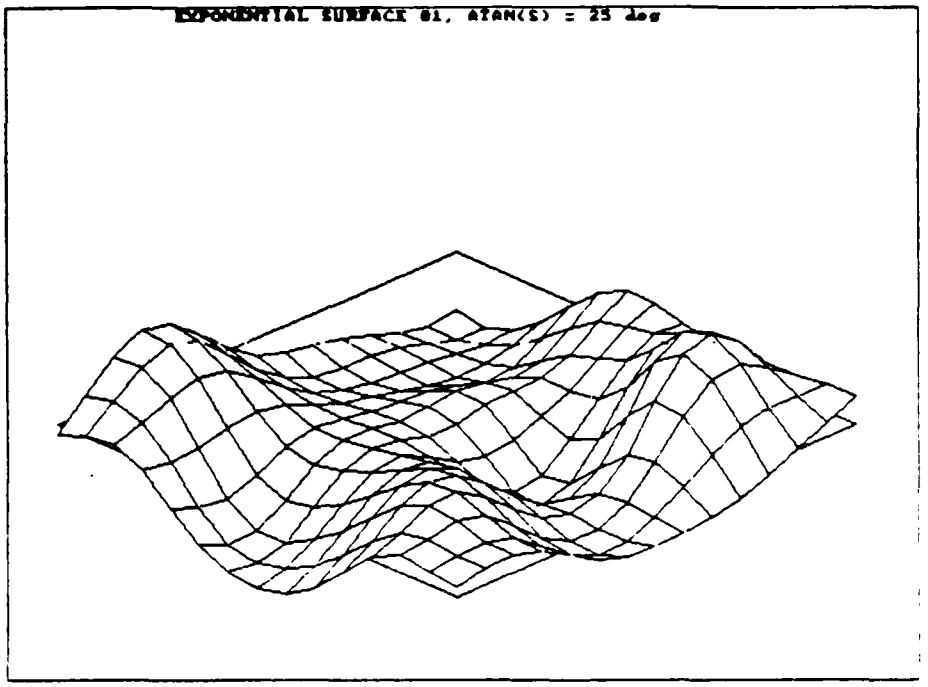

TABLE E.11

<RCS>/Area in dBsm

Ang	Exponential #01				Flat	
	atan(s)=5		atan(s)=25			
	hk=5	hk=27	hk=16	hk=83	k=114	k=357
0	18.97	20.71	5.69	0.63	36.20	46.08
5	3.87	4.24	2.20	-7.63	10.55	5.64
10	8.42	4.30	10.03	-16.53	8.73	7.54
15	0.03	-4.40	-14.36	4.37	6.25	6.13
20	-16.50	-4.63	1.63	-8.13	3.74	-3.96
25	-9.47	-15.38	-1.61	-3.66	1.18	-20.52
30	-8.98	-14.18	-4.76	2.54	-4.28	-5.54
35	-13.16	-38.60	-0.82	0.96	-11.69	-7.33
40	-17.31	-31.93	1.00	4.03	-3.75	-20.65
45	-27.69	-23.44	2.36	0.18	-8.26	-5.93
50	-15.34	-21.01	-2.31	-8.69	-17.30	-22.52
55	-18.95	-21.68	-14.39	-22.60	-14.19	-19.59
60	-20.00	-24.32	-27.06	-23.50	-9.85	-10.08
65	-23.39	-32.61	-19.50	-21.97	-37.22	-41.25
70	-19.18	-26.82	-21.21	-27.95	-17.25	-17.77
75	-22.69	-29.50	-23.58	-20.08	-21.47	-19.83
80	-29.24	-18.16	-19.73	-25.01	-28.48	-31.13
85	-27.54	-30.18	-31.17	-25.06	-28.15	-30.60
90	-38.22	-35.05	-23.79	-20.57	-99999	-99999

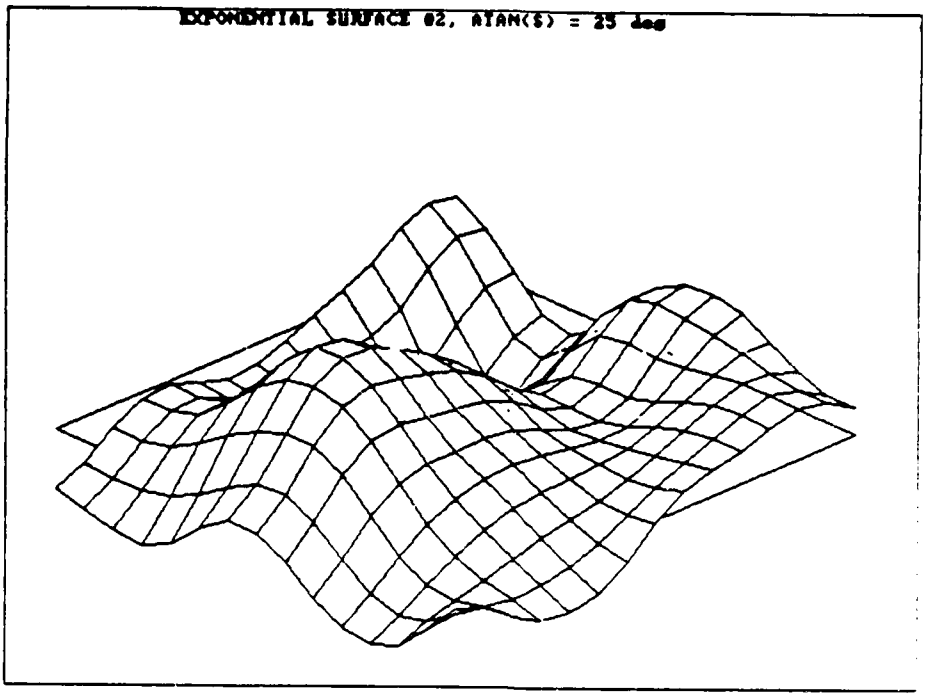

TABLE E.12

<RCS>/Area in dBsm

Ang	Exponential #02 atan(s)=5 hk=5	Exponential #02 atan(s)=5 hk=27	Exponential #02 atan(s)=25 hk=16	Exponential #02 atan(s)=25 hk=83	Flat k=114	Flat k=357
0	1.92	11.15	5.03	-1.26	36.20	46.08
5	16.48	18.05	2.27	4.03	10.55	5.64
10	8.74	-2.41	-14.91	4.62	8.73	7.54
15	-9.48	-8.92	7.26	-2.98	6.25	6.13
20	-9.69	-10.68	6.40	1.27	3.74	-3.96
25	-10.01	-16.48	-0.17	-2.76	1.18	-20.52
30	-15.09	-19.96	5.01	-0.13	-4.28	-5.54
35	-10.25	-20.75	6.76	6.10	-11.69	-7.33
40	-25.84	-23.04	-3.28	5.24	-3.75	-20.65
45	-16.61	-50.81	-2.35	1.14	-8.26	-5.93
50	-21.21	-22.36	-11.05	-14.22	-17.30	-22.52
55	-22.23	-27.80	-20.27	-18.03	-14.49	-19.59
60	-17.26	-25.03	-16.15	-19.45	-9.85	-10.08
65	-28.91	-27.18	-15.28	-29.14	-37.22	-41.25
70	-23.03	-28.48	-33.03	-22.25	-17.25	-17.77
75	-24.91	-37.67	-24.81	-27.26	-21.47	-19.83
80	-27.33	-25.97	-32.36	-26.11	-28.48	-31.13
85	-26.55	-39.14	-20.38	-28.06	-28.15	-30.60
90	-38.37	-43.70	-23.83	-29.16	-99999	-99999

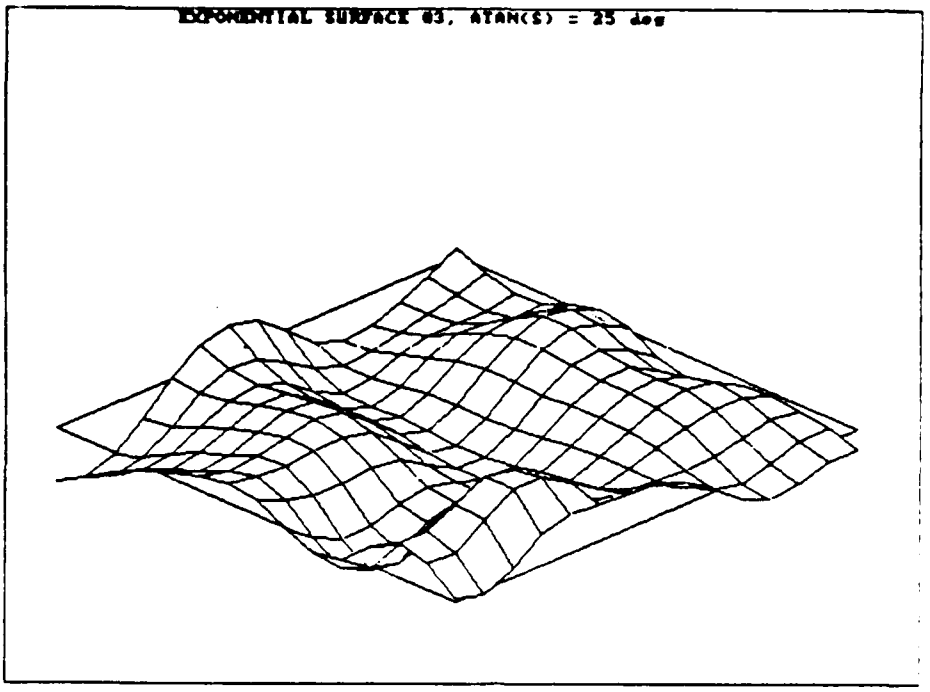

TABLE E.13

<RCS>/Area in dBsm

Ang	Exponential #03 atan(s)=5 hk=5	Exponential #03 atan(s)=5 hk=27	Exponential #03 atan(s)=25 hk=16	Exponential #03 atan(s)=25 hk=83	Flat k=114	Flat k=357
0	22.52	22.25	-0.02	11.71	36.20	46.08
5	18.13	12.19	5.31	0.98	10.55	5.64
10	4.23	0.33	8.72	-3.04	8.73	7.54
15	-6.58	-7.78	4.43	4.14	6.25	6.13
20	-7.73	-13.10	-1.60	-8.99	3.74	-3.96
25	-20.44	-10.21	5.79	3.83	1.18	-20.52
30	-21.87	-22.98	2.61	2.94	-4.28	-5.54
35	-31.18	-12.22	1.20	1.22	-11.69	-7.33
40	-22.62	-15.07	-2.48	3.89	-3.75	-20.65
45	-26.77	-19.91	-9.62	-24.66	-8.26	-5.93
50	-19.14	-20.36	-8.46	-24.16	-17.30	-22.52
55	-38.55	-28.51	-30.94	-25.82	-14.49	-19.59
60	-19.83	-21.14	-17.10	-16.55	-9.85	-10.08
65	-22.37	-29.15	-9.77	-24.15	-37.22	-41.25
70	-15.72	-32.34	-21.99	-16.53	-17.25	-17.77
75	-19.01	-29.61	-21.26	-21.49	-21.47	-19.83
80	-30.51	-18.51	-36.10	-30.14	-28.48	-31.13
85	-23.41	-40.38	-12.12	-32.00	-28.15	-30.60
90	-28.79	-28.91	-14.28	-14.35	-99999	-99999

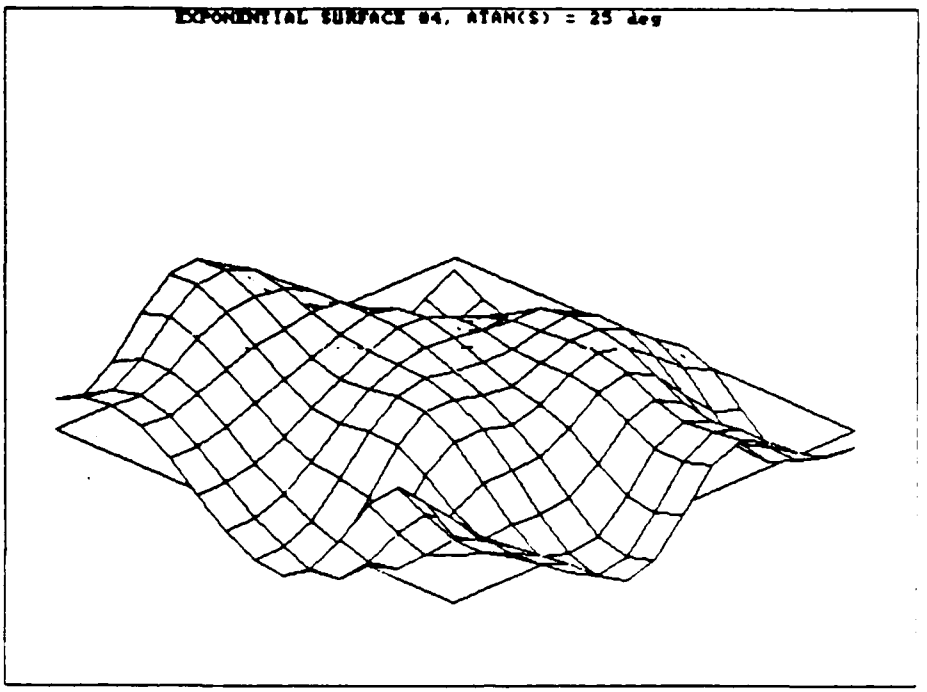

TABLE E.14

<RCS>/Area in dBsm

Ang	Exponential #04 atan(s)=5 hk=5	Exponential #04 atan(s)=5 hk=27	Exponential #04 atan(s)=25 hk=16	Exponential #04 atan(s)=25 hk=83	Flat k=114	Flat k=357
0	20.87	19.08	5.38	1.80	36.20	46.08
5	16.13	2.80	2.61	0.10	10.55	5.64
10	1.46	0.09	7.10	-3.11	8.73	7.54
15	-8.49	-5.61	6.01	-4.02	6.25	6.13
20	-8.52	-20.11	2.31	-1.73	3.74	-3.96
25	-12.16	-22.09	-2.23	1.62	1.18	-20.52
30	-14.88	-18.10	-1.20	-5.84	-4.28	-5.54
35	-24.03	-38.99	8.15	8.07	-11.69	-7.33
40	-25.33	-28.20	1.51	2.04	-3.75	-20.65
45	-21.66	-29.79	-13.01	-19.71	-8.26	-5.93
50	-24.41	-26.96	-37.23	-25.01	-17.30	-22.52
55	-20.87	-30.13	-16.20	-24.14	-14.49	-19.59
60	-27.83	-40.32	-20.62	-34.67	-9.85	-10.08
65	-22.09	-39.75	-22.92	-36.49	-37.22	-41.25
70	-22.71	-24.94	-35.08	-23.44	-17.25	-17.77
75	-25.59	-32.27	-28.65	-37.61	-21.47	-19.83
80	-34.21	-38.39	-34.40	-27.75	-28.48	-31.13
85	-31.68	-42.19	-28.24	-27.97	-28.15	-30.60
90	-33.25	-28.27	-19.23	-13.83	-99999	-99999

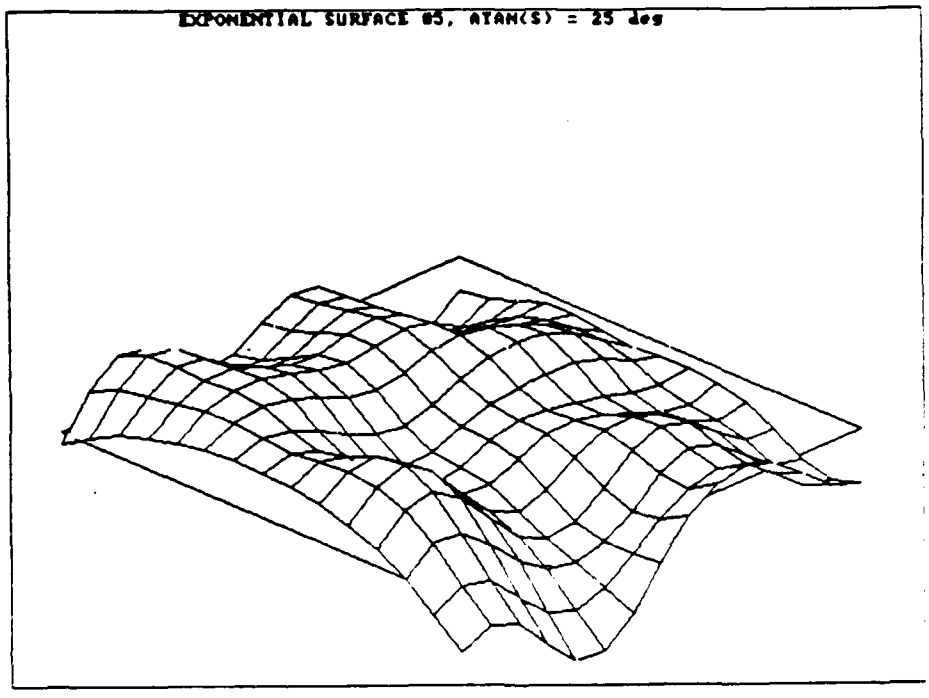

TABLE E.15

<RCS>/Area in dBsm

	Exponential #05				Flat	
	atan(s)=5		atan(s)=25			
Ang	hk=5	hk=27	hk=16	hk=83	k=114	k=357
0	16.92	15.14	4.89	-1.48	36.20	46.08
5	19.02	14.87	0.01	-1.24	10.55	5.64
10	3.16	3.55	-7.49	-1.89	8.73	7.54
15	-5.31	-7.94	-2.23	0.95	6.25	6.13
20	-10.77	-18.29	1.95	2.77	3.74	-3.96
25	-13.74	-39.03	-1.58	7.71	1.18	-20.52
30	-15.73	-22.27	4.69	-0.72	-4.28	-5.54
35	-15.05	-20.62	-1.46	-3.94	-11.69	-7.33
40	-21.66	-20.52	-6.80	-11.76	-3.75	-20.65
45	-16.87	-26.43	-3.41	-4.83	-8.26	-5.93
50	-17.82	-32.96	-11.13	-15.16	-17.30	-22.52
55	-25.56	-28.26	-13.55	-17.59	-14.49	-19.59
60	-37.33	-22.09	-17.39	-29.52	-9.85	-10.08
65	-19.96	-25.07	-18.26	-23.26	-37.22	-41.25
70	-32.70	-23.62	-22.94	-21.38	-17.25	-17.77
75	-41.57	-32.67	-19.06	-17.88	-21.47	-19.83
80	-24.85	-30.32	-19.03	-37.60	-28.48	-31.13
85	-31.52	-27.56	-19.26	-30.57	-28.15	-30.60
90	-29.71	-29.62	-15.16	-15.27	-99999	-99999

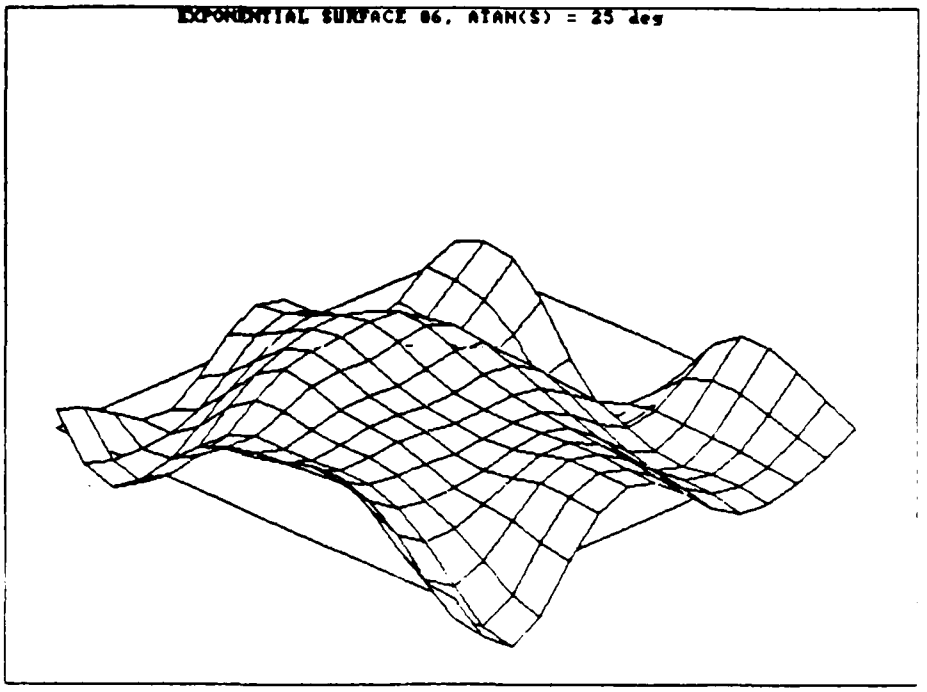

TABLE E.16

<RCS>/Area in dBsm

Ang	Exponential =06				Flat	
	atan(s)=5		atan(s)=25			
	hk=5	hk=27	hk=16	hk=83	k=114	k=357
0	23.18	21.23	-4.07	7.50	36.20	46.08
5	9.97	10.45	11.43	6.56	10.55	5.64
10	8.51	0.12	11.85	11.04	8.73	7.54
15	-4.59	-2.92	3.56	10.19	6.25	6.13
20	-11.13	-11.86	2.49	5.42	3.74	-3.96
25	-11.91	-17.71	-9.31	-3.47	1.18	-20.52
30	-25.57	-18.44	-4.56	0.37	-4.28	-5.54
35	-14.06	-22.60	-4.24	-1.20	-11.69	-7.33
40	-17.51	-25.18	-7.65	-16.74	-3.75	-20.65
45	-12.12	-35.93	-6.82	-5.32	-8.26	-5.93
50	-15.38	-29.64	-5.48	-1.63	-17.30	-22.52
55	-17.46	-28.68	-13.74	-12.16	-14.49	-19.59
60	-16.83	-28.46	-16.80	-21.03	-9.85	-10.08
65	-24.89	-30.77	-22.38	-19.17	-37.22	-41.25
70	-20.65	-28.05	-18.36	-35.45	-17.25	-17.77
75	-23.54	-25.34	-20.49	-29.32	-21.47	-19.83
80	-26.29	-20.85	-22.91	-29.97	-28.48	-31.13
85	-25.42	-30.57	-22.65	-22.20	-28.15	-30.60
90	-41.05	-35.74	-26.51	-21.21	-99999	-99999

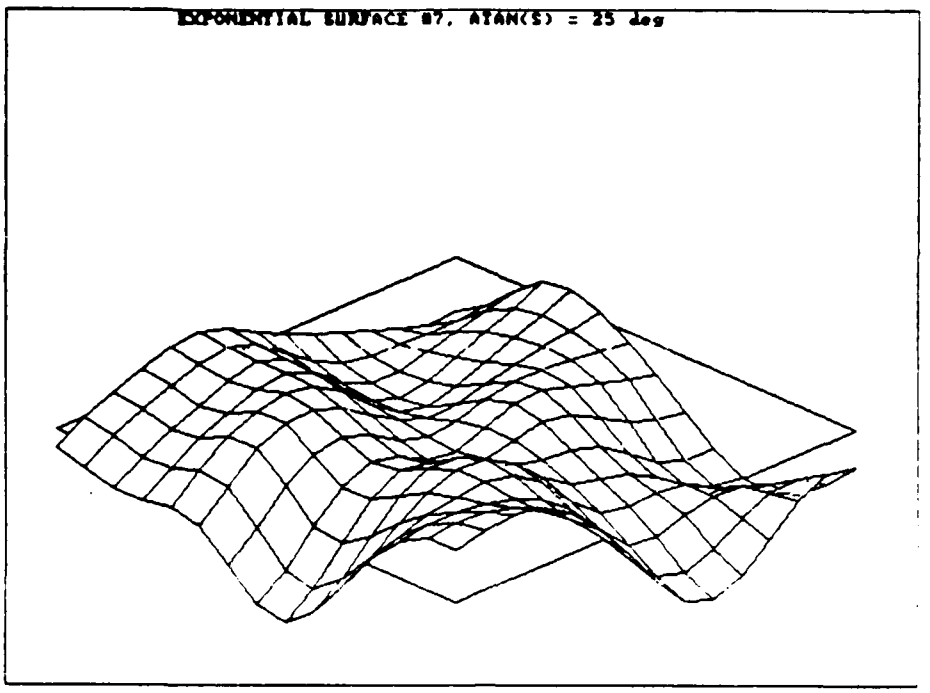

TABLE E.17

<RCS>/Area in dBsm

Ang	Exponential #07				Flat	
	atan(s)=5		atan(s)=25			
	hk=5	hk=27	hk=16	hk=83	k=114	k=357
0	7.68	17.38	0.73	-5.50	36.20	46.08
5	0.77	14.07	1.16	-1.89	10.55	5.64
10	2.24	1.75	-4.32	-0.22	8.73	7.54
15	-5.49	-6.71	-15.47	2.38	6.25	6.13
20	-10.97	-14.54	3.00	3.50	3.74	-3.96
25	-9.58	-23.46	2.91	-5.39	1.18	-20.52
30	-13.04	-13.28	-9.73	-1.83	-4.28	-5.54
35	-19.18	-23.57	-5.54	-1.67	-11.69	-7.33
40	-31.76	-16.78	-8.03	-14.58	-3.75	-20.65
45	-28.50	-27.14	-25.95	-25.22	-8.26	-5.93
50	-14.74	-20.80	-16.64	-38.61	-17.30	-22.52
55	-18.61	-21.26	-15.26	-26.28	-14.49	-19.59
60	-32.00	-19.30	-21.75	-32.71	-9.85	-10.08
65	-18.37	-28.44	-21.63	-34.25	-37.22	-41.25
70	-23.42	-31.21	-26.74	-23.84	-17.25	-17.77
75	-26.04	-33.27	-21.83	-29.63	-21.47	-19.83
80	-25.68	-23.80	-21.74	-25.94	-28.48	-31.13
85	-29.91	-41.39	-22.89	-18.96	-28.15	-30.60
90	-34.30	-29.81	-19.77	-15.27	-99999	-99999

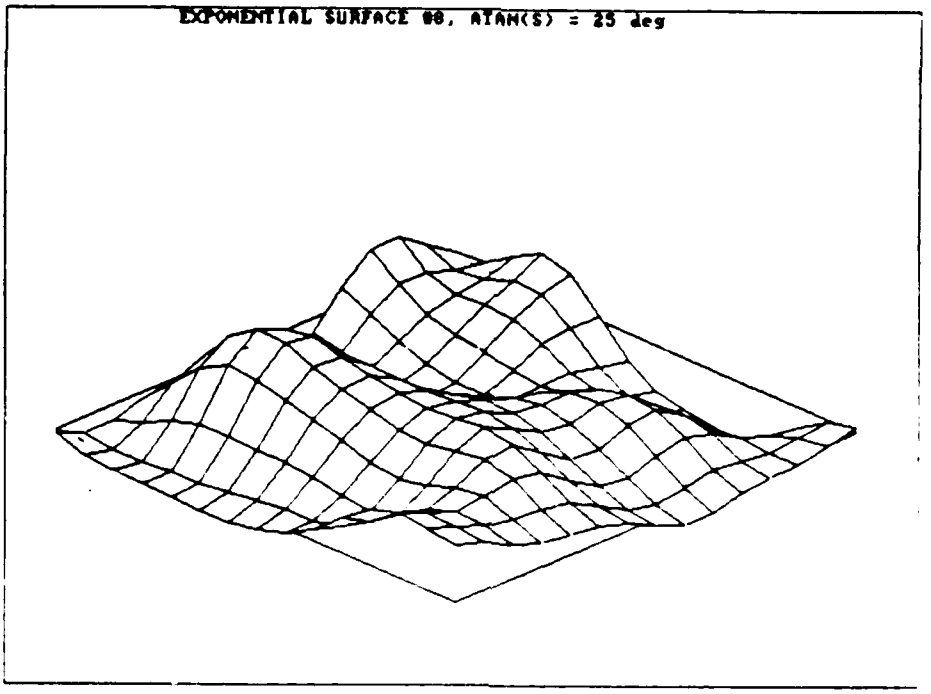

TABLE E.18

<RCS>/Area in dBsm

Ang	Exponential =6d atan(s)=5 hk=5	atan(s)=5 hk=27	atan(s)=25 hk=16	atan(s)=25 hk=33	Flat k=114	k=357
0	17.47	19.16	8.09	-4.77	36.20	46.08
5	12.19	13.11	4.91	-3.63	10.55	5.64
10	-19.76	4.92	-3.01	6.97	8.73	7.54
15	-10.23	-4.97	3.65	2.18	6.25	6.13
20	-15.59	-16.18	-3.40	-0.95	3.74	-3.96
25	-4.88	-18.00	-3.51	1.54	1.18	-20.52
30	-12.95	-16.58	5.92	5.95	-4.28	-5.54
35	-20.14	-20.94	3.58	2.04	-11.69	-7.33
40	-14.65	-16.87	-2.42	-3.76	-3.75	-20.65
45	-20.55	-25.10	-5.07	-17.22	-8.26	-5.92
50	-20.07	-19.29	-14.38	-19.06	-17.30	-22.52
55	-37.82	-26.12	-20.59	-25.39	-14.49	-19.59
60	-13.35	-24.91	-14.88	-20.62	-9.85	-10.08
65	-27.37	-33.37	-23.54	-39.23	-37.22	-41.25
70	-18.38	-29.89	-17.07	-35.02	-17.25	-17.77
75	-21.75	-34.30	-26.50	-29.57	-21.47	-19.83
80	-28.86	-23.59	-28.25	-24.87	-28.48	-31.13
85	-26.99	-35.04	-25.74	-22.38	-28.15	-30.60
90	-31.12	-31.01	-17.28	-15.83	-99999	-99999

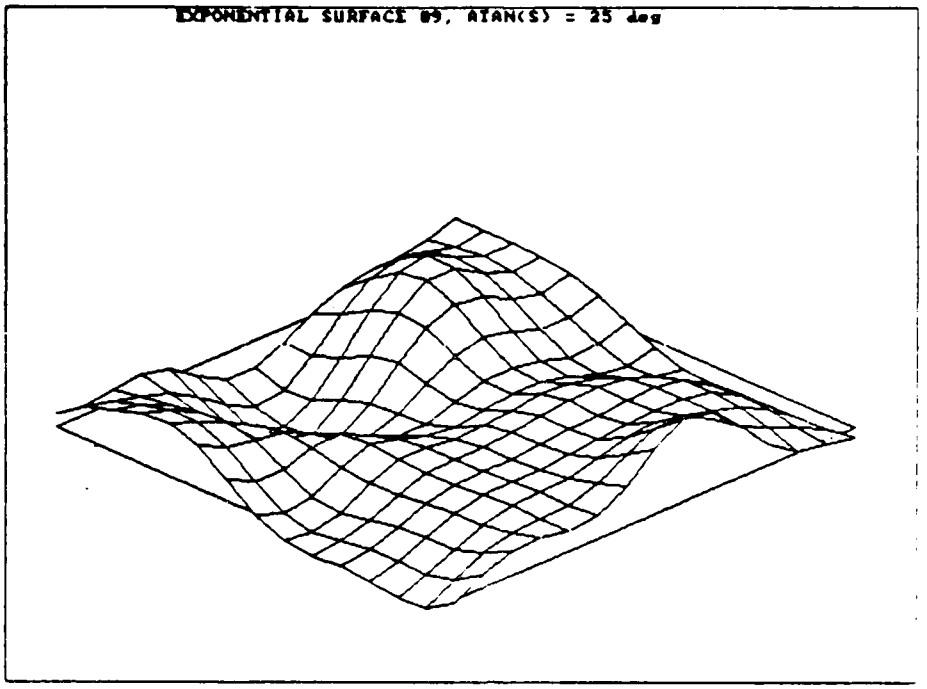

TABLE E.19

<RCS>/Area in dBsm

Ang	Exponential #09 atan(s)=5 hk=5	Exponential #09 atan(s)=5 hk=27	Exponential #09 atan(s)=25 hk=16	Exponential #09 atan(s)=25 hk=83	Flat k=114	Flat k=357
0	24.06	22.11	6.59	15.15	36.20	46.08
5	16.34	15.73	6.28	-18.36	10.55	5.64
10	-4.22	0.26	2.93	4.78	8.73	7.54
15	-3.87	-11.04	-0.12	-14.89	6.25	6.13
20	-4.66	-10.52	-4.70	-6.14	3.74	-3.96
25	-5.64	-9.43	3.22	-1.08	1.18	-20.52
30	-16.10	-14.16	-6.25	-11.31	-4.28	-5.54
35	-23.40	-14.28	-7.60	-10.31	-11.69	-7.33
40	-11.56	-18.15	-19.78	-19.90	-3.75	-20.65
45	-17.85	-18.15	-13.19	-21.92	-8.26	-5.93
50	-21.69	-23.75	-21.52	-32.51	-17.30	-22.52
55	-26.75	-22.89	-20.51	-26.18	-14.49	-19.59
60	-14.73	-25.47	-29.25	-23.10	-9.85	-10.08
65	-22.17	-28.13	-23.03	-25.82	-37.22	-41.25
70	-17.61	-26.87	-21.06	-24.30	-17.25	-17.77
75	-21.03	-24.82	-24.62	-20.64	-21.47	-19.83
80	-35.75	-21.62	-28.56	-30.58	-28.48	-31.13
85	-30.72	-33.95	-38.19	-25.56	-28.15	-30.60
90	-34.72	-33.61	-20.37	-19.90	-99999	-99999

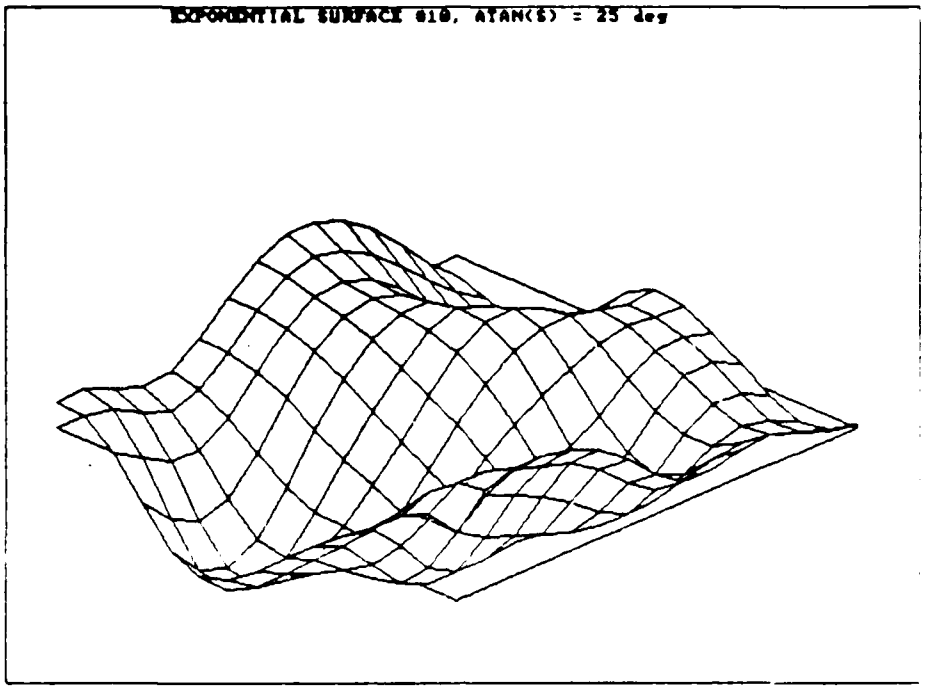

TABLE E.20

<RCS>/Area in dBsm

Ang	Exponential =10				Flat	
	atan(s)=5		atan(s)=25			
	hk=5	hk=27	hk=16	hk=83	k=114	k=357
0	16.48	15.64	0.92	-5.37	36.20	46.08
5	12.64	4.54	-4.17	1.41	10.55	5.64
10	9.60	10.59	-16.42	3.03	8.73	7.54
15	-2.51	-5.35	-14.47	6.07	6.25	6.13
20	-3.75	-12.59	0.58	5.41	3.74	-3.96
25	-4.87	-10.92	-10.55	2.35	1.18	-20.52
30	-10.41	-15.95	-13.76	-7.41	-4.28	-5.51
35	-26.71	-19.43	-14.09	-12.93	-11.69	-7.33
40	-12.23	-19.58	-8.35	-29.99	-3.75	-20.65
45	-19.30	-20.24	-0.50	2.87	-8.26	-5.92
50	-21.58	-25.66	-6.86	-11.41	-17.30	-22.52
55	-19.72	-31.85	-12.40	-22.72	-14.49	-19.59
60	-24.56	-32.05	-13.62	-16.42	-9.85	-10.08
65	-34.82	-30.00	-13.98	-25.39	-37.22	-41.25
70	-22.79	-24.19	-30.77	-29.33	-17.25	-17.77
75	-23.33	-24.80	-26.10	-28.15	-21.47	-19.83
80	-27.91	-30.60	-21.27	-33.22	-28.48	-31.13
85	-26.46	-31.07	-26.13	-21.84	-28.15	-20.60
90	-33.00	-27.29	-19.03	-12.51	-99999	-99999

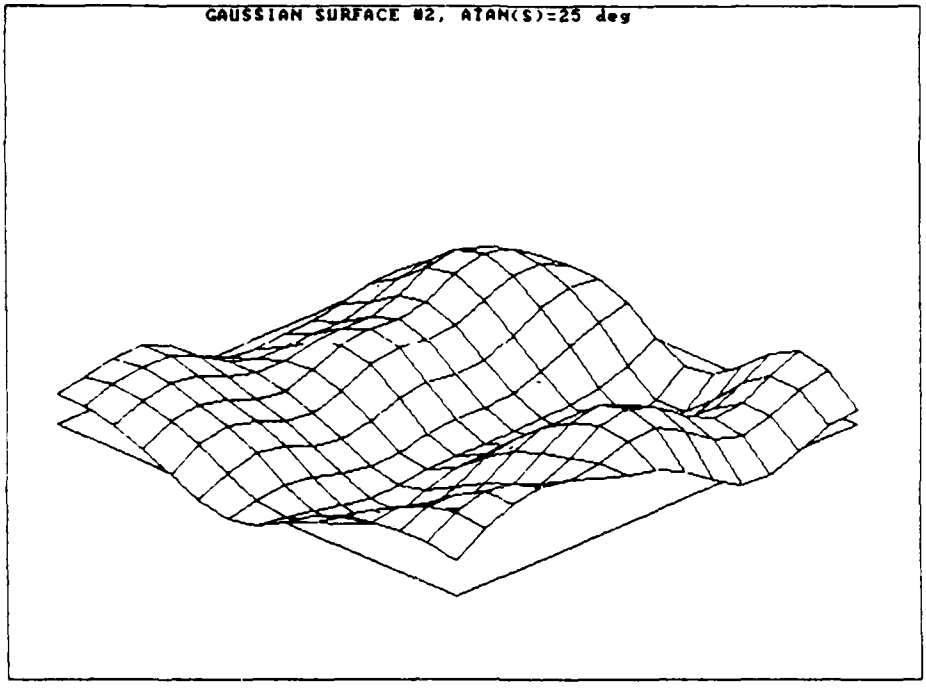

Fig. E1a. Gaussian Surface with Mean Slope of 25°

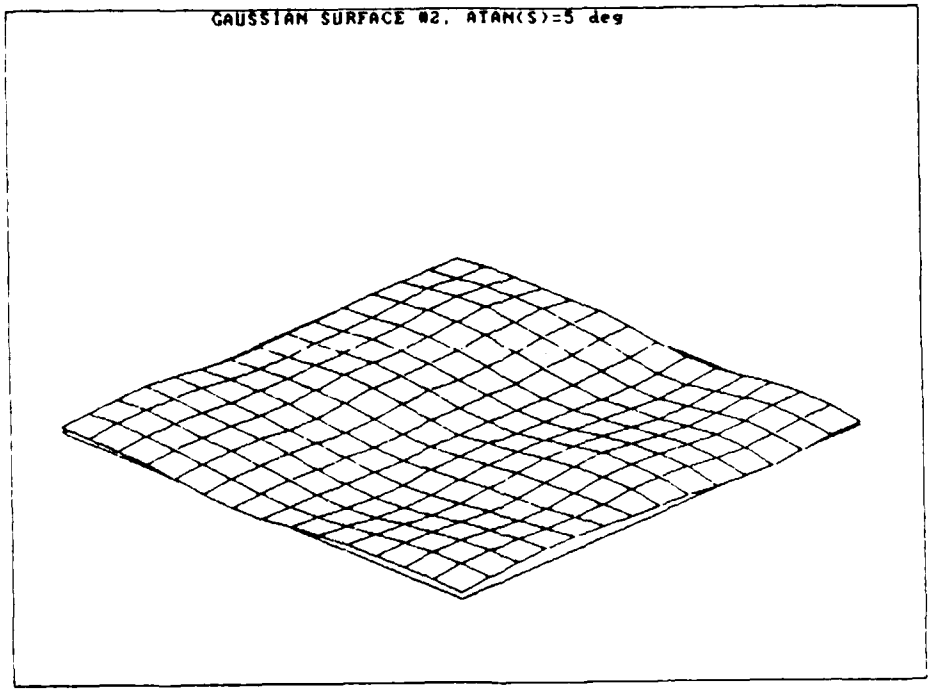

Fig. E1b. Gaussian Surface with Mean Slope of 5°

Bibliography

1. Abramowitz, Milton and Irene A. Stegun. Handbook of Mathematical Functions. Wash D.C.: U.S. Dept. of Commerce, National Bureau of Standards, Applied Mathematics Series No. 55, June 1964.

2. Barrick, Donald E. "A More Exact Theory for the Scattering of Electromagnetic Waves from Statistically Rough Surfaces," PhD Thesis, School of Electrical Engineering, Ohio State University, (1965)

3. Barrick, Donald E. "Rough Surface Scattering Based on the Specular Point Theory," IEEE Trans. Antennas and Propagation Vol. AP-16, No. 4: 449-454 (July 1968).

4. Barrick, Donald E. "Rough Surface Scattering Based on the Specular Point Theory," Radio Science, Vol. 3, No. 8:865-868 (August 1968).

5. Beckmann, Petr and Andre' Spizzichino. The Scattering of Electromagnetic Waves from Rough Surfaces. New York: The MacMillan Company, 1963.

6. Beckmann, Petr. Elements of Applied Probability Theory. New York. Harcourt, Brace and World Inc., 1968

7. Davenport, Wilbur B. Probability and Random Processes. New York: McGraw-Hill Book Company, 1970.

8. Gjessing, Dag T. Remote Surveillance by Electromagnetic Waves. Ann Arbor, Mich.: Ann Arbor Science Publishers Inc., 1980.

9. Harnly, Douglas A. and Robert L. Jensen. An Adaptive Distributed-Measurement Extended Kalman Filter for a Short Range Tracker. MS Thesis, AFIT/GA/EE/79-1. School of Electrical Engineering, Air Force Institute of Technology (AU), Wright-Patterson AFB OH, Dec 1979.

10. Knott, Eugene F. and others. Radar Cross Section. Norwood MA: Artech House, Inc., 1985.

11. Marhefka, Ronald J. Computer Code for Radar Cross Section of Convex Plate and Cone Frustrum Structures. Electroscience Laboratory, Ohio State University, Columbus Ohio, 1986.

12. Maybeck, Peter S. Stochastic Models, Estimation, and Control, Volume 1. New York: Academic Press, Inc., 1979

13. Papa, Robert J. and John F.Lennon. Statistical Characterization of Rough Terrain. Rome Air Development Center Technical Report, RADC-TR-80-9, Feb 1980.

14. Papa, Robert J. et al. Electromagnetic Wave Scattering from Rough Terrain. Rome Air Development Center Technical Report, RADC-TR-80-300, Sep 1980.

15. Papa, Robert J. and John F.Lennon.. Further Considerations in Models of Rough Surface Scattering. Rome Air Development Center Technical Report, RADC-TR-82-326, Dec 1982.

16. Papa, Robert J. and John F.Lennon. "The Dependence of Rough Surface Scattering on the Surface Height Statistics and Correlation Function," IEEE Trans. Antennas and Propagation Vol. AP-35, No. 2: 239-242 (Feb 1987).

17. Pyati, Vittal P. An Exponential Second-Order Probability Density Function. Unpublished report. Air Force Institute of Technology, Dec 1986.

18. Raemer, H.R. and C.K. Chow. Investigations on Statistcs of Terrain Height. Rome Air Development Center Technical Report, RADC-TR-85-178, Sep 1985.

19. Reif, 2Lt Clarence E. Scattering and Shadowing from an Exponentially Random Rough Surface for which Decorrelation Implies Statistical Independence. MS Thesis, AFIT/GE/87D-53. School of Electrical Engineering, Air Force Institute of Technology (AU), Wright-Patterson AFB OH, Dec 1987.

20. Ruck, George T. and others. Radar Cross Section Handbook. New York: Plenum Press, 1970.

21. Schiffer, Ralf. "Reflectivity of a Slightly Rough Surface," Applied Optics, Vol. 26, No. 4: 704-711 (15 Feb 1987).

22. Speigel, Murray R. Vector Analysis. Shaum's Outline Series in Mathematics. New York: McGraw-Hill Book Company, 1959.

23. Stratton, Julius Adams. Electromagnetic Theory. New York: McGraw-Hill Book Company, Inc., 1941.

24. Stutzman, Warren L. and Gary A. Thiele. Antenna Theory and Design. New York: John Wiley & Sons, 1981.

25. Vorburger T.V. and E.C.Teague. "Optical Techniques for On-Line Measurement of Surface Topography," Precision Engineering, Vol 3:61-83, (1981).

VITA

Captain Thomas K. Roseman was born on 26 April 1960 in Euclid, Ohio, a suburb of Cleveland. He graduated from high school in Mentor, Ohio in 1978 and attended Cleveland State University, from which he received a Bachelor's degree in Electrical Engineering. Upon graduation he attended Officers Training School where he earned a commission in the USAF. From there, he was assigned to the Logistics Division of the B-1B Bomber Program Office where he served three until entering the School of Engineering, Air Force Institute of Technology, in May 1987.

Permanent Address: 7722 Goldenrod Dr.

Mentor, Ohio 44060

Unclassified
SECURITY CLASSIFICATION OF THIS PAGE

REPORT DOCUMENTATION PAGE

Form Approved OMB No. 0704-0188

1a. REPORT SECURITY CLASSIFICATION UNCLASSIFIED	1b. RESTRICTIVE MARKINGS
2a. SECURITY CLASSIFICATION AUTHORITY	3. DISTRIBUTION/AVAILABILITY OF REPORT Approved for public release; distribution unlimited
2b. DECLASSIFICATION/DOWNGRADING SCHEDULE	
4. PERFORMING ORGANIZATION REPORT NUMBER(S) AFIT/GE/ENG/87D-55	5. MONITORING ORGANIZATION REPORT NUMBER(S)
6a. NAME OF PERFORMING ORGANIZATION School of Engineering 6b. OFFICE SYMBOL (If applicable) AFIT/ENG	7a. NAME OF MONITORING ORGANIZATION
6c. ADDRESS (City, State, and ZIP Code) Air Force Institute of Technology Wright-Patterson AFB, OH 45433-6583	7b. ADDRESS (City, State, and ZIP Code)
8a. NAME OF FUNDING/SPONSORING ORGANIZATION 8b. OFFICE SYMBOL (If applicable)	9. PROCUREMENT INSTRUMENT IDENTIFICATION NUMBER
8c. ADDRESS (City, State, and ZIP Code)	10. SOURCE OF FUNDING NUMBERS PROGRAM ELEMENT NO. / PROJECT NO. / TASK NO / WORK UNIT ACCESSION NO

11. TITLE (Include Security Classification)
Electromagnetic Scattering by an Exponentially Distributed Rough Surface with the Introduction of a Rough Surface Generation Technique

12. PERSONAL AUTHOR(S)
Thomas K. Roseman, Captain, USAF

13a. TYPE OF REPORT	13b. TIME COVERED	14. DATE OF REPORT (Year, Month, Day)	15. PAGE COUNT
Ms Thesis	FROM 6/87 TO 11/87	1987, 11, 30	180

16. SUPPLEMENTARY NOTATION

17. COSATI CODES			18. SUBJECT TERMS (Continue on reverse if necessary and identify by block number)
FIELD	GROUP	SUB-GROUP	Electromagnetic Scattering, Rough Surface Scattering Diffuse Scattering, Random Media
20	08		
20	14		

19. ABSTRACT (Continue on reverse if necessary and identify by block number)

Electromagnetic Scattering by an Exponentially Distributed Rough Surface with the Introduction of a Rough Surface Generation Technique

Thesis Chairman: Vittal Pyati
Assoc. Professor of Electrical Engineering

Approved for public release: IAW AFR 190-1.
LYNN E. WOLAVER 24 Feb 88
Dean for Research and Professional Development
Air Force Institute of Technology (AU)
Wright-Patterson AFB OH 45433-6583

20. DISTRIBUTION/AVAILABILITY OF ABSTRACT	21. ABSTRACT SECURITY CLASSIFICATION
☐ UNCLASSIFIED/UNLIMITED ☒ SAME AS RPT. ☐ DTIC USERS	UNCLASSIFIED
22a. NAME OF RESPONSIBLE INDIVIDUAL Vittal Pyati	22b. TELEPHONE (Include Area Code) (513) 255-3576 / 22c. OFFICE SYMBOL AFIT/ENG

DD Form 1473, JUN 86 — Previous editions are obsolete — SECURITY CLASSIFICATION OF THIS PAGE

Unclassified

Unclassified

The purpose of this study is to expand the capability of statistical modeling of electromagnetic scattering from radom rough surfaces. Prior studies considered Gaussian and exponential-type surface models. This thesis shows that the exponential-type joint probability density function (jpdf) fails to meet an essential condition imposed by the physics of rough surfaces. An exponential jpdf which satisfies all of the statitical requirements is derived and the scattering properties of surfaces modeled by it are studied.

In the second part of this thesis a technique for generating random rough surfaces on a computer is developed. This is accomplished by borrowing a technique previously used to create spatially correlated noise. This computer generated surface algorithm requires the input of only a monovariate pdf. The scattering properties of Gaussian and exponential computer generated surfaces are then found using a common radar cross section prediction software package.